SIGNAL TRANSDUCTION OF THE ATYPICAL GTPASE RHOH IN INTERLEUKIN-3 DEPENDENT CELL SYSTEMS

DISSERTATION

submitted to the Combined Faculties for the
Natural Sciences and for Mathematics
of the Ruperto-Carola University of Heidelberg, Germany
for the degree of
Doctor of Natural Sciences

presented by
Dipl.-Ing. (FH) Mehtap Gündogdu
born in Hof a.d. Saale

DISSERTATION

submitted to the
Combined Faculties for the Natural Sciences and for Mathematics
of the Ruperto-Carola University of Heidelberg, Germany
for the degree of
Doctor of Natural Sciences

presented by
Dipl.-Ing. (FH) Mehtap Gündogdu
born in Hof a.d. Saale
Oral examination: …….

SIGNAL TRANSDUCTION OF THE ATYPICAL GTPASE RHOH IN INTERLEUKIN-3 DEPENDENT CELL SYSTEMS

Referees:

Prof. Dr. Michael Lanzer

Prof. Dr. med. Alexander Dalpke

Meiner Familie

Table of contents

1. Summary 1

1. Zusammenfassung 2

2. Introduction 3

2.1 Interleukin-3 (IL-3) and the IL-3 receptor 3

2.1.1 The JAK-STAT pathway 4

2.1.2 IL-3 mediated JAK-STAT signalling 5

2.1.3 The physiologic relevance of IL-3 and the IL-3 receptor 6

2.2 Rho GTPases member of the Ras superfamily of small GTPases 7

2.2.1 Structural features of Rho GTPases 8

2.2.2 Important regulation mechanisms of Rho GTPases 9

2.2.3 Function and signalling of Rho GTPases 10

2.3 The atypical GTPase RhoH 10

2.3.1 Structural features of RhoH 11

2.3.2 RhoH in signal transduction 11

2.3.3 RhoH, a negative modulator of hematopoetic proliferation and its function in cancer 12

2.3.4 RhoH, inhibitor of IL-3 mediated proliferation and signalling: Preliminary data 13

2.4 Aim of this study 14

3. Materials and Methods 15

3.1 Material 15

3.1.1 Lab equipment 15

3.1.2 Expandable material 16

3.1.3 Purchaseable kits and buffers 17

3.1.4 General chemicals 17

3.1.5 DNA modifying enzymes 19

3.1.6 Stimuli for cell culture 19

3.1.7 Antibodies and isotypes 20

3.1.8 Size markers 21

3.1.9 Vectors 21

3.1.10 Oligonucleotides 22

3.1.11 Eukaryotic cells 23

3.1.12 Special software & databases 24

3.1.13 Buffers and working solutions 24

3.2 Methods 26

3.2.1 Eukaryotic cells 26

3.2.2 Prokaryotic cells 30

3.2.3 Molecular biological techniques 32

3.2.4 Biochemical and immunological methods 37

4. Results 48

4.1 RhoH modulates IL-3 signalling through regulation of STAT activity and IL-3 receptor expression 48

4.1.1 Regulation of RhoH expression in the IL-3 dependent system 48

4.1.2 RhoH, an inhibitor of IL-3 induced proliferation 49

4.1.3 RhoH overexpression results in increased IL-3 dependent STAT1 activation 51

4.1.4 RhoH modulated IL-3 dependent STAT1 activation correlates with expression of CDKIs 52

4.1.5 RhoH expression modulates IL-3 induced STAT5 activity 54

4.1.6 RhoH- a modulator of CD123 surface expression 56

4.1.7 RhoH reconstitution correlated with a downregulation of prognostic AML markers in THP-1 cells 58

4.1.8 RhoH expression pattern in lymphoma derived cell lines 59

4.1.9 Proteomics of RhoH in IL-3 dependent cell lines 62

4.2 RhoH in IL-3 derived bone marrow MCs 71

4.2.1 RhoH mRNA expression in IL-3 derived murine MCs 71

4.2.2 RhoH null HPCs show elevated IL-3 induced proliferation 72

4.2.3. RhoH null HPCs show lower $p21^{waf/cip1}$ and $p27^{kip1}$ mRNA expression only in early phase of IL-3 cultivation 73

4.2.4. RhoH null progenitors show no differences in the differentiation to MCs 74

4.2.5. RhoH is important for FcεRI mediated degranulation of MCs 75

4.2.6. $RhoH^{-/-}$ MCs show impaired release of IL-6 and TNF-α 76

5. Discussion 78

5.1 RhoH expression is regulated by IL-3 and modulates IL-3 induced proliferation 78

5.2 RhoH: Fine-tuning of IL-3 dependent JAK-STAT signalling 79

5.3 RhoH expression in THP-1 cells, correlates with increased IRF-1 and decreased CD123 expression 82

5.3.1 RhoH is underexpressed in lymphoma derived cell lines with abberant signalling patterns and immunophenotype 83

5.4 RhoH interaction partner binding is IL-3 dependent 85

5.4.1 Similar proteins can bind to RhoH and to its effector domain mutant variant 87

5.4.2 IL-3 treatment determines the subcellular localisation of RhoH interacting proteins 89

5.4.3 RhoH interacts with Cofilin-1 in HEK cells 91

5.4.4 RhoH interacts with PTP1B in HEK cells 92

5.5 Summary and outlook (I): RhoH modulates IL-3 induced proliferation by fine-tuning IL-3 dependent JAK-STAT signalling 93

5.6 The function of RhoH in IL-3 mediated MC differentiation and function 95

5.6.1 RhoH mRNA expression is regulated during MC differentiation 95

5.6.2 RhoH null MC progenitors show enhanced proliferation in early phases of cultivation in IL-3 containing medium 96

5.6.3 No morphologic differences between RhoH null and wt MC 98

5.6.4 The lack of RhoH causes functionial defects in IL-3 derived MCs 100

5.7 Summary and outlook (II): The consequences of RhoH deficiency for IL-3 derived MCs 102

6. Appendix 103

6.1 Supplementary tables 103

6.1.1 Thesis relevant protein hits 103

6.1.2 Gene ontology 104

6.2 RhoH protein sequence (mouse) 105

7. Bibliography 106

8. Publications and Presentations 114

Acknowledgment 115

List of abbreviations

AA	Amino acid
ALCL	Anaplastic large cell lymphoma
ALK	Anaplastic lymphoma kinase
AML	Acute myeloid leukemia
Amp	Ampiciline
AP-1	Activator protein 1
APC	Antigen presenting cell
APC labelled	Allophycocyanin labeled
APS	Ammonium persulfate
Arf	ADP-ribosylation factor
ATCC	American Type Culture Collection
ATP	Adenosine 5`triphosphate
BCA	Bicichinonic
BCL6/LAZ3	B-cell lymphoma 6
BM	Bone marrow
BMC	Bone marrow cell
bp/kb	Base pairs/1000 bases
BrdU	Bromodeoxyuridine
BSA	Bovine serum albumine
C°	Degree Celsius
CD	Cluster of differentiation
Cdc42	Cell division control protein 42 homolog
cDNA	Complementary DNA
c-Kit (CD117)	Tyrosinkinase KIT
CMP	Common myeloid progenitor
C-terminus	Carboxy-terminus
CTG	Cell Titer Glo
Da	Dalton
DC	Dendritic cell
DMEM	Dulbecco's Modified Eagle's Medium,
DMSO	Dimethyl sulfoxide
DNA	Desoxynucleic acid
DSMZ	Deutsche Sammlung von Mikroorganismen und Zellkulturen
E.coli	Echerichia coli
EDTA	Ethylenediaminetetraacetic acid,
ELISA	Enzyme-linked immunosorbent assay
EPO	Erythropoietin
ER	Endoplasmatic Reticulum
ERK	extracellular-signal-regulated kinases
EtOH	Ethanol
FACS	Fluorescence associated cell sorting
FCS	Fetal calf serum
FcεRI	High-affinity receptor for the Fc region of immunoglobulin E (IgE)
FITC	Fluorescein isothiocyanate
GAP	GTPase-Activating Proteins
GAPDH	Glycerinaldehyd-3-phosphate-dehydrogenase
GDI	Guanosine nucleotide dissociation inhibitors
GDP	Guanosine diphosphate
GEF	Guanine nucleotide exchange factors
GFP	Green fluorescent protein
GM-CSF	Granulocyte-macrophage colony stimulating factor
GSH	Gluthatione
GST	glutathione *S*-transferase
GTP	guanosine triphosphate
h	hour
HAA	Hexosaminidase Assay

HCL	Hairy cell leukaemia
HLA	Human leukocyte antigen
HPC	Hematopoietic progenitor cell
HPLC	High-performance liquid chromatography
HRP	Horse radish peroxidase
HSC	Hematopoietic stem cell
IF	Immuno fluorescence
IgE	Immunoglobulin E
IKK	IκB kinase
IL	Interleukin
IP	Immunoprecipitation
IPTG	Isoprypylthio-β-D-galactoside
IRES	Internal ribosomal entry site
IRF-1	Interferon regulatory factor 1
ITAM	Immunoreceptor tyrosine-based activation motifs
IκBα	Inhibitor of kappa B
JAK	Janus-Kinase
JH	Jak homology
JNK	c-Jun N-terminal kinases
k	Kilo
ko	Knock-out
LB	Luria Bertani
LC	Liquid chromatography
LSC	Leukemic stem cell
Lyn	V-yes-1 Yamaguchi sarcoma viral related oncogene homolog
mA	Milli Ampere
MAP	Mitogen-activated protein
MAPK	Mitogen-activated protein Kinase
MC	Mast cell
MetOH	Methanol
Mg^{2+}	Magnesium
min	Minute
Miro	Mitochondrial Rho GTPase
mRNA	Messenger RNA
MS	Massspectrometry
NES	Nuclear Export Signal
NFkB	Nuclear factor kappa-light-chain-enhancer of activated B cells
NHL	Non-Hodgkin lymphoma
NLS	Nuclear Localisation Signal
NPM-1	Nucleophosmin-1
N-terminus	Amino-Terminus
OD	Optical Density
ON	Over night
OVA	Ovalbumin
PAGE	Polyacrylamide gel electrophoresis
PBR	Poly Basic Region
PBS	Phosphate buffered saline
PCR	Polymerase chain reaction
PE	Phycoerythrin
PFA	Paraformaldehyde
PI	Propidium iodide
PI3K	Phosphoinositid-3-Kinase
PKC	Protein Kinase C
P-loop	Phosphate binding loop
PMA	Phorbol 12-myristate 13-acetate
PS	Penicilin/Streptomycin
PTP	protein tyrosine phosphatase
PTP1B	Protein Tyrosin phosphatase 1B
Puro	Puromycin
Rab	Ras related in brain
Rac	Ras-related C3 botulinum toxin substrate

Ran	Ras related nuclear protein
Ras	Rat sarcoma
rE	Relative expression
Rho	Ras homologue
RhoH	Ras homologe H
RLU	Relative Light Units
RNA	Ribonucleic acid
rpm	Rotations per minute
RPMI	Roswell Park Memorial Institute
RT	Room Temperature
RTK	Receptor Tyrosine Kinase
SCF-1	Stem cell factor-1
SCX	Strong cation exchange
SDS	Sodium dodecyl sulfate
Sec	Second
SHP	Src homology region 2 domain-containing phosphatase
SOCS	Suppressor Of Cytokine Signalling
Src	Sarcoma
SRF	Serum Response Factor
STAT	Signal Transducers and Activators of Transcription
Syk	Spleen Tyrosine Kinase
TBS	Tris Buffered Saline
TBST	Tris Buffered Saline and Tween20
TCR	T-Cell Receptor
TNF-α	Tumour Necrotizing Factor alpha
TNP	2,4,6-Trinitrophenol
TTF	Translocation Three Four
Tyk2	Tyrosine kinase 2
U	Units
V	Volt
WB	Western-blot
wt	Wildtype
Zap70	Zeta chain associated protein kinase 70

1. Summary

The hematopoietic, atypical GTPase RhoH is reported to function as a negative regulator of progenitor cell differentiation, proliferation and survival. IL-3 is an important cytokine, signalling mainly via the JAK-STAT pathway and by this promoting hematopoiesis, progenitor cell survival and differentiation of myeloid cells, such as mast cells. This study aimed to investigate the role of RhoH and important components in the signalling network of RhoH in IL-3 mediated signal transduction. It was attempted to link published, as well as the gained, information of this study to profile hematopoietic malignancies with aberrant RhoH expression. Finally, complementary studies were performed with *in vitro* IL-3 derived mast cells to address the role of RhoH in IL-3 mediated cell differentiation and its function in mast cell mediated processes, such as anaphylaxis.

RhoH overexpression in BaF3 cells resulted in inhibition of IL-3 induced proliferation correlating with increased STAT1 and decreased STAT5 activity. Downregulation of RhoH was followed by an increase in IL-3 proliferation associated with enhanced STAT5 phosphorylation. Altered STAT1 activation induced increased expression of the cell cycle inhibitors (CDKIs) $p21^{waf/cip}$ and $p27^{kip}$. Enforced IL-3 induced STAT5 activation in cells with low RhoH expression led to enhanced sensitivity of cells to IL-3, as a result of an upregulation of the STAT5 dependent transcription factor IRF-1 which induced increased IL-3 alpha chain (CD123) surface expression. RhoH expression was tested in lymphoma cell lines which were characterised based on their immunophenotype, STAT and GTPase activity. RhoH was strongly underexpressed in almost every cell line, suggesting that RhoH plays an important role in the formation of hematopoietic cancer types. To gain further insight into the IL-3 dependent signalling networks of RhoH, cytokine treatment dependent proteomic experimebyents were performed with IL-3 dependent BaF3 cells. A cytokine dependent pattern of protein interactions was identified. The interaction with RhoH was verified in HEK cells for two proteins: Cofilin-1 and PTP1B. Both of these proteins were found to have effects that can be related to the previous findings of this study in IL-3 mediated signalling. Finally, experiments in mast cells were performed to identify the role of RhoH for IL-3 dependent cell differentiation and function, indicating that RhoH deficiency does not affect the IL-3 induced differentiation. However, the loss of RhoH has functional consequences on mast cell biology, such as decreased cytokine production and mast cell mediator release.

These findings link RhoH expression and RhoH modulated IL-3 induced proliferation on the one hand to STAT1 dependent induction of CDKIs and on the other hand to the increased STAT5 dependent CD123 expression. It is suggested that RhoH is a tandem regulator of IL-3 dependent STAT5/STAT1 activation, most likely by newly discovered interactions with key signalling proteins such as PTP1B and Cofilin-1. Altered RhoH expression pattern in different hematopoietic disorders also suggests that the identified role of RhoH in IL-3 dependent signalling is transferrable to aberrant signalling in cancerogenous diseases. Furthermore, it was postulated that, although RhoH is dispensable for IL-3 mediated myeloid mast cell differentiation, the lack of RhoH has serious impact on mast cell mediated effects.

1. Zusammenfassung

Die hämatopoetische GTPase RhoH ist ein negativer Regulator für die Vorläuferzelldifferenzierung, Proliferation sowie für das Überleben hämatopoetischer Stammzellen. Die Regulation der Differenzierung und des Überlebens dieser Zellen erfolgt hauptsächlich über den IL-3 abhängigen JAK-STAT Signalweg. Ziel dieser Studie war es die Rolle von RhoH in der IL-3 abhängigen Signaltransduktion zu untersuchen und neue Komponenten der RhoH vermittelten Signaltransduktion zu identifizieren. Zusätzlich wurde anhand von Hinweisen aus der Literatur verschiedene Lypmhoma Zellinien hinsichtlich ihrer RhoH Expression im Zusammenhang mit der Aggressivität der jeweiligen Tumorzellen analysiert. Ausserdem sollte der Einfluss von RhoH auf die IL-3 abhängige Mastzelldifferenzierung und deren Funktion (z.B. Anaphylaxie) mittels *in vitro* generierter Mastzellen geklärt werden.

Die Überexpression von RhoH in der murinen Pro-B-Zelllinie Baf3 korrelierte mit der Inhibition IL-3 vermittelter Proliferation einhergehend mit einer erhöhten STAT1 und verminderter STAT5 Phosphorylierung. Umgekehrt führte die Inhibition der RhoH Expression zu einer verstärkten IL-3 vermittelten Proliferation, verbunden mit einer erhöhten STAT5 Phosphorylierung. Die verstärkte STAT1 Aktivität induzierte eine erhöhte Expression der Zell Zyklus Inhibitoren (CDKIs) $p21^{waf/cip1}$ und $p27^{kip1}$ in RhoH überexprimierenden Zellen, während die erhöhte STAT5 Aktivierung in RhoH defizienten Zellen in einer gesteigerten Expression des STAT5 abhängigen Transkriptionsfaktors IRF-1 resultierte. Dies führt wiederum zur Überexpression der IL-3 α Kette CD123 an der Zelloberfläche.

Verringerte RhoH Expression konnte in verschiedenen Lymphoma Zelllinien nachgewiesen werden, die aufgrund ihres Immunophentoyps sowie ihrer veränderten STAT und GTPase Aktivitäten ausgewählt wurden. In verschiedenen RhoH Proteomanalysen wurden Zytokin abhängige Bindungsmuster mit RhoH interagierenden Proteinen festgestellt. Es konnten Interaktionen von RhoH mit Cofilin-1 und PTP1B in HEK Zellen nachgewiesen werden. Diese beiden Proteine können potentiell an den in dieser Studie gefundenen RhoH abhängigen Modulationen im IL-3 abhängigen Signalweg beteiligt sein. Abschließend konnte in Mastzellen gezeigt werden, dass RhoH keinen Einfluss auf die IL-3 vermittelte Zelldifferenzierung nimmt. Der Verlust von RhoH hatte jedoch schwerwiegende funktionelle Konsequenzen in den Mastzellen, wie eine verminderte Zytokin- und Histaminsekretion. Schlussfolgernd kann gesagt werden, dass RhoH die IL-3 vermittelte Signaltransduktion und vor allem die IL-3 abhängige Proliferation beeinflusst. Dies geschieht zum einen durch eine Modulation der STAT1 Aktivität und der Expression von STAT1 abhängigen CDKIs und zum anderen durch die Veränderung der STAT5/IRF-1 abhängigen CD123 Expression. RhoH wird eine Rolle als Tandem-Regulator in der IL-3 induzierten STAT5/STAT1 Aktivität zugeschrieben, die wahrscheinlich durch die Interaktion mit den Proteinen PTP1B und Cofilin-1 zustande kommt. Anhand der nachgewiesenen Expressionmuster von RhoH in Lymphoma Zellinien wird angenommen, dass RhoH eine wichtige Rolle in der Krankheitsentstehung als auch in deren Verlauf spielt. Für Mastzellen konnte gezeigt werden, dass RhoH keinen Einfluss auf die IL-3 abhängige Zelldifferenzierung nimmt jedoch die Expression von RhoH essentiell für die vermittelten Zellfunktionen ist.

2. Introduction

2.1 Interleukin-3 (IL-3) and the IL-3 receptor

Interleukin-3 (IL-3) is an important cytokine for hematopoiesis, supporting the proliferation and survival of hematopoietic progenitors and promoting the differentiation of myeloid cells (e.g. basophils, erythrocytes, dendritic cells (DCs) and mast cells (MCs))[1] from a common myeloid progenitor (CMP)[2,3]. IL-3 is a four helical cytokine serving as ligand for the IL-3 specific type I cytokine receptor alpha (α) chain, CD123. The (human) IL-3 gene is located on chromosome 5q23-31 and is neighbored by the IL-3 family cytokine genes GM-CSF (Granulocyte macrophage colony-stimulating factor) and Interleukin-5 (IL-5)[4]. IL-3 is produced mainly by $CD4^+$ T-helper (Th) cells and to a lesser extent by other cells, such as MCs, endothelial cells and monocytes.

The IL-3 receptor belongs to the type I cytokine receptor family, which are mediating signal transduction by the formation of receptor heterooligomers. These receptors commonly comprise a shared beta (β) and a cytokine specific α-chain[5;6]. In humans it was found that GM-CSF and IL-5 can compete with IL-3 for receptor binding suggesting that these cytokines share a common β chain [7] **(Fig.2.1)**. This observation does not occur in the murine system, since there is an additional IL-3 specific beta chain (β_{IL-3}) present on murine cells. Ligand binding to the IL-3 receptor α chain (CD123) causes the formation of a high affinity heterodimeric receptor complex[6,8]. The IL-3 βc is quite unique within the type I cytokine receptor family, since the conserved WSXSW motif, usually found within the CHR stretches of type I cytokine receptors, is replaced by a distinctive LSXSW motif[8,9]. The membrane proximal intracellular part of the βc subunit of the IL-3 receptor includes a Box-1 domain which was found to be of importance for the induction of proliferation associated genes (*c-myc*, *pim-1* and *oncostatinM*) [10-12]. Upon ligand binding, this region plays an important role in the interaction with different signal transducing proteins, such as Janus-Kinases (JAKs), STATs (Signal Transducers and Activators of Signal Transduction) , c-Scr (cellular-sarcoma) and PI-3K (phosphoinositid-3-kinase) [13]. The membrane distal region is known to mediate survival signals and growth inhibiting signals induced by the cytokines of the IL3-family[14]. Moreover, the membrane distal region is reported to take part in the activation of Ras (rat sarcoma) as well as in the transcriptional activation of transcription factors[14]. Due to a lack of

intrinsic enzymatic activity, type I cytokine receptors, such as the IL-3 receptor use mainly the JAK–STAT signalling pathway to transmit incoming signals [15].

2.1.1 The JAK-STAT pathway

The investigation of cytokine signalling pathways led to the discovery of four types of JAK proteins containing seven JAK homology (JH) domains[16]. Members of the JAK family are JAK1, JAK2, JAK3 and Tyk2. Except for JAK3, JAKs are ubiquitously expressed. The C-terminal JH domains inhabit the kinase and the pseudo-kinase region. Upon ligand binding to the receptor, receptor associated JAKs become activated through phosphorylation of critical tyrosines in their "activation loop" located within their kinase domain [17]. The FERM (four-point one, ezrin, radixin, moesin) domain is N-terminally located and is thought to mediate the association with the Box1 domain on cytokine receptors (type I and II)[18]. Upon activation JAKs initiate the phosphorylation of specific receptor tyrosine residues which serve as docking sites for the STAT proteins[18]. The seven discovered members of the STAT family STAT1, STAT2, STAT3, STAT4, STAT5a, STAT5b and STAT6 (90-100 kDa), inhabit a SH2 domain which is able to bind to phosphotyrosine residues, provided by JAKs. In resting cells, STATs are mostly located as inactive homodimers within the cytoplasm[18]. Once bound to the phosphorylated receptors sites, the STAT proteins become phosphorylated by JAKs and thereby activated. Activated STATs are released from the receptor and reorient into an anti-parallel dimer. To achieve this conformation, the SH2 domain of one activated STAT has to bind to the phosphorylated tyrosine of another activated STAT. The resulting STAT dimers translocate to the nucleus, where they bind to specific DNA sequences and initiate gene transcription. The regulation of the JAK-STAT signalling pathway is tightly controled by different mechanisms. One important mechanism is mediated by phosphatises, such as Src homology region 2 domain-containing phosphatases (SHP) which are able to dephosphorylate JAK proteins[19]. Members of the protein tyrosine phosphatase (PTP), family such as PTP1B are known to dephosphorylate STAT proteins. Only two of these phosphatases, TC-PTP and SHP-2, are able to dephosphorylate nuclear STATs, which plays an important role for the next regulatory mechanism, nuclear import and export of STATs. This process is driven by nuclear localisation and nuclear export signals in the sequence (NLS and NES) of STAT proteins[19,20]. Another important control function is initiated by members of the family of suppressors of cytokine signalling (SOCS) molecules. These molecules are STAT target genes which directly inhibit STAT activation resulting in a classical "feedback loop". Once these inhibitory mechanisms fail to "turn-off" the cytokine induced reaction, a

hyperactivity of the cytokine receptor results, which is frequently found in diverse cancer types[18].

2.1.2 IL-3 mediated JAK-STAT signalling

The major signalling pathway activated by IL-3 is the JAK-STAT pathway **(Fig. 2.1)**[13]. Upon receptor activation, the membrane proximal receptor associated JAK2 kinase (N-terminally) is activated and induces tyrosine (docking sites for STATs) and serine phosphorylation of βc residues. The α subunit of the IL-3 receptor (CD123), which is reported to be pivotal in IL-3 mediated differentiation of hematopoietic stem cells, is also involved in JAK2 activation. Normally STAT5a and STAT5b can be activated by IL-3 treatment which leads to the transcription of pro-proliferative genes[13,21,22]. To a much lesser extent Tyk2, STAT1 and STAT3 phosphorylation, following IL-3 treatment, has been observed[23].

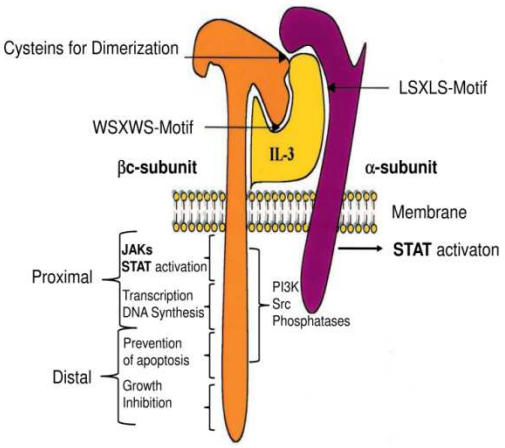

Fig. 2.1 The IL-3 receptor and its associated signalling molecules
Schematic diagram of IL-3 bound to the type I cytokine receptor IL-3. IL-3 comprises an unique ligand binding subunit that is not shared by other members of the IL-3 family receptors. The common β-chain is mostly responsible for cytokine mediated signal transduction and is shared by the IL-5 and GM-CSF receptors (modified from Reddy 2000)

It needs to be highlighted that STAT1 and STAT5, despite both being targets of IL-3, have oppositional effects in cells. In inflammation, STAT1 mediates the recruitment and the activation of immune cells via control of gene transcription of cytokines, chemokines, adhesion factors and proinflammatory mediators[24]. The induction of apoptosis is controlled by STAT1 activation by initiating the transcription of caspases[25] or death receptors and their ligands[26-29]. Also, the activation of STAT1 is known to have an inhibitory effect on the transcription of prosurvival genes such as members of the *bcl-2* family[30]. Moreover, STAT1 is known to be an inhibitor of proliferation by the transcriptional repression of proteins involved in cell cycle progression, such as the cyclin c-myc[31,32], or initiating the cell cycle dependent inhibitors (CDKIs) $p21^{waf/cip1}$ and $p27^{kip1}$ which can bind to the cell cycle dependent kinases (CDK2, 4/6) and by this causing cell cycle arrest in G1 phase[31,33,34]. By regulating cell survival and proliferation STAT1 is a major factor in the control of tumourigenesis[24].

However, STAT5 a key regulator of hematopoiesis, is phosphorylated and activated to a much higher content by IL-3 than STAT1. STAT5 is reported to act "reverse" to different STAT1 dependent processes by counter- regulating overlapping signalling pathways. By regulating genes such as *c-myc*, *bcl-xl* and genes of the *bcl-2* family, STAT5 activity takes part in enhancing cell proliferation[35,36]. Proliferation and cell cycle progression is promoted by STAT5 through the initiation of the expression of cell cycle progressing cyclin protein, as it was demonstated for CyclinA2[37] and CyclinD1[38] or as recent studies suggest by the regulation of $p21^{waf/cip1}$ and $p27^{kip1}$ proteins[39,40]. Apoptosis is thought to be directly inhibited by STAT5 through the regulation of the members of caspase proteins[41,42]. Aberrant STAT5 activation is also frequently found in a variety of malignancies and plays a key role in tumour development and oncogenic transformation and cancer progression[36].

2.1.3 The physiologic relevance of IL-3 and the IL-3 receptor

2.1.3.1 Physiologic relevance of IL-3 for murine mast cells (MCs)

Mast cells (MCs) are inflammatory tissue-based cells of myeloid origin, that function as major effectors of allergic reactions (e.g. anaphylaxis) and to a lesser extent as modulators of innate and adaptive immunity[43]. Different groups of mediators are produced by MCs: preformed mediators such as histamine, which effects the smooth muscle contraction and induces an increase of the vascular permeability; serine proteases and the cytokine Tumour Necrotizing Factor alpha (TNF-α). TNF-α is also reported to be *de novo* synthesised like other cytokines (IL-6, IL-10, IL-4) by MCs upon antigen challenge [43-44]. MCs are carriers of the high-affinity Immunoglobuline E (IgE) receptor (FcεRI)[45]. The release and secretion of MC mediators is triggered after antigen recognition or polyvalent allergen binding to the FcεRI bound IgE. Following antigen challenge the granules fuse to the plasma membrane and the granule contents are released[44]. The FcεRI β-chain inhabits immunoreceptor tyrosine-based activation motifs (ITAMs)[46], which are conserved sequences composed of tryrosine residues found throughout different types of immune-related proteins[47]. Upon IgE binding the crosslinkage of the FcεRI is induced and the ITAMs get phosphorylated and recruit the spleen tyrosine kinase (Syk) kinase. Syk initiates the downstream signalling cascades leading to the activation of the MC[46]. Also STAT5 was found to significantly contribute to the activation and to the maturation of MCs[37], which differentiate to their mature form locally after precursor migration to the target tissue[48]. However, many factors in the micro-environment can dramatically influence the resulting mature MC phenotype in the tissue [49,50]. *In vitro*

hematopoietic stem cells (HSCs) can be triggered to differentiate into MCs in the presence of only one of the required factors, which means either in the presence of SCF-1 or IL-3. However, the details of the influence of the environment and signal transduction leading to MC development are still unknown[43].

2.1.3.2 Physiologic relevance of CD123 in Acute Myeloid Leukemia (AML)

Acute Myeloid Leukemia (AML) is a myeloid clonal stem cell disorder. Characteristic for this disease is the occurrence of clonal chromosomal defects and a low production of healthy cells. A few leukemic stem cells (LSC) are the origin of a vast amount of leukemic cells undergoing an aberrant and poorly regulated process of hematopoiesis[51 52].Characteristic markers and features of AML is the elevated expression of the IL-3 receptor α chain on primitive AML cells, which is associated with an increased cell cycle activity and an increased resistance of these cells against apoptosis, when facing growth factor deprivation[53]. In addition CD123 overexpressing AML blasts showed either spontaneous STAT5 activation or increased levels of STAT5 phosphorylation after IL-3 treatment. It is thought that the increased CD123 surface expression in AML cells, as a result of the elevated expression of the STAT5 dependent interferon regulatory factor-1 (IRF-1) surface[53]. Recent observations indicate that low expression levels of the atypical GTPase RhoH functions as an unfavourable prognostic marker for overall and disease free survival[54].

2.2 Rho GTPases member of the Ras superfamily of small GTPases

There are over 150 highly conserved monomeric G- proteins belonging to the Ras Superfamily of small guanosine-triphosphatases (GTPases)[55]. Due to their sequence homologies and functional similarities, the members of the Ras Superfamily can be subdivided into six main branches: Ras, Rho, Rab, Ran, Arf and Miro. These small GTP-binding proteins act as molecular “switches” in several cellular processes, working in a binary fashion. Stereotypic members of these subgroups cycle between a GTP bound “on” and a guanosinediphosphate (GDP) bound “off” conformation [56].

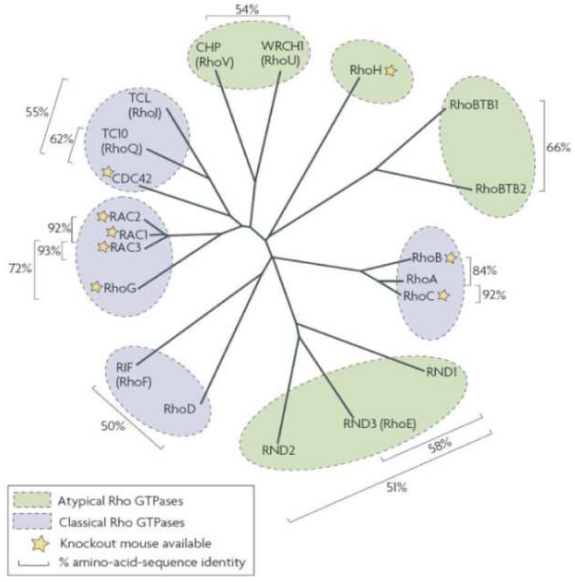

Fig. 2.2 Unrooted phylogentic tree of the 20 members of the Rho GTPases Family
Classification of the members of Rho GTPases based on their amino acid sequence similarities under specifications of the sequence homology (percentage) and indications of their GTPase activity ("classical" and "atypical"), (from Heasman and Ridley 2008)

2.2.1 Structural features of Rho GTPases

Rho GTPases are monomeric 20-30 kDa GTP binding proteins, found in all eukaryotic cells. 22 mammalian genes encode for 25 Rho GTPases, which can be subdivided according to their functional and sequential homologies into 8 clusters **(Fig 2.2)**: the "classical" GDP/GTP binding proteins including RhoA, Rac1 and Cdc42 [57]. These classical GTPases are cycling between an inactive GDP (inactive) and GTP (active) -bound conformation. The cycling is promoted by their intrinsic ability to hydrolyse GTP to GDP. They are thought to interact with their downstream targets and signalling mainly in their GTP-bound form. Besides the typical members there are the so called "atypical" Rho GTPases, which are comprised by the subbranches Wrch-1/Chp, Rnd, RhoBTB and RhoH/TTF **(Fig. 2.2)**. The atypical Rho GTPases are in a constitutively GTP-bound "on" conformation[58].

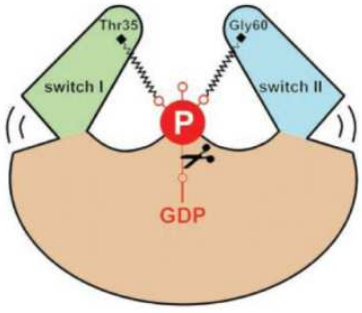

Fig.2.3 Structure and "loaded spring mechanism" of Rho GTPases
Schematic illustration of the universal loaded spring mechanism. Switch I and II domains are bound to the γ-phosphate via amino groups of conserved threonine and glycine residues. Switch region relaxes after release of γ-phosphate following GTPase hydrolysis (from Vetter and Wittinghofer 2001)

Characteristic for Rho family proteins is the Rho-type GTPase like domain, lined up within short N- and C- terminal extensions and inhabiting a Rho specific structural insert of 13 amino acids (aa)[56,59]. In addition to the GTPase domain, GTP-binding molecules have 4 to 5 other conserved sequence elements, of which the switch regions (I and II) and the β- and γ-phosphates located in the phosphate binding loop (P-loop) are of particular interest for nucleotide base binding. The "loaded spring mechanism" describes the conformational change of the GTPase, when the GDP is exchanged for GTP **(Fig. 2.3)**[56,60]. In the GTP-bound form, two hydrogen bonds from the γ-phosphate oxygens are formed to the invariant conserved threonine in the switch I region (37 in RhoA, 36 in RhoH) and to the glycine in the switch II region. The release of γ-phosphate after the GTP hydrolysis allows the switch to relax back to its "off", GDP bound conformation[56].

2.2.2 Important regulation mechanisms of Rho GTPases

2.2.2.1 Gene expression

Rho GTPases are expressionally regulated. Most Rho GTPases are ubiquitously expressed, while other GTPases show tissue specific expression pattern[59]. In addition to the tissue specific gene expression, the control of transcription and translation are important regulatory mechanisms of Rho GTPases. The transcriptional control is of particular interest for the atypical, constitutive active members of Rho GTPases such as RhoH [59,61].

2.2.2.2 Regulation through interactions with GEFs, GAPs and GDIs

Guanine nucleotide exchange factors (GEFs), are proteins that promote the exchange of bound GDP to GTP of Rho GTPases. GTPase activating proteins, (GAPs) are accelerating the weak GTP hydrolysis activity of Rho proteins[62-63]. Guanine dissociation inhibitors, (GDIs) are interacting with the switch I and II region, as well as the C-terminal polybasic domain and CAAX motif of Rho GTPases [64]. GDIs are able to: (1) inhibit the GDP dissociation, (2) inhibit the hydrolysis of GTP and blocking interactions with effector proteins, (3) mediate the cytosol sequestering of Rho GTPases, (4) provide the structural stability of Rho GTPases and facilitate the transport of RhoGTPases between different intracellular compartments [65,66]. The GTPase RhoH was found to interact with GDIs[61]. However, the function and the mechanism of these interactions remain widely speculative. Competition between Rho GTPases for the interaction with overlapping effector and target proteins has been shown to contribute to the regulation of Rho GTPases and their mediated signalling pathways[67].

2.2.2.3 Posttranslational protein modifications

The activity and the mediated function of Rho GTPases also depend on their subcellular localisation. C-terminal CAAX motif determines GTPase localisation, and is known to be targeted for posttranslational lipid modifications. The CAAX motif can be prenylated, geranylated or methylated[68], thereby the -AAX sequence is cleaved off and the free carboxylate anion of the cysteine residue is methylated [59,68]. Rho GTPase activity can also be regulated by direct phosphorylation or ubiquitination[69,70]. The serine phosphorylation within the polybasic region of Rho GTPases was shown to modulate the binding affinity to their GDIs[71]. Ubiquitinylation of Rho GTPases in response to stimuli results in the posttranslational degradation of Rho GTPases[70,72].

2.2.3 Function and signalling of Rho GTPases

Rho GTPases and their effector proteins are well described modulators of the cytoskeleton and related cell functions[61,73,74]. RhoA, Cdc42 and Rac1 are known to stimulate cell cycle progression either by promoting Cyclin D1 induced G1-S transition or by negative regulation of the cell cycle inhibitors $p21^{waf/cip1}$ and ^{p27kip1}. The atypical GTPase Rnd3/RhoE however, blocks cell cycle progression via Cyclin D1[75]. Rho GTPases are also known to control wide ranges of "nuclear factor kappa-light-chain-enhancer of activated B cells" (NFκB)-mediated processes such as cell survival[76,77]. Rho GTPases are also important for cytokine mediated JAK-STAT signalling. The phosporylation, as well as the nuclear translocation, of STAT5 and STAT3 was demonstrated to be facilitated by activated Rac1 and the GAP molecule MgcRacGAP[78,79]. Also interferon-γ induced inflammatory response via STAT1/STAT3 signalling strongly depends on Rac1 activity[80]. Rho GTPases are mediating numerous functions in hematopoiesis such as long-term engraftment, proliferation and migration of HSC or in the differentiation and development of MCs, B- and T- lymphocytes[81]. Apparently dysregulation of Rho GTPases is found to promote tumorigenesis and malignant disorders.

2.3 The atypical GTPase RhoH

RhoH, initially named Translocation Three Four (TTF), was discovered in 1995 by Dallery and co-workers as a fusion transcript from chromosome (3:4) translocation in Non-Hodgkin-Lymphoma (NHL) with the transcriptional repressor B-cell lymphoma-6 (BCL6)/LAZ3[82]. Sequence analysis assigned the sequence to the previously unknown small G like protein RhoH[82]. RhoH is localised on the short arm of chromosome 4, band p13 and has a length of

191 aa. RhoH shares a 27% H-RAS and a 45% relationship to other Rho family members and is GTPase deficient. Thereby RhoH activity is thought to be controlled through interactions with other GTPases, posttranslational modifications and transcription regulation[83]. RhoH expression is restricted on hematopoietic cells, with differential expression levels among the lineages[81-84]. The strongest expression of RhoH was detectable in lymphocytes, lower RhoH expression was also detectable in hematopoietic progenitor cells and myeloid lineages such as *in vitro* derived MCs[61,85].

2.3.1 Structural features of RhoH

RhoH is GTPase deficient, due to absent residues critical to catalytic GTPase activity such as the conserved glycine 12 (RhoA), which is replaced in RhoH by a serine[86] and glutamine 63 (RhoA) that is asparagine in RhoH. The specific Rho family insert of 13 aa was found to be significantly shorter in RhoH with a length of only 7 aa[83]. The conserved CAAX motif on the C-terminus is present in RhoH as a CKIF-motif. The RhoH CKIF-motif was demonstrated to undergo farnesylation and to a lesser extent, geranylation[83].

2.3.2 RhoH in signal transduction

2.3.2.1 RhoH and its inhibitory function on other GTPases

RhoH was found to significantly retard the degradation of IκBα and thereby suppress the NFkB activation[61]. RhoH was also able to reduce the activation of NFκB, induced by the expression of constitutive active RhoA or Rac1. RhoH has an inhibitory effect on Rac1 and Cdc42 dependent TNF induced p38 activation independently of JNK or ERK activation[61]. Furthermore it was demonstrated that RhoH is able to inhibit stromal derived factor-1 (SDF-1) induced, Rac1 mediated chemotaxis and polarisation of HPCs[87]. The inhibitory effect of RhoH on other GTPases is considered as a physiological function, although the exact mechanisms remain unknown.

2.3.2.2 RhoH in T-cell signalling

Studies of RhoH in lymphocytes showed that phorbol 12-myristate 13-acetate (PMA) treatment, which activates Protein Kinase C (PKC) and thereby mimics T-cell receptor (TCR) complex mediated signal transduction, results in the decrease of RhoH mRNA levels[61]. RhoH null mice exhibited substantial blocks at distinct developmental stages leading, to fewer mature T-cells and thereby indicating RhoHs` importance for pre-TCR signalling[88]. Mature T-cells of RhoH-/- mice, despite normal amounts of TCR on their surface, failed to respond with

adequate proliferation in response to stimulation with anti-CD3 antigen. It was found that the spleen tyrosine kinase homolouge Zap70, binds to a putative ITAM in RhoH, which in turn sequesters its recruitment to the CD3ζ-chain following TCR activation leadinding to the initiation of proper downstream signalling[89]. Nevertheless, the interaction of RhoH and Zap70 is contested since Brakebush and co-workers were unable to detect this interaction[88]. RhoH is subject to proteasomal degradation after TCR, but not after B-cell receptor activation, highlighting its distinct role for TCR signalling[72].

2.3.2.2.1 Anaplastic large T-cell lymphoma (ALCL)

Anaplastic large T-cell lymphoma (ALCL) is a biologic and clinically heterogeneous subtype of peripheral T-cell lymphoma (non-Hodgkin lymphoma (NHL))[90]. 50-80 % of all ALCLs contain a chromosomal translocation which brings the orphan tyrosine kinase, anaplastic lymphoma kinase (ALK) under the promoter control of different genes (ALK^+ ALCL)[91]. Most systemic ALK^+ ALCL types inhabit the translocation t(2;5)(p23;35)[92], which brings ALK under the promoter control of the nucleolar phosphoprotein nucleophosmin (NPM)[93]. One hallmark of ALCL subtypes is the aberrant immunophenotype, typicaly lacking the TCR and associated molecules such as CD3 and Zap70, as well as low or no expression of CD4/CD8[94]. NPM-ALK^+ ALCL show enhanced STAT5 phosphorylation correlating with higher cell cycle progression rates and cytokine independent growth[95,96]. Recent studies also reveal an important role of small GTPases (e.g. Rac1, Cdc42) contributing to the oncogenic attributes of NPM-ALK rearrangements in systemic ALCL[97,98].

2.3.3 RhoH, a negative modulator of hematopoetic proliferation and its function in cancer

2.3.3.1 RhoH a negative modulator of hematopoietic cell proliferation and survival

Hematopoietic progenitor cells with enhanced RhoH levels showed decreased proliferation rates in response to the cytokine SCF-1. Additionally, RhoH expression led to impaired colony formation in response to SCF-1. The susceptibility of RhoH overexpressing progenitor cells to undergo apoptosis was enhanced causing decreased cell counts. The explanation of the observed defects was due to an antagonistic effect of RhoH on the GTPase Rac1, which was previously described to have opposing consequences on the described processes in stem cells[85].

2.3.3.2 RhoH involvement in cancer

RhoH is a protooncogene since its coding region is juxtaposed to the immunoglobulin locus. BCL6/LAZ3 translocations with RhoH are frequently found during the process of indolent follicular lymphoma transformation to aggressive large B-cell lymphoma, which indicates a role of RhoH in pathogenesis and as a marker for transformation potential of follicular lymphoma[83]. RhoH involving translocations were also detectable in multiple myelomas, nodal marginal lymphomas and splenic lymphomas. RhoH is located on a hypermutable gene locus, and is thereby targeted by aberrant hypermutation at its non-coding region which indicates altered RhoH expression [61]. Hypermutations in RhoH are considered as a tumor-associated event[99]. RhoH expression is downregulated in hairy cell leukemia (HCL) and AML. It was found that RhoH underexpression is a diagnostic marker for HCL associated with increased proliferation, adhesion and migration of HCL cells[100]. RhoH underexpression in AML supports Rac1 dependent protection from apoptosis and drug resistance and was thereby determined to be a poor prognostic factor for general and disease-free survival of AML patients[4-54]. Overexpression of RhoH also plays a role in leukaemia. Increased RhoH expression levels correlated with Zap70 expression in B-cell chronic lymphocytic leukemia (CLL) leading to enhanced Akt/Erk phosphorylation following B-cell receptor activation[101].

2.3.4 RhoH, inhibitor of IL-3 mediated proliferation and signalling: Preliminary data

Previous work from our lab (Liu, H.) with parental and RhoH overexpressing BaF3 cells showed indications for RhoH as a negative modulator of IL-3 dependent proliferation. Further work suggested that RhoH might eventually modulate IL-3 induced STAT activity leading to the observed proliferation defects. Physiologic relevance of RhoH for IL-3 dependent differentiation and cell function was tested by Liu in initial experiments with RhoH deficient, IL-3 derived MCs. These experiments suggested defect IL-3 dependent MC development due to altered MC marker expression and altered MC functions based on decreased β-hexosaminidase release measurements of RhoH deficient MCs[102].

2.4 Aim of this study

Based on the preliminary findings of Liu aim of the first part of this study was to gain an understanding of the role of RhoH IL-3 induced signalling and its relevance for hematologic malignancies. Subject of investigation was the potential of RhoH to modify specifically IL-3 induced proliferation and cell survival by using the murine model proB cell line BaF3. Next it was attempted to understand how RhoH expression is able to alter IL-3 dependent proliferation by investigating IL-3 mediated JAK-STAT signalling in BaF3 cells with distinct RhoH levels. In this context it was further aimed to understand the alterations in gene expression induced by RhoH modulated JAK-STAT signal transduction with focus on the expression of STAT dependent CDKIs and CD123 surface expression. Complementary studies were assessed to outline a possible role of RhoH in the aberrant signal transduction of the myeloid malignancy AML, in which RhoH was reported to be underexpressed, transferring the previously gained knowledge from the BaF3 model system. Furthermore it was aimed to test RhoH expression in different lymphoma types with aberrant immunophenotypes and STAT signalling to gain insight into a potential role of RhoH in disease progression. To extend the knowledge about RhoH and the signalling networks involved in controlling IL3- mediated signal transduction it was planned to find novel interaction partners of RhoH by using mass spectrometry.

The second part of this work addressed the role of RhoH for IL-3 dependent cell differentiation and function using *in vitro* derived murine MCs. It was sought to understand the consequences of RhoH deficiency on MC mediated functions using IL-3 derived bone marrow MCs from RhoH ko mice. Additionally, it was attempted to relate the previous findings of RhoH as a modulator of STAT activation in the BaF3 model system, to MCs differentiation and function.

3. Materials and Methods

3.1 Material

3.1.1 Lab equipment

Agarose Gel Elektrophoresis system	PerfectBlue ™ Mini S, Pequlab, Erlangen
Bacteria Shaker	Incubator 1000, Unimax, 1010 Shaker, Heidolph Instruments GmbH Co. KG, Schwabach
Bunsen burner	Gasprofi 2^{scs},WLD-TEC GmbH, Göttingen
Cell Counting Chamber	Neubauer 0.0025 mm²/0.1 mm, Brand GmbH Schwerin
Centrifuges	1. Biofuge fresco, Heraeus Instruments, Hanau 2. Biofuge pico, Heraeus Instruments, Hanau 3. Biofuge stratos, Heraeus Instruments, Hanau 4. Sorvall RC 5B Plus, Thermo scientifc, Bonn
Chemical Balance	EW600-2M, Kern & Sohn GmbH, Balingen
Extractor Hood	Variolab Mobilien W90, Waldner-Laboreinrichtungen GmbH, Wangen
FACS	BD FACSCanto™, BD Bioscience, Heidelberg
Gel documentation system	1. Infinity Video ducumentation system 3000, Peqlab, Erlangen 2. Chemi-Smart 5000, Peqlab, Erlangen
Ice Flakes Device	Scotsman® AF-30, ENODIS Germany GmbH, Herborn
Incubators	1. BBD 6220, Heraeus Instruments, Hanau 2. B5060 EK/CO_2, Heraeus Instruments, Hanau
Luminometer	LUMIStar OPTIMA, BGM Labtech, Offenburg
Magnetic agitator (with heating)	IKA® RCT basic, IKA® RCT labtech, Staufen i.Br.
Microscopes	1. Invers-microscope, Axiovert 25 CFL, Carl Zeiss Jena GmbH, Jena 2. Incident-light microscope, Leica DMLS, Leica Microsystems GmbH, Wetzlar 3. Confocal Microscope, Leica TCS SMD FCS, Leica Microsystems GmbH, Wetzlar
Microtiter-Plate reader	SUNRISE Absorbance Reader, Tecan, Salzburg, Austria
Microwave oven	R-234, Sharp Electronics GmbH, Hamburg
pH meter	SevenEasy ™ , Mettler Toleado GmbH, Gießen
Pipettes	Gilson, Middletown, Wisconsin, U.S
Pipettor	Pipetboy acu, Integra Bioscience AG, Chur, Switzerland
Power supply	Consort Power Supply E835, Pequlab, Erlangen
Refrigerator	1. divers equipment, Liebherr home equipment Ochsenhausen GmbH, Ochsenhausen 2. HERA Freeze®(-80°C), Heraeus Instruments, Hanau
Safety cabinet	HERAsafe classII, Heraeus Instruments, Hanau
SDS PAGE System	1. SE400 Sturdier Vertical Electrophoresis Unit, Hoefer Inc., San Francisco, U.S

	2. PowerEase 500 Pre-Cast Gel System, Invitrogen GmbH, Karlsruhe
Semi-Dry Transfer Unit	Standard Semi Dry Unit, Hoefer Inc., San Francisco, U.S
Shaking devises	1. Vortexter, MS 1 Minishaker, IKA Works Inc., Wilmington, USA
	2. RS-24 (orbital shaker), Lab4You GmbH, Berlin
Sonicator	1. Branson Sonifier B-R, Branson Sonic Power Company, Danbury, U.S.
	2. Sonoplus, Badelin electronic GmbH & Co. KG, Berlin
Thermocycler	1. quantitative RT-PCR: 7900 HT Fast Real-Time PCR System, Applied Biosystems, Darmstadt
	2. Primus 96 advanced® Gradient, Pequlab, Erlangen
Thermomixer	Thermomixer Comfort, Eppendorf AG, Hamburg
UV/Vis Spectrometer	NanoDrop® ND-1000, Peqlab, Erlangen
Vacuum pump	Laboport® N811 KN, 18, KNF Neuberger GmbH, Freiburg
Waterbath	WB/OB 22, Memmert GmbHCo. KG, Schwabach

3.1.2 Expandable material

Blotting paper	Whatman® GB003, GE Healthcare, Dassel
Canula	27G, 0,4 mmx19 mm, BD Biosciences, Heidelberg
Cover slides	Round, Ø12mm, Carl Roth GmbH Co. KG, Karslruhe
Cyro tubes	Cryotubes™, Nunc GmbH Co.KG, Wiesbaden
Disposable inoculation loop	Looplast®, LP ITALIANA SPA, Milan, Italy
FACS tubes	BD Falcon ™ 5 ml polystyrol tubes, BD Biosciences, Heidelberg
Falcon tubes	Cellstar, polypropylen, sterile, Greiner Bio-One GmbH, Frickenhausen
Flat bottom 96 Well plate	PS-Microplate, 96-well, non-sterile, Greiner Bio-One GmbH, Frickenhausen
Luminometer plate	CulturePlate™, white, 96-well, non-sterile, Perkin Elmer, Rodgau-Jügesheim
Nitrocellulose membrane	Whatman® Protan Nitrocellulose Membranes BA83(0,2 µm), GE Healthcare, Dassel
Object plate	Double smoothed, Süße GmbH, Gudensberg
Parafilm	American National Can™, Chicago, US
Pasteur pipettes	WU, Mainz
PCR plate sealing foil	Absolute QPCR Seal, ABgene House, Epsom, UK
PCR-plates	Thermo-Fast®, 96 Detection Plate, ABgene House, Epsom, UK
Petri dishes	Greiner Bio-One GmbH, Frickenhausen
Pipette tips	1. TipOne® , Pippette Tips, Starlab, GmbH, Ahrensburg
	2. TipOne® , Filter Tips, Starlab, GmbH, Ahrensburg
Precast gels	1. Anamed Elektrophorese GmbH, Gross-Bieberau
	2. Invitrogen GmbH, Darmstadt
Reaction tubes	1. Safe Lock, Eppendorf AG, Hamburg
	2. PP-PCR tubes, Greiner Bio-One GmbH, Frickenhausen
Sterile filter	Millex®-GS 0,22 µm, Millipore, Billerica, U.S.
Syringe	BD Discardit II, BD Biosciences, Heidelberg
Tissue flasks	Cellstar, polystyrol, sterile, Greiner Bio-One GmbH, Frickenhausen

Tissue petri-dishes	polystyrol, sterile, Nunc GmbH & Co. KG, Wiesbaden
Tissue plates	Cellstar, polystyrol, sterile, Greiner Bio-One GmbH, Frickenhausen

3.1.3 Purchaseable kits and buffers

Absolute™ QPCR SYBR Green ROX Mix	Thermo Fisher Scientific Inc., Waltham, U.S.
Annexin-V-FLUOS Staining Kit	Roche, Penzberg
BCA™ Protein Assay Reagent Kit	Pierce Biotechnology, Rockford, U.S.
BD OptEIA™ mouse IL-6 ELISA Kit	BD Biosciences, Heidelberg
BD OptEIA™ mouse TNF ELISA Kit	BD Biosciences, Heidelberg
CellTiter-Glo Luminescent Cell Viability Assay System	Promega, Madison, Wisconsin, U.S.
Dual-Glo Luciferase System Assay System	Promega, Madison, Wisconsin, U.S.
FITC-BrdU-Flow Kit	BD Biosciences, Heidelberg
High Pure RNA Isolation Kit	Roche Diagnostics, Penzberg
High Speed maxi Kit	Quiagen, Hilden
High Speed mini Kit	Quiagen, Hilden
NEB 5-alpha	New England Biolabs GmbH, Frankfurt/Main
Platinum®Pfx DNA Polymerase	Invitrogen GmbH, Darmstadt
QIAquick Gel Extraction Kit	Qiagen, Hilden
QIAquick PCR Purification Kit	Qiagen, Hilden
Restore Western Blot Stripping Buffer	Pierce Biotechnology, Rockford, U.S.
RevertAid™ First Strand cDNA Synthesis Kit	MBI Fermentas, St. Leon-Rot
SuperSignal West Pico Chemiluminescent Substrate	Pierce Biotechnology, Rockford, U.S.
Taq DNA Polymerase	MBI Fermentas, St. Leon-Rot

3.1.4 General chemicals

If not stated otherwise, all chemicals and solvents were purchased from Merck (Darmstadt), Roth (Karlsruhe), Sigma-Aldrich (Taufkirchen) or AppliChem (Darmstadt).

4',6-diamidino-2-phenylindole (DAPI)	Molecular probes Inc. Eugene, U.S.
A/G Agarose	Santa Cruz Biotechnology, Santa Cruz, U.S
Acetic Acid (100%)	Merck, Darmstadt
Acetone	Roth, Karslruhe

Acrylamide rotiphenol	Roth, Karslruhe
Adenosine-5'-triphosphate (ATP)	Sigma-Aldrich, Taufkirchen
Agar bacteriological	Agar No. 1, Oxoid GmbH, Wesel
Agarose ultra pure	Gibco BRL, Life technologies^{TM}, Eggenstein
Ammonium Persulfate (APS)	Sigma-Aldrich, Taufkirchen
Ampicilin	Kanamycine
Aprotinin	Sigma-Aldrich, Taufkirchen
Aqua ad iniectabilia (10 ml)	Braun, Melsungen
Bovine serum albumine (BSA)	AppliChem GmbH, Darmstadt
Bromphenole Blue	Sigma-Aldrich, Taufkirchen
Complete Protease Inhibitor Cocktail	Roche, Penzberg
Dimethylsulfoxide (DMSO)	Sigma-Aldrich, Taufkirchen
Dithiothreitol (DTT)	Sigma-Aldrich, Taufkirchen
Doxurobicine	Sigma-Aldrich, Taufkirchen
Dulbecco's modified Eagle's medium (DMEM)	Biochrom AG, Berlin
Ethanol	AppliChem GmbH, Darmstadt
Ethidium bromide	Merck, Darmstadt
Ethylendiaminetetraacetic acid (EDTA)	Sigma-Aldrich, Taufkirchen
FACSClean^{TM}	BD Biosciences, Heidelberg
FACSFlow^{TM}	BD Biosciences, Heidelberg
Fetal calf serum (FCS)	Biowest, Nuaillè, France
Geneticin (G418, 50 mg/ml)	PAA Laboratories, Pasching, Austria
Glycerol	Sigma-Aldrich, Taufkirchen
Glycine	Sigma-Aldrich, Taufkirchen
Hydrogen chloride (37%) (HCl)	Merck, Darmstadt
Immersion oil	Merck, Darmstadt
Indole-3-acetitc acid (IAA)	AppliChem GmbH, Darmstadt
Isopropanol	Roth, Karslruhe
Isopropyl β-D-1-thiogalactopyranoside (IPTG)	AppliChem GmbH, Darmstadt
Kanamycin	AppliChem GmbH, Darmstadt
Leupeptin (-hydrochloride)	Sigma-Aldrich, Taufkirchen
L-Glutamine, 200 mM (100x)	Biochrom AG, Berlin
Luria-Bertani- borth	AppliChem GmbH, Darmstadt
Magnesium chloride-Hexahydrate ($MgCl_2x6H_2O$)	Merck, Darmstadt
Metafectene	Biontex, Munich
Methanol	AppliChem GmbH, Darmstadt
MOPS (3-(N-morpholino)propane sulfonic acid)	Sigma-Aldrich, Taufkirchen
Mounting medium	AF1, Citifluor Ltd., London, UK
N,N,N`, N`-Tetramethylethylethyllendiamin (TEMED)	Sigma-Aldrich, Taufkirchen
Paraformaldehyde	Merck, Darmstadt
Penicilin/Strepromycin solution (100x)	PAA Laboratories, Pasching, Austria
Pepstatin A	Sigma-Aldrich, Taufkirchen
Phenylmethylsulfonylfluorid (PMSF)	Sigma-Aldrich, Taufkirchen

Phosphate buffered saline (PBS)	PAA Laboratories, Pasching, Austria
Phosphatic acid (H_3PO_4)	Merck, Darmstadt
PhosSTOP Phosphatase Inhibitor Cocktail	Roche, Penzberg
Polybrene	Sigma-Aldrich, Taufkirchen
Poly-D-Lysin	Sigma-Aldrich, Taufkirchen
Puromycine	Sigma-Aldrich, Taufkirchen
Roswell Park Memorial Institute 1640 medium (RPMI)	Biochrom AG, Berlin
Sequencing grade modified trypsine	Promega, Madison, Wisconsin, U.S.
Serva Blue G	Serva, Heidleberg
Sodium chloride (NaCl)	AppliChem GmbH, Darmstadt
Sodium hydroxide (NaOH)	Merck, Darmstadt
Sodiumdeoxycholate	Sigma-Aldrich, Taufkirchen
Sodiumdodecysulfate (SDS)	Roth, Karslruhe
Sodiumfluoride (NaF)	Sigma-Aldrich, Taufkirchen
Sodiumorthovanadate (Na_3VO_4)	Sigma-Aldrich, Taufkirchen
Staurosporine	Sigma-Aldrich, Taufkirchen
Thioglycolate	BD Pharmingen, Heidelberg
Tris-Base	Sigma-Aldrich, Taufkirchen
Tris-HCL	Sigma-Aldrich, Taufkirchen
Triton-X-100	Sigma-Aldrich, Taufkirchen
Trypan-Blue	Sigma-Aldrich, Taufkirchen
Trypsin/EDTA (10x)	PAA Laboratories, Pasching, Austria
Tween 20	Sigma-Aldrich, Taufkirchen
β-Mercaptoethanol	Sigma-Aldrich, Taufkirchen

3.1.5 DNA modifying enzymes

BamHI	New England Biolabs GmbH, Frankfurt/Main
NotI	New England Biolabs GmbH, Frankfurt/Main
NotI	New England Biolabs GmbH, Frankfurt/Main
T4-DNA-Ligase	Roche, Penzberg
XhoI	New England Biolabs GmbH, Frankfurt/Main

3.1.6 Stimuli for cell culture

Anti- Trinitrophenol(TNP)-ovalbumin(OVA) -IgE (x100)	N.N. (University Freiburg)
Lipopolysaccharide (LPS)	Sigma-Aldrich, Taufkirchen
Mouse IL-3	ImmunoTools, Oldenburg
Mouse IL-4	ImmunoTools, Oldenburg
Mouse INF-γ	ImmunoTools, Oldenburg
TNP-OVA (2μg/μg)	N.N. (University Freiburg)

3.1.7 Antibodies and isotypes

Antibody	Target species	≈kDa	Details (dilution, isotype)	Company
Anti-mouse IgG, HRP-linked Antibody (heavy chain)	Secondary		1:1000	Cell Signalling Technology, Danvers, U.S.
Anti-rabbit IgG, HRP-linked Antibody (heavy chain)	Secondary		1:1000	Cell Signalling Technology, Danvers, U.S.
APC-CD123	human		as prescribed by Mouse IgG_1 κ	eBioscience, Frankfurt
Cofilin-1	human, mouse	20	Detection 1:1000 IP 1µg	Cell Signalling Technology, Danvers, U.S.
FITC-CD4	human		as prescribed by Mouse IgG_1 κ	BD Biosciences, Heidelberg
FITC-FcεRI,	mouse		as prescribed by	eBioscience, Frankfurt
FITC-pSTAT1 (Y701)	human, mouse		as prescribed by Mouse IgG_{2a}, κ	BD Biosciences, Heidelberg
FTIC-pSTAT5 (Y694)	human, mouse		as prescribed by Mouse IgG_{2a}, κ	BD Biosciences, Heidelberg
Green Fluorescent Protein (GFP)	tag	20	Detection 1:1000 IP 1 µg	Santa Cruz Biotechnology, Santa Cruz, U.S
Hemaglutinin (HA)	tag	5	1:1000	Santa Cruz Biotechnology, Santa Cruz, U.S
N-DYKDDDDK-C (FITC-FLAG)	tag	9	Detection 1:1000 IP1:100	Sigma-Aldrich, Taufkirchen
$p21^{cip1}$	mouse	20	1:1000	Cell Signalling Technology, Danvers, U.S.
$P27^{Kip1}$	mouse	30	1:1000	Santa Cruz Biotechnology, Santa Cruz, U.S
PE-CD123	mouse		as prescribed by Rat IgG_{2a} κ	eBioscience, Frankfurt
PE-c-Kit, CD117	mouse		as prescribed by	eBioscience, Frankfurt
pSTAT1 (Y701)	human, mouse	90	1:1000	Cell Signalling Technology, Danvers, U.S.
pSTAT5 (Y694)	human, mouse	90	1:1000	Cell Signalling Technology, Danvers, U.S.
PTP-1B	human, mouse	50	1:1000	Abcam, Cambridge, UK
RhoH-Serum	murine	20	Detection 1:200 IP N.N.	Eurogentec, Seraing, Belgium
STAT1	human, mouse	90	Detection 1:5000 IP: 1µg	Santa Cruz Biotechnology, Santa Cruz, U.S.

STAT5	human, mouse	90	Detection 1:5000 IP: 1µg	Santa Cruz Biotechnology, Santa Cruz, U.S
β-Actin	human, mouse	45	1:1000	Cell Signalling Technology, Danvers, U.S.
MCPt-1	mouse	36	1:1000	Abcam, Cambridge, UK

*Isotypes for FACS Analysis

Isotypes used in this work were purchased from the same company which provided the target antibody, labelled in the same fashion and were used in the same concentration as target antibody.

3.1.8 Size markers

3.1.8.1 Protein marker

P7711S ColorPlus Prestained Protein Ladder, Broad Range (10-230 kDa)

New England Biolabs GmbH, Frankfurt/Main

161-0324 Kaleidoscope Prestained Standart, Bio-Rad Laboratories, Hercules, U.S.

3.1.8.2 DNA marker

Depending on the expected size of the analysed DNA fragements, different DNA marker ranges were used. If not otherwise stated, markers were purchased from New England Biolabs GmbH, Frankfurt/Main or MBI Fermentas, St. Leon-Rot.

3.1.9 Vectors

Plasmid name	**Basic vector**	**Describtion**	**Source**
pGEX-2T-GST-RhoH pGEX-2T-GST-T36A pGEX-2T-GST	pGEX-2T	bacterial expression vector, amp resistance, IPTG inducible promoter, GST-tag	Institute for Experimental and Clinical Pharmacology and Toxicology, University Freiburg
pMX-IRES-GFP-HA-hRhoH pMX-IRES-GFP-mRhoH-flag)	pMX-IRES-GFP (PIG)	mammalian, retroviral, amp resistance	Institute for Experimental and Clinical Pharmacology and Toxicology, University Freiburg
pMX-IRES-CD4-PURO-mRhoH-flag	pMX-IRES-CD4-PURO	mammalian, retroviral, amp resistance, puromycin	generated by D. M.

pMX-IRES-CD4-PURO		selection gene	
p-EGFP-N1-Cofilin-1	p-EGFP-N1	CMV promoter, amp. resistance	Institute for Immunology, University Heidelberg
BSSK-ptp1b	Blue-Scripe-KS^{+}	Amp. resistance	Addgene, Cambridge, U.S
pSilencer-RhoH	pSilencer-Retro 5.1 U6	Amp.Resistance, puromycin selection gene	Ambion, Austin, USA

3.1.10 Oligonucleotides

All oligonucleotides were obtained from MWG Biotech, Eberberg or Apara Bioscience GmbH, Sexau/Freiamt.

3.1.10.1 Primer sequences for quantitative real-time PCR (qPCR)

To avoid amplification of genomic DNA primer for qPCR, primers were chosen according to their intron / exon boundaries.

Gene	**species**	**Sequence 5`→3`**
GAPDH	human	fw ACGGATTTGGTCGTATTGGGC
		rv TTGACGGTGCCATGGAATTTG
GAPDH	mouse	fw TTCACCACCATGGAGAAGGC
		rv GGCATGGACTGGACTGTGGTCATGA
Interleukin-2	human	fw AACTCACCAGGATGCTCACATTT
		rv TTAGCACTTCCTCCAGAGGTTTG
IRF-1	human	fw GCTGGACATCAACAAAGGAT
		rv TGGTCTTTCACCTCCTCGAT
IRF-1	mouse	fw GGAGATGTTAGCCGGACACT
		rv TGCTGACGACACACGGTGA
p21	mouse	fw GCAGACCAGCCTGACAGATT
		rv GCAGGCAGCGTATATACAGGA
p27	mouse	fw AGGGCCAACAGAACAGAAGA
		rv CTCCTGGCAGGCAACTAATC
RhoH	human	fw GACTTCGGCACAGGAACTTGCTT
		rv GCA AGA GCT CGATATTTGGTTATTAT
RhoH	mouse	fw GCTACTCTGTGGCCAACCAT
		rv AGGTCCCACCTCTCTCTGGT
β-Actin	human	fw AGCTACGAGCTGCCTGAC
		rv AGCACTGTGTTGGCGTACAG
TCR beta	human	fw 1 CAGGAT AGG GCC AAACC
		fw 2 GTGTTTGAGCCATCAGAAGC
		rv CACGAGGGCACTGACCAG

3.1.10.2 Primer sequences for genotyping

Name	Sequence 5`→3`
Rh1	fw GTG TAC GAG AATACGGGTGT
Rh2	rv GTGGCCACAACCAGCACC
Rh4	fw CTTGTGTAGCGCCAAGTGC

3.1.10.3 Primer sequences for gene mutation, sequencing and cloning

plasmid / gene	primer	Sequence 5`→3`
PIG	rv IRES-3	CCAACTTAATCGCCTTGCAGCA
PIG-RhoH	fw BamHI-RhoH	GATGCTGGATCCATGCTGAGCTCAA
PIG	rv IRES EcoRI-mRhoH	CGAGGAATTCGTTAGAAGATCTTGCA
RhoH	fw RhoH-T36A	GCCTACAAACCCGCGGTGTACGAGAAT
RhoH	rv RhoH-T36A	ATTCTCGTACACCGCGGGTTTGTAGGC
PIG-HA	rv PIG-HA	GAC CAC CCC ACC GCC CTC AAA GTA GAC GG
PIG	fw MX6	CGC CTC GAT CCT CCC TTT ATC
PIG	rv pMX HindIII	TGT CTT CAA GAA GCT TCC AGA GGA

3.1.11 Eukaryotic cells

Cell lines were either obtained from DSMZ (German Resource Centre for Biological Material), ATCC (American Tissue Culture Collection), or were generously provided by the Megan Lim lab, (Ann Arbor, Michigan).

Name	Origin	Culture Medium
BaF3	Murine pro-B cell line	RPMI/10%FCS (not heat inactivated)/1% PS/ 1-0,5% IL-3 containing supernatant
DEL	human	RPMI/1%PS/10% FCS
FL-18	Human B-cell B-NHL	RPMI/1%PS/10% FCS
FL-518	Human B-cell B-NHL	RPMI/1%PS/10% FCS
Granta 519	Human B-cell Mantle cell	RPMI/1%PS/10% FCS
HEK293	Human Embryonic Kidney	DMEM/1%PS/10% FCS
HH	Human T-cell CTCL	RPMI/1%PS/10% FCS
HUT78	Human T-cell CTCL	RPMI/1%PS/10% FCS
Jurkat	Human T-cell	RPMI/1%PS/10% FCS
Karpas 299	Human T-cell ALCL	RPMI/1%PS/10% FCS
KG-1	Human AML	RPMI/1%PS/10% FCS
KG-1a	Human AML	RPMI/1%PS/10% FCS
Mac2A	Human T-cell ALCL	RPMI/1%PS/10% FCS
NCEB	Human B-cell Mantle cell	RPMI/1%PS/10% FCS
OCI-LY1	Human B-cell B-NHL	RPMI/1%PS/10% FCS
Phoenix-Eco	Human Embryonic Kidney (packaging cell line)	DMEM/1%PS/10% FCS
SKW-3	Human	RPMI/1%PS/10% FCS
SR-788	Human	RPMI/1%PS/10% FCS

SUDHL-1	Human	RPMI/1%PS/10% FCS
SUDHL-4	Human B-cell B-NHL	RPMI/1%PS/10% FCS
SUDHL-6	Human B-cell B-NHL	RPMI/1%PS/10% FCS
SUPM2	Human	RPMI/1%PS/10% FCS
THP-1	Human AML	RPMI/1%PS/10%FCS
X63Ag8-653	Murine myeloma cells	RPMI/1%PS/10%FCS/ 2 mM L-Glutamin, $1x10^{-5}$M β-Mercaptoethanol

3.1.12 Special software & databases

Name	**Application**
BioProfile	Western-blot spot quantification
Clustal W	Gene search and Alignments
Ingenuity	Pathway Analysis Software
Mascot	Protein identification based on MS data
Primer 3	Primer search
Serial Cloner	Molecular biology software
Weasel	FACS data analysis

3.1.13 Buffers and working solutions

10 x TNE Buffer	100 mM Tris, 2 M NaCl, 10 mM EDTA, pH 7,4
Bacteria Lysis Buffer	20 mM Tris-HCl (pH 7,4), 10 mM NaCl, 5 mM $MgCl_2$, 1% Triton X-100 (not for MS), 5 mM DTT, Protease Inhibitors
Buffer	Contents
Coomassie-Staining solution	1,25 g Coomassie Brilliant Blue R-2510, 227 ml methanol, 46 ml acetic acid (96%), aqua bidest. ad 500 ml
Destaining-Solution	150 ml acetic acid (96% v/v), 100 ml Methanol, aqua bidest. ad 2 l
ELISA substrate	3,3',5,5'-Tetramethylbenzidine (TMB)
ELISA wash Buffer	PBS, 0,05% Tween 20
ELISA-Block-Buffer	PBS/ 10%FCS
ELISA-Coating-Buffer	0,1 M Na_2CO_3, pH 9,5
ELISA-Stop Solution	1 M H_3PO_4, 1 mM H_2SO_4
Ethidium Bromide Solution	10 mg/ml ethidium bromide in H_2O
FACS Washing/Blocking Buffer	PBS / 2% FCS
Freezing medium	10% (v/v) DMSO, 90% (v/v) FCS
Gluthation Elution Buffer (10 ml)	1 M Tris (pH8), 5 M NaCl,, 0.001 % β-mercaptoethanol, 0.0301 g Gluthatione , pH 7- pH 8
GST-Fish Buffer	150 mM NaCl, 50 mM Tris-HCl (pH 7.4), 5 mM $MgCl_2$, 1 mM EDTA, Protease Inhibitors

HAA Lysis Buffer	0.5% (v/v) Triton X-100
HAA-Stop-Solution	0.2 % (w/v) glycine, pH (10,7)
HAA-Substrate Buffer	3.8 mM p-Nitrophenyl-glycNAc 4-Nitrophenyl N-acetyl-β-D-glucosaminide, 0.05 M tri-sodiumcitrate-dihydrate, pH 4.5
High Salt Buffer	240 mM NaCl, 20 mM HEPES (pH 7.9), 10 mM KCl, 1.0 mM EDTA, 10 % Glycerol (v/v), 0.2% NP40 (v/v), Protease Inhibiotrs
Hypotonic Buffer	20 mM HEPES (pH 7.9), 10 mM KCl, 1.0 mM EDTA, 10 % Glycerol (v/v), 0.2% NP40 (v/v), Protease Inhibiotrs
Membrane-Blocking Buffer	3% (w/v) BSA, 0.1 % (v/v) Tween 20, solubilised in 1x TBS
MS- Lysis Buffer (mammalian cells)	150 mM NaCl, 50 mM Tris-HCl (pH 7.4),5 mM $MgCl_2$, 1 mM EDTA, Protease Inhibitors
NP-40 Lysis Buffer (2x)	2% NP-40, 300 mM NaCl, 40 mM Tris (pH 7.4), 20 mM NaF, 2 mM EDTAx2 H_2O (pH 8), 2mM MgCl2x6 H_2O, 2mM Na_3VO_4, 20% Glycerin, Protease/Phosphatase Inhibitors
PBS	8 g NaCl, 1.78 g KCl, 1.15 g $Na_2HPO_4 \times 2\ H_2O$, 0.2 g KH_2PO_4 aqua bidest ad 1000 ml, pH 7,5
PonceauS-Solution	0.15 % (w/v) PonceauS, solubilised in 0.5 % (v/v) acetic acid
Protein Sample Buffer (4x)	200 mM Tris-Hcl (pH 6,8) , 8% SDS (w/v), 40% Glycerol (v/v), 0,02% (w/v) Serva Blue G 2% (w/v), 20% (v/v) β-Mercaptoethanol
RIPA Lysis Buffer	50 mM Tris, HCl (pH 7,4), Igepal 1% (v/v), Sodiumdeoxycholate 0.25% (v/v), 150 mM NaCl, 1 mM EDTA, Protease/Phosphatase Inhibitors
Running Buffer MOPS (Novex) (20x)	1 M MOPS, 1 M Tris-Base, 69,3 mM SDS, 20,5 mM EDTA; pH 7,7
SDS- Stacking-Buffer (2x)	250mM Tris-Hcl (pH 6.8), 0.2% (w/v) SDS
SDS-Separation-Buffer (3x)	1.125 M Tris-Hcl pH (8.8), 0.3% (w/v) SDS
TAE Buffer (50x)	2 M Tris-Acetate (pH 8.0), 100 mM EDTA
Tail-Lysis-Buffer	100 mM Tris (pH 8), 5 mM EDTA, 0.2% SDS, 200 mM NaCl, 10 mg/ml Proteinase K
TBS (Tris buffered saline) (10x)	100 mM Tris-HCl (pH 8.0), 1.5 M NaCl
TBST (Membrane Wash Buffer)	0.1% (v/v) Tween 20 in 1x TBS
TE(Tris-EDTA)- Buffer	10 mM Tris-HCl (pH 8.0), 1 mM EDTA
Transfer Buffer	25 mM TRIS, 192 mM Glycin, 0.5 mM Na_3VO_4, 10% Methanol (v/v), 0,1 % SDS (10%) (v/v)
Tris-Glycine Running Buffer (10x)	0.25 M Tris, 1.92 M Glycin, 1% SDS (w/v); pH 8.25
Tyrode Buffer	137 mM NaCl, 2,7 mM KCl, 11.9 mM $NaHCO_3$, 0.3 mM NaH_2PO_4, 5.6 mM D(+) Glucose, 1 mM $MgCl_2$ x 6 H_2O, 2 mM $CaCl_2$ x $6H_2O$, 2% FCS

3.2 Methods

3.2.1 Eukaryotic cells

3.2.1.1 Murine bone marrow preparation and mast cell differentiation

Bone marrow cells (BMCs) were isolated from murine femurs of BL6 mice. The cells were rinsed from the bone using RPMI medium, washed once with PBS and then cultivated in RPMI medium containing 1-0.5 % IL-3 supernatant from X63Ag8-65, 20% heat inactivated fetal calf serum and 0,1 μM β-mercaptoethanol. Cells were obtained in culture for 3-4 weeks to allow differentiation into murine MCs. To avoid impurities and growth of adherent fibroblastic cells, growth surface was changed once a week during differentiation by carefully collecting cells containing supernatant. After differentiation MC maturation was controlled by analyzing FceRI and c-Kit expression, after activation of MCs with 1.0 % IgE stimulation (overnight or at least 6 hours).

3.2.1.2 Cultivation of mammalian cells

Mammalian cells were cultivated in incubators at 37°C, 5% CO_2, in humidified atmosphere. Suitable centrifugation for tissue culture was at room temperature (RT), 3 min. at 1300 rpm. Mammalian cells were cultivated in media with appropriate supplements (as described in section 3.1.11) and passaged in ratios recommended by the cell line distributers, Deutsche Sammlung von Mikroorganismen und Zellkulturen (DSMZ) and/or American Type Culture Collection (ATCC). For cell passaging, supernatant covering adherent monolayer was removed. Cells were washed once with pre-warmed PBS (37°C) and covered with an appropriate amount of Trypsin-EDTA solution. The protease trypsin digests peptide bonds, leading to the loss of the adherent cell assembly. Ethylenediaminetetraacetic acid (EDTA) is supporting this process by binding metal ions, required for the formation of cell clusters. Trypsin digestion was stopped after 5 minutes (min) by addition and resuspension with fresh growth medium in a ratio 1:10 regarding trypsin amount. From this cell suspension cell seeding was performed.

3.2.1.2.1 IL-3 dependent cell lines

The IL-3 dependent cell line BaF3 was cultivated in RPMI medium containing 10% FCS (not heat inactivated) and 1-0.5% IL3 containing supernatant from X63Ag8-653 cell line.

3.2.1.3 IL-3 production with X63Ag8-653 cells

As shown previously by Fritz Melcher`s lab, transformation with a bovine papilloma virus-based expression vector pBV-IMTHA of X63Ag8-653 cells allows these cells to stably express copies of murine IL-3 and to secrete this in high amounts and quality [103]. For this work X63Ag8-653 cells were cultivated in medium containing 0.3 mg/ml G418 to select for transfected cells. After confluent expansion of cells on approximately (approx.) 20 petri dishes, cells were washed with PBS to remove any remaining G418 and distributed for two daysin a ratio lower than 1:2 on 30 petri dishes. Cells were kept in culture for further 48 hours (h), then the supernatant was collected and aliquots of appropriate volumes were prepared. Aliquots were stored at -20°C until usage.

3.2.1.4 Cell counting

Cell counting was accomplished using a Neubauer-cell counting chamber. 10 µl cell suspension was mixed with 90 µl Trypan Blue which allowed exclusion of non-vital cells during count.

3.2.1.5 Cryo-conservation of mammalian cells

Approximately $1x10^6$ cells were spun down; pellet was resuspended in 1 ml Freezing medium and transferred to a fresh cryo tube. The tube was immediately placed into a pre-cooled isopropanol containing “Mr. Frosty” freezing device and stored for 24 h at -80°C. After this time period, cryo tubes were transferred into liquid nitrogen containing cell storage container.

3.2.1.5.1 Recultivation of mammalian cells

Cells were thawed at 37°C and immediately transferred to 9 ml pre-warmed growth medium. After spinning down, supernatant was discarded and the cell pellet was resuspended in 10 ml fresh, warm growth medium and cultivated for 24 hours in a T25 tissue flask. The next day, growth medium again was changed to remove any toxic remains of the freezing medium.

3.2.1.6 Liposome-based transfection of mammalian cells

To obtain altered target gene protein expression or in order to produce viral supernatants, cells need to be transfected with expression vectors.

To transfect adherent human embryonic kidney (HEK) or Phoenix-eco cells, cells were seeded out at desirable scale 24 hours prior to tranfection and either Metafectene or Lipofectamin was used, according to the manufacturer's instructions. To obtain optimal protein expression, cells were allowed to further incubate for 24-72 hours.

THP-1 cells were transfected using Metafectene and an adapted form of the manufacturer's transfection protocol. $1x10^6$ cells/well (6-well) were seeded 24 h prior to transfection. A DNA: Metafectene ratio of 1:4 was used, cells were allowed to incubate 48 h post transfection.

3.2.1.7 Retrovirus production

To stably transduce BaF3 cells, it was required to use retroviral gentransfer in order to deliver target gene expression in the cell line. The Phoenix-eco packaging cell line is based on the 293T cell line. Transfection of this cell line is highly efficient using liposome-based methods. The cell line was created by insertion into 293T cell constructs capable of producing gag (proteins of the virus nucleus) –pol (reverse transcriptase and integrase), and envelope (hill) protein for ecotropic (Phoenix-"eco") viruses. This cell is capable of carrying episomes for long-term stable production of retrovirus. In order to produce virus particles, the cell line has to be transfected with retroviral vectors containing 5`and 3` the "packaging-signal" long-terminal-repeat. This retroviral vector also contains the target gene which needs to be stably transferred into the BaF3 cell line. Transfection with a retroviral vector enables the Phoenix-eco cell line to produce "safe" virons which are able to stably infect cells but which are not able to induce their own reproduction in the host-cell line. To obtain high virus titer, Phoenix-eco cells are seeded 24 hours prior to transfection in a ratio 1:4 after trypsin proteolysis (as described above) [104] into a 6-well plate. 70-80% confluent cells were transfected using the appropriate retroviral vector containing the desirable target gene. 48-72 hours post transfection, virus-containing supernatant was collected and stored for at least two hours or until usage at -80°C.

3.2.1.7.1 Retroviral infection and puromycine selection

In order to retroviral transduction of BaF3 cells, the virus must enter the host-cell to be able to properly integrate viron information into the host genome.

$5x10^5$ BaF3 cells were resuspended in 850 µl of freshly thawed virus supernatant. After addition of 16 µg/ml polybrene, cells were spun for 2 h at 37°C. After this time period, cells were resuspended in fresh growing medium and transferred into a T25 flask and checked for protein expression after 48 h. For selection antibiotics (puromycin 1.5 ng/ml) were added after 48 h and cells cultivated for 48 hours to ensure that only successfully transfected cells remained.

3.2.1.8 Proliferation assays

To investigate the time dependent proliferation rate changes in response to equal doses of cytokine over time, a proliferation assay was performed. $2.5x10^5$ BaF3 cells were seeded out in 2 ml of growth medium containing equal amounts of cytokine. Cells were counted every day using a Neubauer-counting-chamber until cells reach saturation of proliferation (approx. after five days). For Cell Titer Glo (CTG) assay starved (3 h) cells were seeded out in appropriate numbers and stimulated with IL-3 (indicated time/concentration) ATP measurements were performed according to manufacturer`s instructions.

3.2.1.9 Survival assay

To check for changes in resistance to cytokine deprivation $5x10^5$ BaF3 cells were washed three times with PBS and seeded out in 2 ml of RPMI Medium containing 10% bovine serum albumin (BSA). Cells were counted and stained with focus on declining viability rates. Immediately after reaching theoretical limit of viability (less than $1x10^4$ vital cells), cells were spun and taken up in fresh growth medium containing IL-3.

3.2.1.10 Cytospins

Prelabeled glass slides were placed onto the rubber inlay of the metal holder. 200 µl of single cell solution (approx. $0.5x10^6$ cells/ml) was loaded in a cytospin cuvette. By centrifugation at 1300 rpm for 5 min, cells were absorbed onto the glass surface. Remaining liquid was carefully removed and the cells were washed once with 500 µl PBS. After centrifugation, the supernatant was removed. Cells on the glass surface were fixed for 20 minutes (min) with 0.4 % paraformaldehyde (PFA) containing PBS at room temperature (RT). After two additional PBS wash steps, cells were stained according to manufacturer`s protocol.

3.2.2 Prokaryotic cells

The gram negative bacterium *Escherichia coli* (*E. coli*) was used as host for the production of plasmid DNA and recombinant eukaryotic proteins. Bacterial growth was determined by photometric measurement of the optical density (OD) of bacterial cell suspension versus growth medium. Measurement was performed at a wavelength of 600 nm in a plastic cuvette (1cm).

3.2.2.1 Cultivation and storage of *E. coli*

Bacteria were either cultivated on solid growth Luria-Bertani broth (LB) medium (LB-Agar) or in liquid LB media (inoculated with a single colony), containing the appropriate antibiotics in sufficient amount. In the case of ampicilin resistance ampicilin concentration of 100µg/ml was used. For plasmid DNA, cells were then cultivated overnight between 14-16 h at 37°C. For protein expression, overnight culture was used for inoculation of (6 litre/RhoH, 6 litre/RhoH-T36A, 1 litre/GST) growth medium in a ration of 1:10 and cultivated for approx. 3 h until optical density (OD) of 0.9 was reached. Kryo-conservation of bacterial culture was obtained by mixing of 500 µl overnight cultured bacteria suspension with 500 µl of sterile glycerol (80%) and storage at -80°C.

3.2.2.2 Preparation of competent *E. coli* cells

In order to enable exogenous DNA uptake of bacterial cells, *E. coli* were chemically treated with calcium chloride solution. Bacterial cell membrane is permeable to chloride but non-permeable to calcium ions. Water molecules accompany the charged chloride ions upon entrance into the cell, resulting in swelling. This uptake of water is necessary for the introduction of plasmid DNA. Competent cells were prepared by inoculation of 50 ml antibiotic free LB medium with a single colony of freshly grown *E. coli* from LB-agar plate. The bacteria suspension was incubated at 37°C until OD of approx. 0.5 was reached. The culture was centrifuged at 4000 rpm for 10 min at 4°C. After discarding the supernatant, the pellet was resuspended in 2 ml of 0.1 M calcium chloride solution. After adding 0.4 ml of Glyerol, 50 µl aliquots of competent cells were stored at -80°C until usage.

3.2.2.3 Bacterial cell transformation

Transformation represents an efficient method to introduce exogenous DNA molecules into competent bacterial cells. The calcium chloride solution in the aliquots of the previously

prepared competent bacteria cells along with an induced heat shock after DNA supplement supports the uptake of the plasmids. Competent cells were thawed on ice. 10 µl of ligation reaction or plasmid DNA between 50 ng and 1 µg was added to the bacteria with gentle mixing, and then incubated on ice for 10 min . Cells then were heat shocked for 2 min at 37°C and incubated for further 5 minutes on ice and transferred into preheated liquid LB medium (37°C, without antibiotics) and incubated for 20 min at 37°C. This step allows bacteria to recover from the treatment and leads to an increase in the number of clones carrying the antibiotics resistance. Bacteria were then pelleted by centrifugation (10000 rpm/ 30 sec). Supernatant was discarded and bacteria were resuspended in the remaining LB medium in the tube and streaked onto a LB-agar plate, containing appropriate antibiotics.

3.2.2.4 Recombinant protein expression

The *E.coli* strain BL-21 was used for protein expression. Bacterial cells were freshly transformed with the GST-2T expression vectors containing the appropriate gene variation of RhoH (wt RhoH, RhoH T36A) and streaked onto antibiotic containing agar plates. After overnight incubation at 37°C, a single colony was used for inoculation of an overnight liquid culture. The next day this overnight liquid culture was transferred in the ration 1:10 in new growth medium and was allowed to grow to an OD of approx. 0.9. Expression of recombinant proteins was induced by the addition of 0.2 to 1 mM isoprypylthio-β-D-galactoside (IPTG). Binding of IPTG inactivates the lac repressor which leads to the expression of downstream regions. Optimal expression temperature, time and IPTG concentration can vary depending on the expressed protein. In the case of wt RhoH and RhoH-T36A expression, 600 ml overnight culture was scaled up to 6 litres. The expression of the tag protein GST was scaled up 1:10 to 1 litre volume. IPTG was added in a concentration of 1 mM and expression proceeded for 4 to 5 hours at 37°C. Cells were pelleted by centrifugation (4°C, 4000 rpm, 15 min, GSA rotor, Sorvall). Bacterial pellets were washed one time with PBS and either used directly for lysis or were stored at -20°C. Bacteria pellets were resuspended with suitable bacteria lysis buffer containing protease inhibitors (Roche Protease Inhibitor Mix). Cells were then lysed by sonication on ice, for 3x pulses of 40 seconds (amplitude 42 %) with a break of 10 seconds after each pulse. The lysate was cleared by centrifugation for 30 minutes at 15,000 rpm (SS34 rotor, Sorvall®) and the resulting supernatant was used for affinity chromatography.

3.2.3 Molecular biological techniques

3.2.3.1 Genomic DNA extraction from mouse tail biopsy

For genomic DNA extraction, (approx. 0.5 cm) tail biopsies of four to five week old mice were used. Each tail was incubated overnight in 710 µl of "Tail-Buffer" supplemented with 10 mg/ml Proteinase K. After digestion, tubes were mixed for 5 min, after which 250 µl of 5 M NaCl was added and the tubes were mixed again. Samples were centrifuged down at 14,000 rpm/5 min/RT to remove tail debris. Supernatant was transferred to a new tube and DNA was precipitated using 550 µl Isopropanol. After vigorous shaking for 2 min, samples were again spun down for 5 min (14000 rpm at RT). The DNA pellet was washed with 70% Ethanol and centrifuged at same conditions. After discarding supernatant, pellet was air-dried for 10 minutes and finally resuspended in 100-200 µl 1x TE-Buffer or ddH_2O and incubated for at least two hours at 37°C.

3.2.3.2 Purification of plasmid DNA

Methods and Kits for Plasmid purification were dependent upon the required amount of DNA for each respective experiment. Large and small amounts of Plasmid DNA were obtained by usage of Qiagen Plasmid Maxi- Kit and Mini-Kit (Quiagen, Hilden) and PureYield Plasmid Midiprep System (Promega, Mannheim) was used for intermediate amounts of plasmid DNA. Qiagen Gel Purifcation Kit (Quiagen, Hilden) was also used for preparative DNA purification from agarose gel slices. PCR products were purified with PCR-Purification Kit (Promega, Mannheim). The preparation was performed according the manufacturer`s instruction. The underlying principle for the plasmid purification is based on a modified alkaline lysis procedure, followed by binding of plasmid DNA to an anion exchange matrix under appropriate low-salt and pH conditions. Washing the matrix with a medium salt buffer removes RNA, protein, and other impurities. In the final step, nuclease-free water is used to elute bound DNA from the matrix. Long-Term storage of DNA was kept at -20 °C.

3.2.3.3 DNA quantification

DNA concentration was determined using the Nano-Drop Spectrometer by measuring the absorption maximum of double stranded DNA at 260 nm. Potential contaminants, such as proteins and single stranded DNA particles, have an absorption maximum of 280 nm, the ratio of OD at 260 nm and 280 nm is a parameter describing the purity of the DNA sample. Ratios between 1.8 and 2.0 indicate pure DNA.

3.2.3.4 Restriction enzyme digestion

Restriction enzymes recognize and cut double stranded DNA at specific sites, also called restriction sites. Restriction sites are often composed of 4 to 8 palindromic nucleotides. Depending on the type of DNA processing enzyme, the resulting fragment can either have "sticky ends" which are overlapping ends that can be religated or "blunt ends" which result in a smooth cut that usually prevents religation of the DNA. According to manufacturer's instructions, the DNA (5-10 µg preparative digestion, 0.5-2 µg analytic digestion) was incubated with the appropriate buffer system with or without BSA and the chosen restriction enzymes at the optimal concentration at 37°C for 1 to 2 hours. If double digestions were not possible, sequential digestion after the DNA precipitation step was performed.

3.2.3.5 Polymerase chain reaction (PCR)

Defined DNA fragments of a DNA template were amplified by using PCR with appropriate oligonucleotide primer pairs. These oligonucleotides are complementary to the DNA sequence and are defining the starting region of the region to be amplified. The 5` prime sites of oligonucleotides used for the replication of vector gene inserts normally contain restriction sites for further cloning of the PCR product. Thermostable polymerases were used to perform PCR reactions. The PCR reaction takes approx. 30 cycles comprised of a denaturation step performed at 95°C (30 sec) , a primer annealing and elongation step at 60° to 65°C (2 min) and the final elongation step (4-7 min at 72°C). The resulting PCR product was analysed with agarose gel electrophoresis. Depending on the following procedure the whole reaction was either directly purified using a PCR purification kit, or first separated with agarose gel electrophoresis and isolated from the gel matrix using a gel-purification kit. Isolated DNA fragments were either used for another PCR reaction or digestion to their included restriction sites.

3.2.3.5.1 PCR based site directed mutagenesis

A standard mutagenesis PCR was performed using the Pfx DNA polymerase kit (Invitrogen, Darmstadt) and performed according to manufacturer's instructions. A template concentration between 10 pg and 200 ng was appropriate for optimal results. A standard program was used starting with a DNA denaturation step at 95°C (2 min) followed by 35 cycles of DNA amplification:

94°C 30 sec

60°C 2 min

72°C 4 min

The reaction was finished with an elongation step of 10 min at 72°C. DNA was stored until usage at either 4°C or -20°C.

3.2.3.5.2 Genotyping PCR

Mice were genotyped using a touchdown PCR. This form of PCR is used to prevent the amplification of nonspecific products. For this type of PCR, a primer annealing temperature just below the optimum is used to allow binding of only highly specific primer sequences to the DNA. To distinguish RhoH genotypes of mice, two different PCRs were set up. The "wild-type (wt) detection" PCR reaction contained the primer Rh1 (located within the RhoH coding region) and Rh2 (located outside of RhoH coding region) which amplified a 240 base pair (bp) product. This product represented the wt allele. The "knockout (ko) detection" PCR contained primer Rh2 and Rh4 (located within the neomycin resistance cassette) and an amplification product of 325 bp resulted. The genotypes were analysed after agarose gel electrophoresis. Heterozygote and homozygote wt mice reacted positive for the Rh1+Rh2 PCR, no product was detectable for homozygote KO mice. In the Rh2+Rh4 PCR, no product was detected for homozygote wt mice. For genotyping mice, the Fermentas (Fermentas, St. Leon-Rot) Taq DNA Polymerase kit was used. For the reaction, 2 µl of 10x PCR buffer was mixed with 50 mM $MgCl_2$, 10 mM dNTPs, 100 pmol/µl primer and 5 U/µl Taq polymerase. Template DNA was added to a maximum concentration of 200 ng. Finally, the reaction mixture was diluted to a final volume of 20 µl with ddH_2O. A touch down PCR program from 65 to 55°C was used. The standard program started with a DNA denaturation step at 95°C (3 min) followed by 9 cycles of DNA amplification:

95 °C 30 sec

54 °C 30 sec

72 °C 30 sec

Followed by a second amplification cycle with 35 repetitions:

55 °C 30 sec

72 °C 30 sec

The reaction was finished using an elongation step of 10 min at 72°C. DNA was stored until usage at either 4°C or -20°C.

3.2.3.5.3 Quantitative real-time PCR

To avoid contaminations with genomic DNA, DNases or RNases all preparative steps were performed with the usage of gloves, RNase and DNase free tips and tubes. To quantify target gene expression on mRNA levels, target gene-specific primers and the Absolute qPCR SYBR green ROX mix (Thermo-Fisher, Waltham, U.S.) was used to analyse template cDNA. The 2x PCR mixture contains a Thermo-Start DNA polymerase which prevents non-specifc amplification during the reaction. To activate this enzyme, an initiate PCR step of 95°C for 15 min was required. The mixture contains the proper reaction buffer system including optimized $MgCl_2$ concentrations and PCR enhancers to improve amplification rates, dNTPs, and the intercalating cyanid fluorescent SYBR Green I. This dye fluoresces after binding to the newly synthesised double stranded DNA .The detected overall fluorescence increases proportionally to the increasing concentration of double stranded DNA. The passive reference dye ROX was also supplied to the reaction mixture and was used by the PCR apparatus to normalise detected SYBR Green signals. The term real-time PCR refers to the measurement of the fluorescence signal after each PCR cycle which, in contrast to end-point measurements, allows the monitoring of gene amplification in real-time. The data is measured at the exponential phase of the PCR reaction, which is the optimal time point to analyze data. 2.5 ul of template cDNA, 12.5 pmol of forward and reverse primer, and 12.5 ul of SYBR Green Rox mixture were used for each 25 µl PCR reaction. PCR reaction and signal detection were performed in the 7900 HT Fast Real-Time PCR System (AB Applied Biosystems, Darmstadt) in a 96-well format (program: 95°C (15 min); 40x [95°C, 15s, 60°C; 1min]). Measurements were usually performed in duplicates. Automatic detection of baseline and threshold values was used and the determined Ct values were subtracted from the Ct values of an endogenous constitutively expressed reference gene (GAPDH) resulting in a ΔCt for each target gene. Relative expression (rE) was calculated as rE=1/2 DCt and PCR reactions were verified for similar efficiencies. For reaction specificity, “no reverse transcriptase” and “no template” controls were performed with each reaction. Additionally, the dissociation curves of each target gene were determined.

3.2.3.6 RNA isolation

To isolate RNA for further procedures including cDNA synthesis, the High Pure RNA isolation kit (Roche, Penzberg) was used. The nucleic acid contents were absorbed by a Silica fleece located in the purification column in the presence of chaotrophic salt. Isolation of pure RNA was obtained by a digestion step with DNase. The isolation procedure was performed

using $1x10^6$ cells. DNA was digested for 20 min at RT and RNA was eluted using 50 µl of the provided RNA elution buffer following to manufacturer's instructions. RNA was either directly used for cDNA synthesis or stored until usage at -80°C.

3.2.3.7 cDNA synthesis

RevertAID first strand cDNA Sythesis kit (Fermentas, St. Leon-Rot) was used to generate cDNA from RNA templates. 11 µl of the RNA isolated as described above was mixed with 1 µl of the provided oligo dT_{18} primer. This primer selectively binds to the poly(A) tail of the RNA and marks the starting point of the reverse transcription. Only 0.5 µl of the supplied RiboLock RNase Inhibitor and 0.5 µl of the reverse transcriptase were needed to get cDNA of appropriate yield and quality. Manufacturer's recommended incubation steps for synthesis reaction were performed using a Thermo-cycler. For quantitative real-time PCR, cDNA was diluted in a ratio of 1:4 and stored until usage at -20°C.

3.2.3.8 Agarose gel electrophoresis

To analyze or purify digested DNA fragments, agarose gel electrophoresis was used. This method allows for the separation of DNA by size using an electric field. The phosphate-containing sugar backbone of DNA strands is negatively charged and migrates once loaded on a gel matrix towards the positive charge. Depending on the mass of the migrating strand and the pore size of the DNA gel matrix, differing migration rates are observed resulting in the separation of the fragments. By co-loading a DNA ladder, which marks different DNA masses, the size of the migrated fragment can easily be determined. Depending on the expected DNA fragment size, gel concentrations between 0.3-2.0 % [w/v] agarose solubilised in 1x TAE buffer were used. 1-2 µg Ethidium bromide was added to the gel to make DNA visible under UV light (302 nm). DNA samples were mixed with 6x DNA loading buffer and loaded onto the gel which was placed in the electrophoresis unit containing the appropriate amount of 1xTAE buffer and run between 120 and 140 V. DNA bands migrating according to the expected mass were cut from the gel using a clean scalpel under ultraviolet (UV) light. DNA damage was avoided with short time periods of UV light exposure.

3.2.3.8.1 DNA elution after gel electrophoresis

DNA isolation of preparative agarose gel was performed using the QIAEX Agarose Gel extraction Kit (Quiagen, Hilden) according to manufacturer's instructions. DNA was eluted

from ion exchange matrix by incubation with 50 µl of preheated nuclease-free water for 1-5 minutes prior to a final centrifugation step.

3.2.3.9 DNA ligation

The enzyme T4-ligase catalyses the formation of covalent phosphodiester bonds between adjacent 3′hydroxyl ends of one nucleotide with the 5′ phosphate end of another via ATP turn over. This enzyme is used for introduction of DNA inserts into cloning vectors. Typically, 100 ng of linearised vector was combined in a ratio of 1:5 with the DNA insert, 0.5 Units of T4-ligase and appropriate amount of 10x reaction buffer containing ATP. When required, ATP was also added to the reaction. The reaction was incubated between 1-2 h at 16°C. This reaction was used for transformation of competent *E.coli*. To check for background, clones resulting from self-ligation control reaction containing only vector (in the absence of insert DNA) were used for bacteria transformation.

3.2.3.10 DNA sequencing

Sequencing was performed commercially by GATC (Konstanz): 2-3 µg plasmid DNA was analysed with either standard or specifically designed primer. Results were analysed by alignments with the theoretical sequences using the alignment program CLUSTALW2 (www.ebi.ac.uk/tool/clustalw2)

3.2.4 Biochemical and immunological methods

3.2.4.1 Enzyme-linked immunoabsorbent assay (ELISA)

Enzyme-linked immunoabsorbent assay (ELISA) is one of the most commonly used quantitative immunoassays. In this method, a combination of an enzyme, namely streptavidine-horseradish-peroxidase conjugate and a biotinylated detection antibody is used as marker for determining antigen concentrations via substrate turn-over. Either an antigen or antibody is immobilised on a solid surface allowing for the rinsing and removal of unbound components. For sandwich ELISA based detection of IL-6 and TNF-α $1x10^6$ cells/ml were seeded out in a volume of 200 µl into a 96-well plate and stimulated either for 6 hours or overnight with 1% anti-TNP-OVA-IgE. Antigen challenge triggers cytokine release of MCs. Therefore different concentrations of the Antigen TNP-OVA were used. Cells were incubated either overnight or at least for 5 hours with the antigen. Supernatant was then collected and

either frozen at -20°C or directly applied in different dilutions with PBS for ELISA. The assay was performed according to the manufacturer's instructions.

3.2.4.2 Hexosaminidase assay (HAA)

To measure MC mediator release following antigen challenge, the β-hexosamindase assay (HAA) was performed[105]. When compound exocytosis is triggered, MC granule membranes fuse with the plasma membrane leading to the release of their components into the surrounding environment. The amount of the enzyme β-hexosaminidase released, directly correlates with those of histamine and chymase. By measuring the enzyme activity of this one component in the supernatant of MCs under high purity, one can quantify and determine the efficiency of MC degranulation. $2x10^6$ cells/ ml were activated by incubation with 1% anti TNP-OVA-IgE (hen egg OVA) conditioned medium overnight or for at least six hours. Cells were then washed once with Tyrode buffer before resuspending in 100 µl Tyrode Buffer. Antigen challenge was performed with varying concentrations of TNP-OVA (10.0 ng/ml) solubilised in Tyrode buffer at 37°C for 1 hour. TNP-OVA as well as anti-TNP-OVA IgE were produced and generously provided by Prof. Aktories group (University Freiburg). To measure released mediators, supernatant was mixed 1:1 with HAA-substrate solution. To determine the remaining unreleased mediators, cells were lysed by addition of 10 µl of Tyrode-TritonX lysis Buffer and mixed in a ratio 1:2 with HAA-substrate solution. After incubation for 1 h at RT, the reaction was aborted by adding 100 µl of HAA-stop solution. Enzyme activity was measured by the turn over of the substrate 4-nitrophenyl-2-acetamido-2-deoxy-β-D-glucopyranosid. The product of the colorimetric reaction is the yellowish p-nitrophenol which can be measured photometrically at 405 nm.

3.2.4.3 Fluorescence activated cell sorter (FACS)

The underlying principle of the FACS is the laser-stimulated light emission of cells stained with different fluorescently labelled molecules. In this case, antibodies were used to mark certain cell population with specific properties such as activation, size and granularity. Different fluorescent dyes and labels require different laser types to acquire fluorescent spectra. The scattering of monochromatic laser light is dependent upon the properties of the samples. Forward diverted rays (Forwardscatter) correlate with the cell size while rays radiated at a 90° angle correlate with cell granularity (Sidwardsscatter). In the case of fluorescent labelled cells, additional absorption of the monochromic light is absorbed by the

dye and light of higher wave length is emitted by the fluorescent molecules. To guarantee specific results and avoid staining artefacts, one sample included antibody stained samples, unstained cells, as well as cells labelled with isotype control of the antibody with appropriate labelling into the measurements. In the case of double stained samples it was required to measure samples stained with only one of each dye to be able to identify problematic staining and wave length interferences.

3.2.4.3.1 Extracellular FACS staining

Approx. $1x10^6$ cells per probe were harvested and pelleted by centrifugation (30 sec, 10,000 rpm). Cells were washed once with PBS/2%FCS. Prior to staining, nonspecific antibody binding was avoided using a blocking step. Therefore, cells were resuspended in 100ul PBS/2%FCS and incubated on ice for 30 min. An appropriate amount of antibody was then added directly to the cell suspension and incubated in the dark and on ice for 45 min. To remove the remaining nonspecific staining, samples were washed twice with PBS/2%FCS prior to FACS analysis.

CD123 staining:

CD123 staining of murine primary or BaF3 cells was performed by the addition of 0.2 µg of murine CD123-APC antibody. CD123 staining of THP-1 cells was done using 10 µl of human-CD123-APC antibody.

All experiments were performed using the appropriate isotype staining.

c-Kit (CD117) / FcεRI:

MCs were treated for at least 6 h with IgE prior to staining for maturation marker using 1 µl (0.2 µg) of PE-labelled anti-c-Kit antibody together with 1 µl (0.2 µg) of FITC-labelled anti-FcεRI.

3.2.4.3.2 Intracellular FACS staining

Approximately $1x10^6$ cells were pelleted by centrifugation (30 s, 10 000 rpm). Cells were washed once with PBS. For intracellular staining, cells were fixed 20 min at RT with PBS/4%PFA. Fixation is required to prolong stability of the intracellular proteins. After fixation, cells were washed twice with PBS/2%FCS and permeablised overnight with either incubation with 1 ml 90% methanol at -20°C overnight, or with 0.1% saponin detergent containing PBS at RT for 20 min. Following permeabilisation, cells were again washed twice

with PBS/2%FCS resuspended in 100 µl of the same buffer. Antibody in appropriate amounts was added to the sample and incubated 45 min at RT in the dark.

Intracellular staining of phosphorylated STATs

Cells were washed three times with PBS and cultured under IL-3 deprivation conditions for three hours prior to stimulation with 50 ng/ml IL-3 for different time points (5 min, 10 min, 30 min) or left untreated. Stimulation was aborted by washing cells with cold PBS (30 s, 10,000 rpm) followed by fixation using the procedure described above.
All experiments were performed under the usage of the appropriate isotype staining.

Propidium Iodide (PI) staining (Dye exlusion method)

Propidium iodide is an intercalating, florescent dye commonly used for intracellular DNA staining as a parameter for cell viability. Necrotic cells with their porous membrane are strongly positive for PI while viable cells have an intact membrane which is inaccessible to PI. PI can not only be used for the detection of necrotic cells but also to exclude nonspecific staining of cells when probed with labelled antibodies. Necrotic cells would also nonspecifically take up fluorescence-tagged molecules. To exclude necrotic populations, double-positive cells were left out of the measurement by appropriate gating. For dye exclusion, appropriately antibody-stained cells were co-stained with 1 µl of PI (50 µg/ml) and analysed immediately by FACS.

3.2.4.3.3 Annexin V- PI staining (Apoptose assay)

Apoptosis was determined using the Roche Annexin-V-FLUOS-staining Kit.
These proteins exhibit high binding affinity for negatively charged phospholipids in a calcium dependent manner. Annexin V, however, is a protein with high affinity for phosphatidylserine which is a phospholipid component normally localised at the inner leaflet of the cell membrane. Cells undergoing apoptosis, however, expose phosphatidylserine on the outer leaflet of their membrane. Using the provided FITC labelled Annexin V reagent, this PS can be stained. Since necrotic cells also have phosphatidylserine exposed on their cell membrane, it is required to co-stain with PI. Necrotic cells have a highly cavernous membrane leading to strong PI staining. This enables one to distinguish between highly PI and Annexin V positive necrotic cells and apoptotic cells highly positive for Annexin V and low for PI.
For the measurement of RhoH-induced apoptosis, cells were starved in the absence of IL-3 for 3 hours and $2.5x10^5$ BaF3 cells/ml were seeded in a 6-well plate. Cells were either incubated

in RPMI medium (10% FCS) overnight or under other stress conditions (e.g.treatment with 1 µM Doxurobucin or 1 µM Staurosporine). For analysis, cells were stained with Annexin-V and PI according to the Annexin-V-FLUOS kit protocol provided by the manufacturer.

3.2.4.4. Toluidine Blue staining of MCs

MC cytoplasm contains granules (metachromatic) composed of heparin and histamine. Toluidine blue should stain MCs red-purple (metachromatic staining of sulphated polysaccharides) and the background blue (orthochromatic staining of nucleic acids). For staining of MCs, previously prepared cytospins were incubated for two minutes in Toluidine Blue staining solution. Cytospins were then washed twice with PBS.

3.2.4.5 Sodium dodecyl sulphate polyacrylamided gel electrophoresis (SDS-PAGE)

SDS-PAGE seperates proteins according to their electrophoretic mobility. The migration of the proteins is not determined by their intrinsic electric charge of the polypeptides but by their molecular weight. The substance SDS is a strongly anionic detergent which denatures secondary and non-disulfate linked tertiary structures. This is achieved by wrapping the hydrophobic tail around the backbone of the polypeptide. SDS thereby confers a negative charge to each protein proportional to its mass. Specific molecular weight standard range markers allow for the estimation of the molecular weight. Complete unfolding of protein structure is achieved by the usage of disulfide-reducing agents such as β-mercaptoethanol. SDS-PAGE was performed by using discontinuous buffer systems with two layer gels containing a stacker and a resolving gel layer. The stacking gel layer containing 5% acrylamide and Tris-HCL (pH 6.8), was used to concentrate proteins in a thin starting zone before being resolving in the second Tris-Glycine gel layer. The acrylamide content of the resolving gel was specifically-chosen to accommodate the size of the target protein. Acrylamide concentrations in the resolution part can vary between 10-20%. Higher acrylamide concentrations are suitable for resolving proteins of lower sizes and vice versa. Continues gel systems containing an acrylamide concentration gradient (4-20%) were used to obtain optimal resolution for proteins of different or unknown sizes.

3.2.4.5.1 Protein detection in SDS-gels with Coomassie Blue

One method to visualize protein bands nonspecifically after SDS page is Coomassie Blue staining of the gel. The Coomassie mechanism for protein attachment is through ionic interactions and non-covalent bonds to non-polar regions via Van-der-Waals interactions as

the dye Coomassie is negatively charged and stable in the anionic form. The gel was washed twice for 5 min with water, then the proteins were fixed by incubating the gel for 1 h at RT with fixing/destaining buffer (40% methanol, 10% acetic acid, and 50% H_2O). Gel was rinsed three times (5 min) with water and then covered with Coomassie Blue staining solution. After 45 min of gentle shaking at RT, the gel was again rinsed several times with water. Destaining of the gel was performed to make individual bands visible by incubating the gel in fixing/destaining buffer 2 h or overnight. After this procedure, gel was stored in buffer containing 1% acetic acid.

3.2.4.6 Eukaryotic cell lysates

To obtain protein lysates for SDS Page from eukaryotic cells, different methods were used. All working steps for the preparation of cell lysates for protein analysis were performed on ice with cooled buffers (4°C) containing Roche Phosphatase Inhibitors and Protease Inhibitors (Roche, Penzberg), and cooled (4°C) centrifuges.

PBS- lysates

$1x10^6$-$1x10^7$ cells were collected and washed twice with PBS (30 s, 10,000 rpm). Cells then were resuspended in 250 µl PBS. To prevent high viscosity of the lysates via nucleic acids, samples were frozen at -80°C for at least two hours. After thawing, the cells were lysed through sonication with using 3x 10 sec pulses sepearated by five seconds each. Cell debris was pelletted by centrifugation and the supernatant was collected and either stored at -80°C or directly used for SDS-PAGE after determination of protein concentration.

NP40-lysates

Stimulated cells in solution were quickly lysed by the addition of an equal volume of 2xNP-40 lysis buffer containg the appropriate amount of protease and phosphatase inhibitors. After resuspending the cells with lysis buffer, samples were spun for 45 min at 4°C. The lysates were then centrifuged at maximum speed for 30 min. Supernatant was then collected and either stored at -80°C until usage or directly used for determining protein concentration and SDS PAGE.

RIPA-lysates

At least $1x10^6$ cells were washed three times with PBS and resuspended in 350 µl of RIPA Buffer. Cells were incubated while rotating upside down for 15-30 min at 4°C. Cell debris

was pelleted by maximum speed centrifugation for 20-30 min. Supernatant was then collected and either stored at -80°C until usage or directly used for determining protein concentration and SDS PAGE.

3.2.4.7 Bicichinonic assay (BCA)

For the measurement of protein concentrations of lysates and of GSH-matrix eluates, the BCA was used. The "biuret reaction" is the underlying principle of the BCA. Peptides containing more than two aa residues form a chelating complex with cupric ions (Cu^{2+}) in an alkaline environment. One cupric ion forms a complex with 4 to 6 nearby peptides bonds which absorbs visible light. The blue color intensity, resulting from the reduction of cupric ion to cuprous ion, is proportional to the number of peptide bonds participating in the reaction. This reaction is combined with a second reaction in which the chelation of BCA with the cuprous ion of the former reaction yield an intense purple color. The reaction products are formed by the chelation of two molecules of bicichinon (BC) with one cuprous ion. The BC/copper complex is water soluble and exhibits a strong linear absorbance at 562 nm with increasing protein concentrations.

3.2.4.8 Immunoprecipitation (IP) and Co-IP

Immunoprecipitation (IP) is used to precipitate, and thereby concentrate and isolate, a single protein type out of a mixed solution by using immobilised antibodies. Cell lysates are prepared with suitable lysis buffer and are mixed with 30 µl of freshly resuspended Protein A/G Sepharose Beads (Santa Cruz, San Diego). 1-5 µg of the antibody is added to the reaction. After rotating incubation for at least 6 h at 4°C, beads are centrifuged at 13,000 rpm for 30 sec. Supernatant is either collected and stored at -80°C or discarded. Beads were washed twice with 350 µl lysate buffer and once with TNE-buffer to remove any remaining detergents. Beads were mixed with 30 µl of 2x sample buffer (Lämmli) and heated for 3-5 min at 96°C. After centrifugation for 3 min at maximum speed, the supernatant was loaded onto a SDS page gel and proteins were detected via enhanced chemiluminescence. This method was also used to co-precipitate potential interaction partners of the target protein.

3.2.4.8.1 Immunoprecipitation of STAT proteins

$1x10^7$ starved (3 h) BaF3 cells in 250 µl RPMI medium were either stimulated with 50 ng/ml IL-3 or left untreated. Cells were lysed using 250 µl 2x NP40 lysis buffer. A/G Sepharose

beads as well as 5 µl of either STAT1 or STAT5 antibody were added to the reaction. Samples were run on 12% SDS-Page.

3.2.4.8.2 Co-Immunoprecipitation of RhoH interaction partner

100 µl of generated RhoH antibody serum (Eurogentec, Seraing, Belgium) was preincubated overnight with 30 µl of protein A/G sepharose per sample. Beads were collected after centrifugation and the serum supernatant was stored and reused up to three times. Lysates of $1x10^7$ BaF3 cells of $1x10^6$ transfected HEK cells were incubated with the RhoH antibody-coupled beads over night. Samples were run on an acrylamide concentration gradient (4-20%) gel (Anamed, Bad-Ems).

3.2.4.9 Western-blot (semi-dry)

After SDS–PAGE, the separated proteins were transferred onto a nitro cellulose membrane using a semi-dry blotting technique which allows for protein detection with antibodies. Nitrocellulose and filter paper (Whatman) were soaked with Transfer buffer. Four to eight soaked layers of Whatman paper were stacked between the positive and negative electrode of the blotting unit. Then the soaked membrane was placed on top of the staple of Whatman paper. The SDS gel was positioned onto the nitrocellulose membrane and was covered again with equal layers of Whatman paper. To avoid discrepancies during transfer, air bubbles were removed. Proteins were transferred vertically toward the anode for one hour under a current of approximately 0.8 mA per cm² gel. Transfer of proteins to the membrane was checked using Ponceau S.

3.2.4.9.1 Antibody-mediated detection of immobilized proteins

After protein transfer, the membrane was incubated with 3% lactose or 5% BSA containing TBST-buffer for 1 h/ RT to block nonspecific binding. The membrane was then probed with the antigen-specific antibody overnight at 4°C. The following day, the antigen-specific antibody was removed, washed three times with TBST (5 min, RT), and the membrane was incubated (1 h, RT) with horse radish peroxidase (HRP) coupled secondary antibody directed against the Fc portion of the primary antibody. After discarding the secondary antibody and three additional washing steps with TBST, detection of bound antibody was performed using luminol. Luminol serves as a substrate for HRP and during oxidation of the agent chemiluminescent molecules are formed. The luminescence signal is proportional to the amount of target protein and can be detected and visualised with the detection unit Chemi-

Smart 5000 (Peqlab Erlangen). For analysis and quantification of resulting bands the software ChemiCapt (Peqlab, Erlangen) was used.

3.2.4.9.2 Stripping

Stripping was performed to remove primary and secondary antibodies from the membrane in order to re-probe chemiluminescent western-blots. The membrane was incubated for 1 h at 37°C in the appropriate amount of Restore Western Blot Stripping Buffer (Pierce). After discarding Stripping buffer, membrane was washed with TBST several times to remove residual buffer. Finally, the membrane was blocked as described above and probed again with the primary antibody of interest.

3.2.4.10 Nuclear extracts

$1x10^8$ cells per sample were washed with 5 ml of cold PBS. Cells were transferred into falcon tubes and spun 5 min at 1000 rpm (4°C). The cell pellet was resuspended in 400 µl hypotonic buffer and allowed to swell on ice for 10 min. Again cells were centrifuged for 1 min at 12,000 rpm and 4°C. Supernatant containing cytoplasmic extracts were either kept at -80°C or used directly for SDS-PAGE. Nuclear pellets were resuspended in 50 µl of high salt buffer and rocked or vortexed for 30 min at 4°C. Suspension was centrifuged for 10 min at 12,000 rpm and 4°C. Protein content was quantified using BCA and either kept at -80°C until storage or 50 µl of the lysates were directly used for SDS PAGE.

3.2.4.11 Affinity chromatography: GST-pulldown assay

GST tagged proteins were purified using Glutathione Sepharose TM 4 fast flow (GE Healthcare). The gluthatione beads were conditioned to supernatant settings by three rinsing steps using appropriate bacteria lysis buffer. Equilibrated glutathione coupled beads were then incubated at 4°C for 2 h with bacteria supernatant. After this period beads, together with supernatant, were transferred to a column (Bio Rad). After five washing steps with bacteria lysis buffer, matrix bound proteins were eluted with 1 ml of reduced Gluthation-Buffer. For enhanced efficiency, this step was repeated three times. Next, the protein concentration of the eluate was determined colorimetrically using 10 µl of eluate which was mixed with 1 ml Coomassie Plus Bradford Protein reagent. Protein concentration dependent absorption was measured after 10 min at RT (595 nm) and the resulting protein concentration was from the pre-determined calibration curve.

3.2.4.12 Sample preparation for protein in-solution trypsin digestion

In order to analyze and identify proteins by liquid chromatography (LC)-tandem mass spectrometry (MS/MS) methods, proteins are proteolyzed (e.g. digestion with trypsin) into their corresponding peptide fragments. For efficient digestion, the proteins should be denatured and solubilized in an aqueous solution buffered at an optimal pH (~ 7.5). The procedure for denaturing and digestion of the proteins was as follows: First, the proteins were precipitated overnight at -80°C by adding ice cold acetone in at a ratio 1:4. The next day, precipitated protein was pelleted by centrifugation (maximum speed, 45 min, 4°C). Supernatant was discarded and pellet was allowed to dry at RT for 15 to 20 minutes. Protein pellet was resuspended in 6M Urea containing Ammonium Bicarbonate Buffer (0.1 M). This step denatures the protein structure. 5mM dithiothreitol (DTT) was added break disulfide bonds between different cysteinyl residues and this step, combined with denaturation, enhances the accessibility of proteolytic cleavage sites within the proteins. To prevent reforming of disulfide bonds, an alkylating agent, 15 mM iodoacetamide (IAA) was added to the mixture. After 30 min incubation at RT in the dark, DTT was added to the reaction to quench any excess IAA. In the final step, the mixture was diluted to a final concentration of 2 M urea and trypsin (Promega) was added in a ratio of 1:20. Trypsin digestion was performed overnight at 37°C.

3.2.4.13 Peptide fractionation and mass spectrometric analysis

The peptides from each of the sample digestion mixtures were separated using two orthogonal fractionation techniques composed of strong cation exchange (SCX) followed by reversed-phase HPLC of each fraction. Fractionation was performed on a polysulfoethyl aspartamide column (200 × 2.1 mm; 5 µm; 200 Å) (PolyLC Inc., Columbia, MD) using a Paradigm MG4 HPLC system (Michrom BioResources, Inc., Auburn, CA). Peptides were loaded onto the SCX column with mobile phase A (5 mM KH_2PO_4 (pH 2.7)/30% acetonitrile) and eluted with an increasing salt gradient from phase B (mobile phase A containing 500 mM KCl). The flow rate was set at 200 µl/min and elution was monitored with a UV-visible detector (214 nm). Fractions were collected at 2 min intervals (30 fractions) and then pooled (based on absorbance) for a total of twelve fractions for subsequent reversed-phase LC-MS/MS analysis. Reversed-phase separations were performed on C18 media (5 µm particles; Applied Biosystems, Foster City, CA) packed in fused silica capillary tubing (8cm × 50 µm i.d.). An acetonitrile gradient was delivered by a binary nano-LC pump (nanoLC•2D^{TM}; Eksigent). Buffer A was composed of 0.1% formic acid and buffer B was composed of 90% ACN/0.1%

formic acid. Peptides were delivered to the column at 3% buffer B and separated via a linear gradient of increasing buffer B to 60% at 45 minutes. It was held at 60% B for five minutes and then the composition was reset to 3% B for the duration (65 min/run). Eluates were analysed with an ion trap/Orbitrap hybrid mass spectrometer (LTQ Orbitrap, Thermo Fisher Scientific, San Jose, CA) equipped with a Nanomate nanospray ion source (Advion Biosciences, Ithaca, NY, USA). Settings included: spray voltage 1.3 kV; spray current 100 µA; capillary voltage 35 V; ion transfer tube temperature 220°C. The mass spectrometer was operated in the data-dependent mode to automatically switch between Orbitrap-MS and ion trap-MS/MS acquisition. Survey full scan MS spectra (from *m*/*z* 400–2000) were acquired in the orbitrap at a resolution of 30,000 (based on *m/z* 400). The four most intense ions were isolated for fragmentation in linear ion trap using collision-induced dissociation with a normalised collision energy setting of 27.0.

3.2.4.13.1 Data analysis and interpretation

MS/MS peak lists from the raw files were extracted (.dta format) using Bioworks Browser version 3.3.1 SP1, ThermoFisher Scientific Inc. (San Jose, CA, USA). The combined list of .dta files from each set of LC-MS/MS runs (from 12 SCX fractions each) were then converted to .mgf format (as one concatenated file) using a Perl script (merge.pl) available from Matrix Science Inc. (Boston, MA, USA). The .mgf peak lists were then analysed using the Mascot database searching software from Matrix Science Inc. (Boston, MA, USA) using the IPI mouse database.The following fixed settings and modifications were used in the searches: trypsin as the protease allowing for up to two missed cleavage sites; carbamidomethylation (C); precursor mass tolerance of 20 ppm (ion mass tolerance of 1 Da). The variable modifications included deamidation (N and Q) and oxidation (M). Peptide identifications and residue modifications were accepted if their scores were above the confidence threshold (95% confidence interval) as established by Mascot. The data from biological replicates were combined and sorted by IPI protein accession number in Microsoft Excel. Proteins identified by a single peptide hit were removed from the list and stored in a separate file. The data was then sorted by peptide aa sequence to identify redundant peptides. The total data from all of the 2D-LC-MS/MS experiments, including the duplicates wt RhoH ± IL3 and mutant T36A RhoH ±IL3 and the GST control, was then combined. The number of unique and/or redundant peptides were then entered into the appropriate sample column for each protein identified. Two unique peptides were required for a protein identification to be considered as a solid hit.

4. Results

4.1 RhoH modulates IL-3 signalling through regulation of STAT activity and IL-3 receptor expression

4.1.1 Regulation of RhoH expression in the IL-3 dependent system

The IL-3 dependent proB cell line BaF3 was used as a model system. RhoH is a constitutively active GTPase and it is assumed that transcriptional regulation is a major mechanism to control RhoH initiated signalling. Less is known about the induction of RhoH expression and only two modulators of RhoH expression are known[61,106]. To gain insight into the integrity of the chosen system and whether RhoH expression would be transcriptionally regulated by IL-3, parental BaF3 cells were cultivated under diverse conditions and subjected to different treatments. RhoH expression on mRNA level was determined using quantitative real-time PCR and GAPDH as reference gene. BaF3 cells were either cultured under "normal conditions" in IL-3 containing medium or were starved (withdrawal of IL-3) for 3 hours. Starved cells were then either restimulated with IL-3 (5h) or kept under starving conditions (5h). RhoH expression remained stable when IL-3 dependent cells were either continuously starved or cultivated in IL-3 containing medium. Interestingly, BaF3 cells which were previously starved and restimulated with IL-3 for 5 hours showed a decrease of RhoH mRNA levels, indicating a transcriptional regulation of RhoH expression induced by IL-3 **(Fig.4.1)**. This experiment clarified that RhoH expression is downregulated by IL-3, indicating a negative role for RhoH during the initial induction of IL-3 signalling.

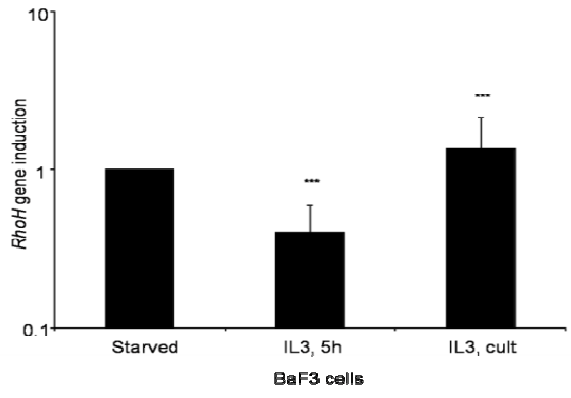

Fig. 4.1RhoH mRNA regulation after IL-3 stimulation of starved BaF3 cells
RhoH mRNA levels of parental BaF3 cells, either cultivated under IL-3 withdrawal for 3 hours (starved), starved for 3 hours and then transferred back in IL-3 containing medium for 5 hours (5h IL-3) or continuously kept in IL-3 containing growth medium (cult.) mRNA levels were detected by quantitative SYBR Green Real-Time PCR using *RhoH* specific primers and *GAPDH* as reference gene. Data is presented as induction of RhoH mRNA levels compared to starved cells. Statistical significance was determined using Student`s t-test (n=3, mean ± SD and *P≤0.05; ***P ≥0.005)

4.1.2 RhoH, an inhibitor of IL-3 induced proliferation

To address the question of an inhibitory role of RhoH in IL-3 dependent, next BaF3 cells overexpressing RhoH (RhoH cells), BaF3 cells which were retrovirally transfected with a vector containing short hairpin shRNA directed against RhoH (siRhoH cells), and a control cell line of BaF3 cells, transduced with the corresponding empty vector (Mock) were generated. All vectors were containing a puromycin resistance gene for antibiotic selection. BaF3 cells were several times tested upon their IL-3 dependency to ensure solid and reliable results. To guarantee that only transduced cells were analysed, cells were kept continuously in puromycin containing medium. Due to a lack of a functional antibody against endogenous RhoH, the altered expression levels of RhoH in siRhoH, RhoH overexpressing and control cells were checked by quantitative real-time PCR and RhoH cDNA specific primers, that were suitable to detect endogenous and transduced RhoH expression **(Fig. 4.2A)**. Short hairpin RNA mediated knock-down of RhoH reduced endogenous expression of RhoH up to 90% of that of control cells while overexpression of RhoH enhanced RhoH mRNA expression approximately fivefold the mRNA levels detected in cells transduced with the control vector. It was previously reported that simultaneous expression of multiple genes in mammalian cells, transduced with IRES (internal ribosomal entry site) sequence containing vectors, are highly comparable[107]. Therefore CD4 was cloned into the IRES containing vector and was used for surrogate measurements to determine transduction efficiency. To demonstrate successful transduction, cells were analysed by FACS upon their CD4 surface expression. The CD4 expression in both samples was about 80% compared to untransfected cells **(Fig. 4.2B)**.

(A) (B)

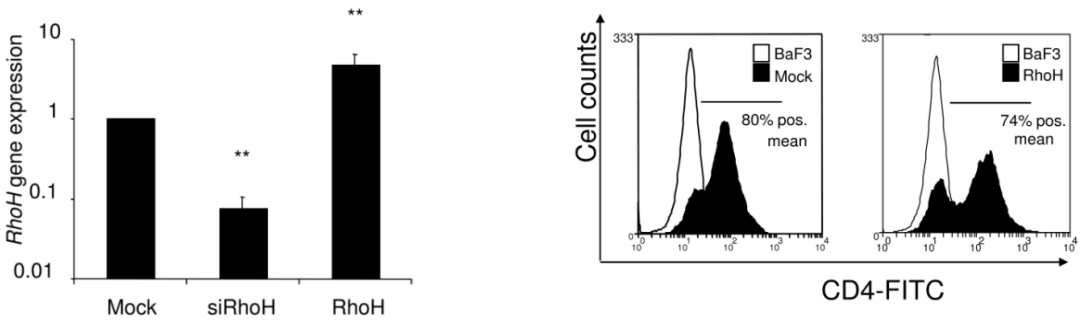

Fig. 4.2 Generation of BaF3 cells with distinct RhoH expression levels

(A) RhoH mRNA levels of BaF3 cells retrovirally tranduced with either empty vector (pMX-IRES-CD4-Puro) indicated here as Mock, with shRNA directed against RhoH containing vector, indicated as siRhoH or RhoH overexpression vector (pMX-IRES-CD4-Puro-RhoH) were analysed by quantitative SYBR Green Real-Time PCR using *RhoH* cDNA specific primer and *GAPDH* as reference gene. Statistical significance was determined using Student`s t-test (n=2, mean ± SD and *P≤0.05; **P≤0.01) (B) Human CD4 expression after puromycin selection of Mock or RhoH overexpression vector transduced BaF3 cell measured using FACS analysis. Parental BaF3 cells served as negative control.

To determine whether RhoH expression levels would impact IL-3 induced proliferation of cells, a proliferation assay was performed. The time-dependent proliferation rates of RhoH overexpressing cells, siRhoH and control cells with constant IL-3 concentration in the growth medium, when seeded out with equal cell counts were compared **(Fig 4.3A)**. When observing the proliferation of cells with different RhoH levels over 5 days it became apparent that cells with shRNA mediated knock-down of RhoH showed an increased proliferation in response to IL-3, while cells overexpressing the protein showed a decrease of proliferation compared to empty vector transduced BaF3 cells. The differences became most prominent at day 5 when cell proliferation rate exit log phase. At day 5 both RhoH overexpressing and siRhoH cells differed from control cells in a cell count of about $4x10^5$ cells. To clarify whether this observations correlated with a IL-3 dependent dose-response sensitivity caused by modified RhoH expression levels, a cell viability assay with varying IL-3 concentrations (0.001-1 ng/ml) in the medium, was performed. In this assay the ATP levels of cells are measured. ATP levels are increasing with rising cell counts **(Fig. 4.3B)**. ATP levels measured after 48 hours of culture in different IL-3 concentrations confirmed and even clarified the observations which were made in the time-dependent proliferation assay. RhoH overexpressing cells showed 70% lower proliferation potential than control cells, while siRhoH cells proliferation showed an increase of 160% in proliferation compared to Mock transfected cells. The inhibitory effect RhoH had on proliferation was not able to be compensated with increasing IL-3 concentration. To address the question whether RhoH expression would have similar effects on proliferation rates when using a growth factor other than IL-3, BaF3 and RhoH overexpressing BaF3 cells were co-transduced with erythropoietin receptor (Epo-R) and were cultivated together with parental (untransduced) BaF3 cells in medium containing erythropoietin (Epo) as growth factor. In this experiment again ATP levels were determined **(Fig. 4.3C)**. Parental cells, as expected showed no proliferation in response to Epo and interestingly RhoH overexpressing cells were growing with a proliferation rate, similar to that observed in EpoR tranduced cells with lower RhoH expression levels. These results supported the hypothesis that the RhoH modulated IL-3 dependent proliferation effects previously observed in cells with distinct RhoH levels were specifically in response to the cytokine IL-3.

(A)

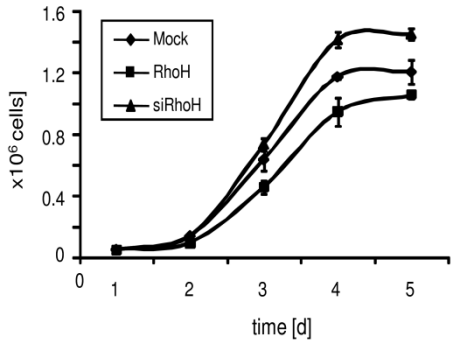

(B)

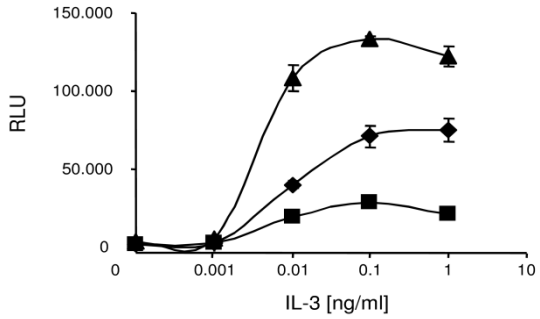

(C)

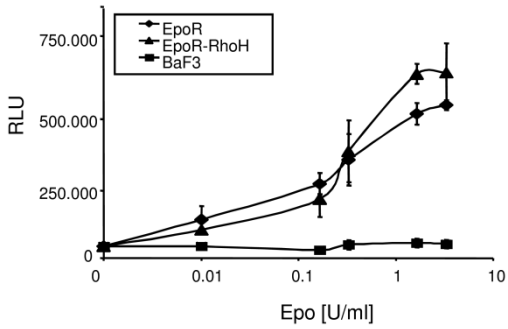

Fig. 4.3 RhoH modulates IL-3 stimulated proliferation
(A) Time dependent proliferation of $0.25x10^5$ cells over 5 days in of RhoH, Mock and siRhoH BaF3 cells, cultivated in 0.5% IL-3 containing growth medium. Cell numbers were analysed using Neubauer`s cell counting chamber. Presented results from one represented experiment performed in dublicates ± SD (n=2) (B) IL-3 dose response curve of RhoH, Mock and siRhoH cells cultivated for 48 hours in medium with indicated IL-3 concentrations. Viability of cells was determined in a CTG assay. Presented results from one representative experiment performed in triplicates ± SD (C) Epo dose response curve of parental BaF3 cells (BaF3), BaF3 cells transduced with Epo-Receptor (EpoR) and RhoH overexpressing BaF3 cells co-tranduced with Epo-receptor (RhoH-EpoR) cultivated for 24 hours in growth medium containing indicated concentrations of Epo. Viability of cells was determined in a CTG assay. Presented results from one representative experiment performed in triplicates ± SD (n=2).

4.1.3 RhoH overexpression results in increased IL-3 dependent STAT1 activation

RhoH was previously reported to induce apoptosis in hematopoietic progenitor cells via an unknown signalling pathway[85]. IL-3 is known to induce not only factors important for survival but to a much lesser amount also growth inhibiting and proapoptotic transcription factor STAT1[23]. To address whether RhoH levels can modulate STAT1 activation in response to IL-3, siRhoH, RhoH and control cells were starved prior to stimulation with IL-3 and phosphorylated STAT1 levels were determined by FACS analysis **(Fig. 4.4A).** The treatment of control and siRhoH cells with IL-3 resulted in only slight or no phosphorylation of STAT1 compared to unstimulated cells, while the IL-3 treatment of RhoH cells resulted in a strong phosphorylation of STAT1. To confirm FACS analysis, STAT1 immunoprecipitation (IP) was performed to detect tyrosine phosphorylated STAT1 (pSTAT) using western-blot analysis. Since no significant difference in phosphorylation has been detectable between Mock and siRhoH transfected cells using FACS analysis, only control and RhoH cells were starved and stimulated with IL-3 for IP **(Fig. 4.4B)**. The results

confirmed that enhanced STAT1 activation can be observed in RhoH overexpressing cells after IL-3 treatment. The quantification of different experiments clarified that there is a 1.5 fold increase of IL-3 induced STAT1 phosphorylation in RhoH overexpressing cells compared to the activation of STAT1 in control cells. These observations lead to the conclusion that RhoH expression causes enhanced IL-3 dependent phosphorylation of STAT1, which most likely causes the inhibition of IL-3 induced proliferation.

(A)

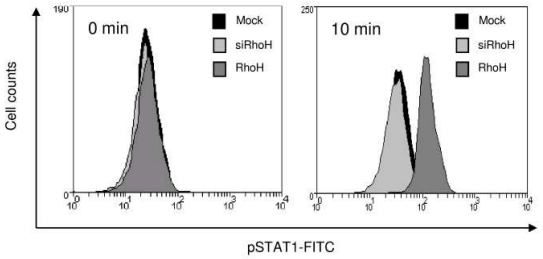

(B)

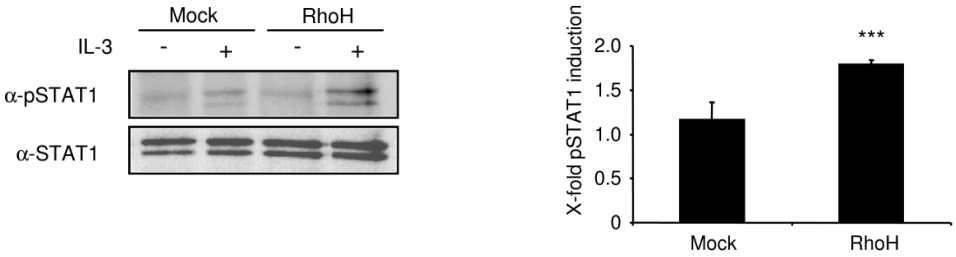

Fig. 4.4 RhoH overexpressing cells show increased IL-3 induced STAT1 phosphorylation
(A) Mock, siRhoH and RhoH BaF3 cells were starved for 3 h and then stimulated for 10 min with 50 ng/ml IL-3. FACS analysis of pSTAT1 was performed using a FITC labeled pSTAT1 antibody. Results from one representative experiment is shown (n=3). (B) (Left panel) Mock and RhoH cells were lysed for STAT1-IP, either directly after 3 h of cytokine withdrawal or after 10 min stimulation with 50 ng/ml IL-3 following 3 h starvation. For STAT1-IP STAT1 specific antibody was used, detection of pSTAT1 and total STAT1 was performed by enhanced chemiluminescence. (Right panel) Quantification of pSTAT1 levels was performed after normalisation to STAT1 levels in control cells and is presented as induction of phosphorylation compared to the unstimulated samples. Statistical significance was determined using Student`s t-test (n=3, mean ± SD; ***P≤ 0.005)

4.1.4 RhoH modulated IL-3 dependent STAT1 activation correlates with expression of CDKIs

To check the induction of STAT1 dependent apoptosis mediated through the activation of pro-apoptotic signalling pathways such as the activation of caspases 1 and 11 or through the inhibition of pro-survival signalling pathways[29], apoptosis was induced in cells with different RhoH expression levels. To trigger distinct apoptotic mechanisms cells were kept under different stress conditions. RhoH, siRhoH and control cells were either kept under IL-3 withdrawal, or treated with either doxorubicine (doxorub) or staurosporine (staurosp). As negative control for apoptosis, cells cultured in IL-3 containing medium were used **(Fig. 4.5**

A). Apoptosis was detected using FACS analysis. The results showed that cells with different RhoH levels did not differ in their ability to undergo apoptosis, indicating that the observed proliferation inhibition caused by RhoH overexpression is not the result of STAT1 induced apoptosis. STAT1 activation can result in growth inhibition by the induction of the CDKI $p21^{waf/cip1}$ [34]. Investigations of $p21^{cip1}$ mRNA levels in siRhoH, RhoH and control cells showed that indeed RhoH overexpression results in enhanced mRNA levels of $p21^{waf/cip1}$ **(Fig. 4.5B)**. Suprisingly the mRNA expression of the CDKI $p21^{waf/cip1}$ measured in siRhoH cells seemed to be slightly elevated in comparison to control cells. Next it was confirmed that the enhanced mRNA levels of $p21^{waf/cip1}$ also result in an accumulation of $p21^{waf/cip1}$ on protein level **(Fig. 4.5B).** To quantify the detected $p21^{waf/cip1}$ protein amounts, the $p21^{waf/cip1}$ signal intensity was corrected using β-actin loading control signal and normalised against the signal measured in control cells (100%). RhoH overexpressing cells showed 100 fold higher signal intensity of $p21^{cip1}$. On protein level siRhoH levels showed insignificantly lower $p21^{waf/cip1}$ expression than control cells.

The CDKI $p27^{kip1}$ is is known to be regulated by STAT1[31] and IL-3 treatment[108]. Therefore it was assumed that this protein could be also a potential target of RhoH mediated cell cycle inhibition. The mRNA expression levels of the *$p27^{kip1}$* gene were quantified in control, RhoH and siRhoH cells **(Fig 4.5C).** RhoH overexpression resulted in enhanced $p27^{kip1}$ mRNA levels. Investigation of the $p27^{kip1}$ protein levels in control, siRhoH and RhoH cells showed the same result. RhoH overexpression lead to an upregulation of $p27^{kip1}$ protein expression, while control cells and siRhoH cells showed comparably low $p27^{kip1}$ levels **(Fig. 4.5C)**. Quantification of the results revealed an approximate increase of $p27^{kip1}$ protein expression of 30% compared to control cells. These results demonstrated that RhoH modulated enhanced IL-3 dependent STAT1 activation inhibits cell proliferation by upregulation of cell cycle inhibitors rather than by the induction of apoptosis.

(A)

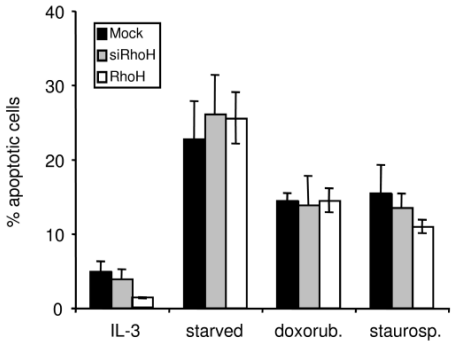

(B)

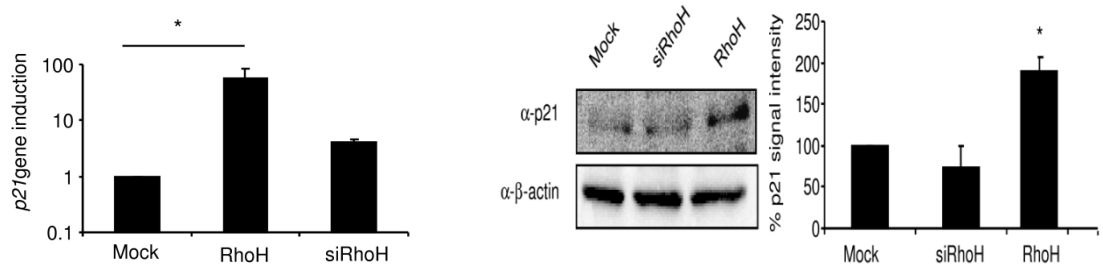

(C)

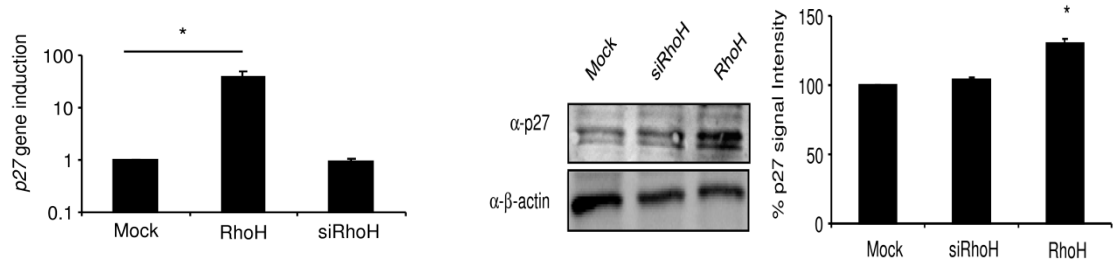

4.5 RhoH dependent STAT1 activation after IL-3 stimulation correlates rather with increased CDKI expression than with induction of apoptosis

(A) Apoptosis was measured using FACS analysis of Annexin V/PI staining of Mock, siRhoH and RhoH cells. Apoptosis was measured after cultivation in normal growth medium, under IL-3 withdrawal (ON) or in growth medium containing 1 µM doxorub. (12h) or 1 µM staurosp. (3h). (n=3, mean ± SD). (B)&(C) mRNA levels of $p21^{waf/cip1}$ (B) and $p27^{kip1}$(C) in control, RhoH and siRhoH cells was performed by quantitative SYBR Green Real-Time PCR and primers against *$p21^{waf/cip1}$* (B) or *$p27^{kip1}$*(C) and the reference gene *GAPDH* (n=3, mean±SD) statistical significance was determined using Student`s t-test (*P≤0.05). Data is presented after normalization of $p21^{cip1}$ (B) or $p27^{kip1}$ (C) to mRNA levels detected in control cells. For western-blot analysis of $p21^{waf/cip1}$ (B) or $p27^{kip1}$(C) whole cell lysates of Mock, siRhoH and RhoH cells were prepared and separated by 4-20% gradient SDS-PAGE. Protein levels were detected using enhanced chemiluminescence. For quantification $p21^{waf/cip1}$ (B) or $p27^{kip1}$(C) levels were normalised to correlating β-actin levels (right panel). Data is presented as percentage of $p21^{waf/cip1}$ (B) or $p27^{kip1}$(C) levels detected in control cells. Statistical significance was determined using Student`s t-test (n=3, mean ± SD; *P≤0.05).

4.1.5 RhoH expression modulates IL-3 induced STAT5 activity

One of the major pro-proliferative signalling pathways activated by IL-3 treatment is the induction of the JAK2-STAT5 pathway[22] resulting in the expression of cell cycle progression and survival supporting genes[21]. To address the question whether the enhanced proliferation of siRhoH cells could be connected to an increase of STAT5 activation, IPs of total STAT5 (followed by the detection of the amount of phosphorylated STAT5) was performed. For this purpose control, RhoH and siRhoH cells were starved and restimulated with IL-3 **(Fig 4.6A)**. After comparing IL-3 induced phosphorylation levels to the untreated sample a significant decrease in STAT5 phosphorylation of RhoH overexpressing cells (50% compared to control) was observed. The phosphorylation differences between Mock and siRhoH cells were hard to distinguish using IP, since total STAT5 levels seem to vary between samples. However the comparison of different, to the total STAT5 levels normalised experiments **(Fig 4.6A)**, showed a slight enhancement of STAT5 phosphorylation in cells with RhoH knock-down. In

an effort to further characterise this slight difference in STAT5 activation, FACS experiments were performed using Mock and siRhoH cells **(Fig 4.6B)**. Using FACS analysis made it possible to detect a stronger difference in phosphorylation between control cells and cells with lower RhoH expression **(Fig. 4.6B)**. STAT5 activation is known to play a pivotal role in the mediation of cytokine independent proliferation and enhanced survival under cytokine deprivation conditions[109].

(A)

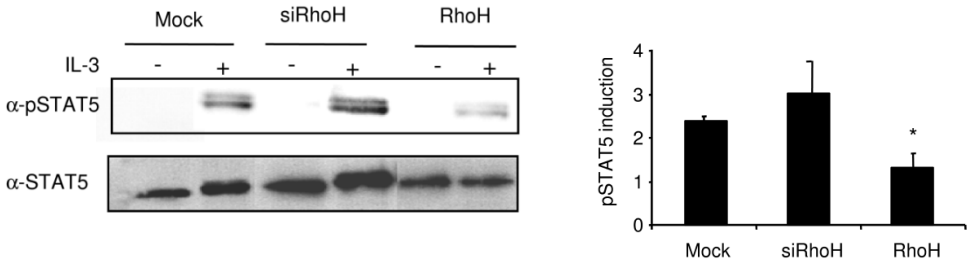

(B)

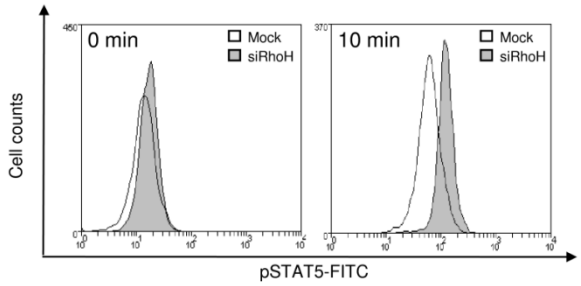

Fig 4.6 Low RhoH levels are correlating with enhanced STAT5 phosphorylation (A)Mock, siRhoH and RhoH BaF3 cells were lysed for STAT5-IP, either directly after 3 h cytokine withdrawal or after 10 min stimulation with 50 ng/ml IL-3, following 3 h of cytokine starvation. For STAT5 IP STAT5 specific antibody was used, detection of pSTAT5 and total STAT5 was performed by enhanced chemiluminescence. Quantification of pSTAT5 levels was performed after normalization to detected STAT5 levels in control cells. Data is presented as induction of phosphorylation compared to unstimulated sample. Statistical significance was determined using Student`s t-test (n=2, mean ± SD; *P≤ 0.05) (B) FACS analysis of pSTAT5 in Mock and siRhoH cells after 10 min treatment with 50 ng/ml IL-3, following 3 h of cytokine starvation was performed using a FITC labeled pSTAT5 antibody. Presented data from one representative experiment is shown (n=3).

It was tested whether the increased STAT5 activation in response to IL-3 would impact the survival of siRhoH cells. Parental cells and BaF3 cells with a shRNA mediated knock-down of RhoH were tested in a survival-assay **(Fig. 4.7)**. After removal of any IL-3 from the growth medium, the decreasing cell viability and the correlating decreasing cell counts were documented. After day 3 no vital cells were detectable using Trypan Blue cell staining, indicating that less than $1x10^4$ cells per ml medium were vital. At this time point IL-3 was re-added to the growth medium and cells were allowed to recover from starvation period for several days before counting of vital proliferating cells started. The outcome of this

experiment showed that there is no increased survival of cells underexpressing RhoH after IL-3 removal, highlighting that the increased levels of phosphoSTAT5 (pSTAT5) were a direct result of IL-3 treatment. Instead, siRhoH cells showed a more unfavourable reaction to the IL-3 withdrawal than parental cells since cell counts of siRhoH cells declined with an increased rate in comparison to parental cells. However when IL-3 was re-added to the growth medium, cells with less RhoH expression exhibited the ability to recover from IL-3 starvation in contrast to parental BaF3 cells with higher RhoH expression.

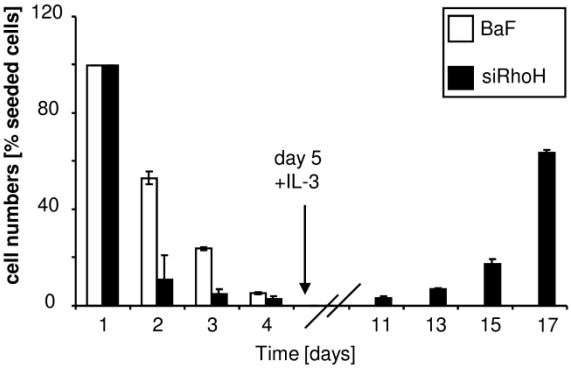

Fig. 4.7 Low RhoH expression correlates with increased recovery from IL-3 starvation
Increased IL-3 sensibility of siRhoH cells was detected by daily counting of siRhoH cells and control cells using Trypan Blue and Neubauer`s cell counting chamber. Cells were kept 4 days in medium without IL-3 until reaching of theoretical viability limit then IL-3 was readded into medium and again cell number and viability was determined for further 12 days (n=2, ±SD).

siRhoH cells seem to recover from starvation indicates that these cells may inhabit a stronger susceptibility to both IL-3 withdrawal and recovery. These experiments pointed out that RhoH overexpression not only inhibited the proliferation in these cells by the induction of IL-3 dependent STAT1 activation but also by the inhibition of IL-3 induced pro-proliferative signals via decreased STAT5 activation. At the same time low expression of RhoH resulted in an enhancement of STAT5 phosphorylation and an increased sensitivity to IL-3 stimulation in response to IL-3 which explains the previously observed IL-3 dependent proliferation advantage of siRhoH cells.

4.1.6 RhoH- a modulator of CD123 surface expression

To explain the enhanced STAT5 phosphorylation and the observed increased sensitivity to IL-3 in cells with low RhoH protein levels, the RhoH dependent surface expression of IL-3 receptor α chain (CD123) was measured. It was assumed that altered IL-3 receptor expression, and thereby distinct levels of ligand binding to its receptor in cells with altered RhoH levels, would consequently led to differences in the activation and the outcomes of IL-3 dependent downstream signalling, such as STAT5 activation and recover from starvation. To check this hypothesis Mock, siRhoH and RhoH cells were stained for the surface expression of CD123, and analysed via FACS **(Fig. 4.8A)**. The analysis of the cells attested that expression of CD123 was altered depending on the amount of RhoH present in the cells. RhoH overexpressing cells showed only about 30% CD123 surface expression compared to

that measured on control cells. Controversially, CD123 expression on the surface of siRhoH cells was enhanced. Previous reports suggest that an enhanced expression of surface CD123, observed in AML cells can be initiated by a STAT5 dependent upregulation of the transcription factor IRF-1[110]. To analyse RhoH and siRhoH and Mock cells for their IRF-1 expression levels, quantitative SYBR-green real-time PCR was performed **(Fig. 4.8B)**.

(A)

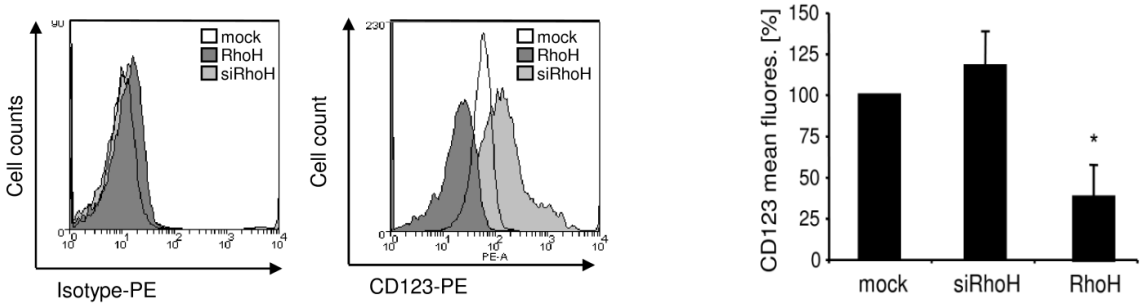

(B)

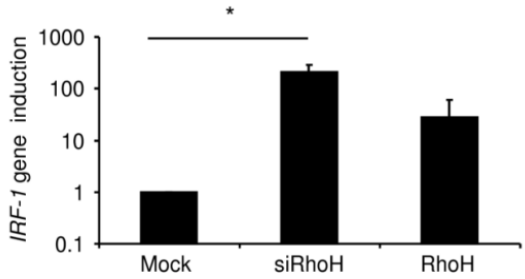

Fig. 4.8 RhoH levels modulate IRF-1 dependent CD123 surface expression in BaF3 cells
(A) (Left panel) FACS analysis of CD123 surface expression on control, siRhoH and RhoH cells was performed using a CD123-PE antibody. Specifity of staining was controlled by the usage of correlating PE-labeled antibody isotype reagent. (Right panel) Quantification of CD123 surface expression was determined using mean fluorescence values, and is presented as percentage of detected CD123 mean fluoresecence signal in control cells (n=3, mean±SD, *P≤0.05). (B) *IRF-1* mRNA in control, siRhoH and RhoH cells were determined using quantitative SYBR Green Real-Time PCR, *IRF-1* specific primers and *GAPDH* as reference gene. Obtained data was normalised against *GAPDH* reference gene expression and presented as fold induction of IRF-1 gene expression detected in empty vector transduced cells induction of *IRF-1* gene expression detected in control cells. Statistical relevance was determined using Student`s t-test (n=3, mean ± SD; *P≤0.05).

Interestingly siRhoH cells exhibited increased mRNA levels of IRF-1 compared to control cells, although RhoH overexpressing cells showed a prominent upregulation of IRF-1 mRNA levels as well. The upregulation of IRF-1 in siRhoH cells lead to the conclusion that a lack of RhoH in the cells induces IL-3 dependent STAT5 activation, eventually resulting in enhanced IRF-1 expression and by this leading to an increased expression of CD123 on the cell surface. These findings were also in line with the previously observed increased sensitivity to IL-3, since the increased CD123 surface expression may allow these cells to react with higher

efficiency to the addition of IL-3, than cells with less CD123 on their surface. IRF-1 is a well known target of STAT1 activation and is reported to have tumour suppressor functions[26]. The elevated IRF-1 expression detected in RhoH cells could be a result of the enhanced STAT1 activation caused by RhoH overexpression with other transcriptional consequences in the cells than the regulation of CD123 expression.

4.1.7 RhoH reconstitution correlated with a downregulation of prognostic AML markers in THP-1 cells

As mentioned above overexpression of the IL-3 receptor is a characteristic prognostic marker of AML cells[111,112]. Additional studies showed that there might be a correlation of constitutive STAT5 activation on the expression of the transcription factor IRF-1 finally resulting in the overexpression of CD123[110]. Moreover, recent publications highlighted the fact that AML cells also show decreased RhoH expression levels, which is associated with bad prognosis for patients[54]. To check whether the phenotype observed in AML cells could be caused by a lack of RhoH- and thereby be compensated through the reconstitution of RhoH, experiments with the AML cell line THP-1 were performed.

(A)

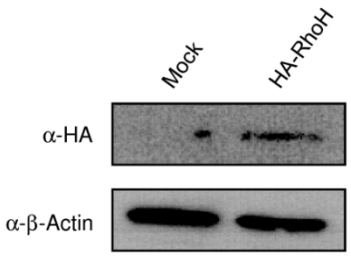

Fig. 4.9 AML cell line THP-1 mimics siRhoH phenotype
(A) THP-1 cells transfected with either pMX-IRES-HA-RhoH or pMX-IRES empty vector (Mock) were lysed 48 h post transfection. Samples were separated using 4-20% gradient SDS-PAGE. HA-expression and β-actin loading control were detected using enhanced chemiluminescence. (B) FACS analysis of CD123 in Mock and RhoH transfected THP-1 cells was performed using a CD123-APC antibody, specifity was determined with APC-labeled isotype control. Quantification of CD123 expression was determined using mean fluorescence values. Presented as percentage of detected CD123 mean fluorescence signal in control cells (n=3, mean ± SD, *P≤0.05). (B) *IRF-1* mRNA levels in Mock and RhoH overexpressing THP-1 cells, determined using quantitative SYBR Green Real-Time PCR, *IRF-1* specific primers and *GAPDH* as reference gene. Data was normalised against reference gene expression and presented as fold induction of *IRF-1* gene expression detected in control cells. Statistical relevance was determined using Student`s t-test (n=3, mean ± SD; ***P≤0.005).

(B)

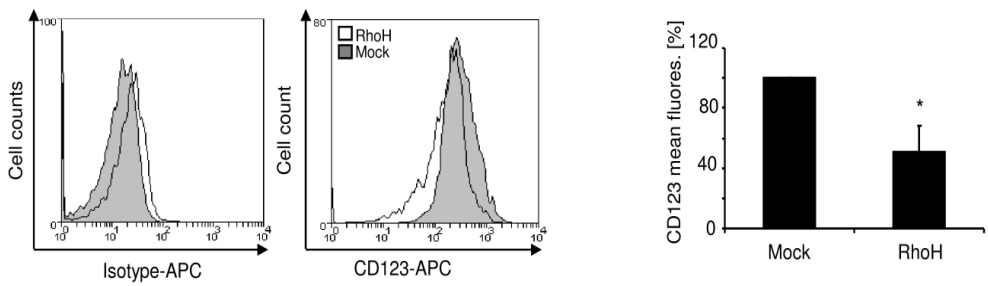

(C)

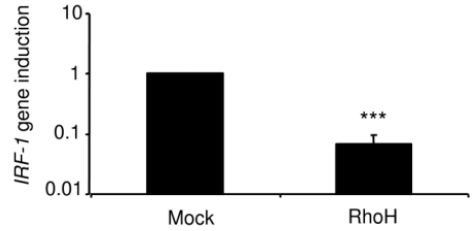

The monocytic THP-1 lineage is generated from a patient suffering from AML. First, human HA-tagged RhoH and the corresponding empty vector were transduced into THP-1 cells and expression was proved via western-blot **(Fig. 4.9A)**. Next, cells were FACS analysed for CD123 expression **(Fig 4.9B).** Comparing control cell with HA-RhoH transfected cells it became apparent that the overexpression of RhoH, led to an approximate decrease of 60% in CD123 surface expression **(Fig. 4.9B)**. To prove that the RhoH induced reduction of STAT5 activity would consequently lead to a decrease of IRF-1 expression in these cells, control and RhoH transfected cells were analysed for IRF-1 expression on mRNA levels **(Fig 4.9C)**. The observed IRF-1 levels in RhoH transfected versus control cells confirmed that through the reconstitution of RhoH into the AML cells, the THP-1 characteristic prognostic markers, CD123 and IRF-1 expression were downregulated, most likely through the RhoH induced inhibition of STAT5, and thus it was able to link the prognostic CD123 expression in AML cells to RhoH expression levels.

4.1.8 RhoH expression pattern in lymphoma derived cell lines

CD123 overexpression[53] as well as low RhoH expression levels[54] were independently from each other described as two negative prognostic markers for acute myeloid leukaemia. In an attempt to analyse other hematopoetic cell lines derived lymphoma for a yet unknown correlation with RhoH expression patterns, different leukaemia cell lines were subject to investigations. 40 to 60% of diagnosed ALCL inhabit a chromosomal rearrangement leading to the formation of the fusion protein NPM-ALK. Patient prognoses of NPM-ALK$^+$ (positive for NPM-ALK) lymphoma are generally considered worse than that of patients negative (-) for this specific rearrangement. This is due to the fact that the rearrangement results in the formation of a constitutively active version of the anaplastic lymphoma kinase, which seem to be involved in the activation of various tumorigenic signalling pathways[113]. In regard to the previous observations made in RhoH underexpressing BaF3 cells and AML cells, it was of particular interest to determine whether an underexpression of RhoH would be detectable in

different ALCL subtypes and if these findings would correlate with the expression pattern of the NPM-ALK fusion protein. To further specificy the observed phenomena on their lineage specifity, not only NPM-ALK positive and negative lineages were tested for their RhoH expression, but also other lymphoma derived lineages, such as B-cell Non-Hodgkin Lymphoma subtypes and mantle cell lymphoma types. As a positive control for RhoH expression, the human T-cell line Jurkat, with known expression, of RhoH[61], and as a negative control for RhoH expression the breast cancer cell cline MCF-7 was analysed on mRNA level. Data were first normalised against the expression of the reference gene *HPRT* and than normalised against the *RhoH* levels detected in Jurkat cells **(Fig. 4.10)**.

(A)

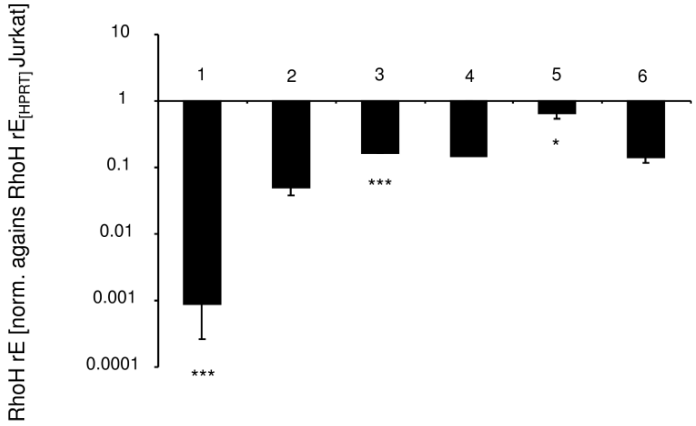

(A)	Cell line	Lineage/ cell type	Classification translocation t(2:5)
1	MCF-7	epithelial	Adenocarcinoma
2	SR-789	T-cell	ALCL, NPM+
3	Karpas 299	T-cell	ALCL, NPM+
4	DEL	T-cell	ALCL, NPM+
5	SU-MP2	T-cell	ALCL, NPM+
6	SU-DHL-1	T-cell	ALCL, NPM+

(B)

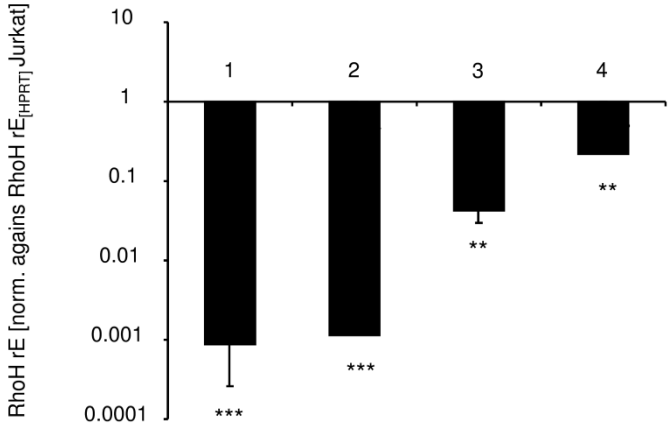

(B)	Cell line	Lineage/ cell type	Classification translocation
1	MCF-7	epithelial	Adenocarcinoma
2	Mac2A	T-cell	ALCL, NPM- t(8:9)
3	HH	T-cell	ALCL, NPM-
4	HUT78	T-cell	ALCL, NPM- t(2:8)

(C)

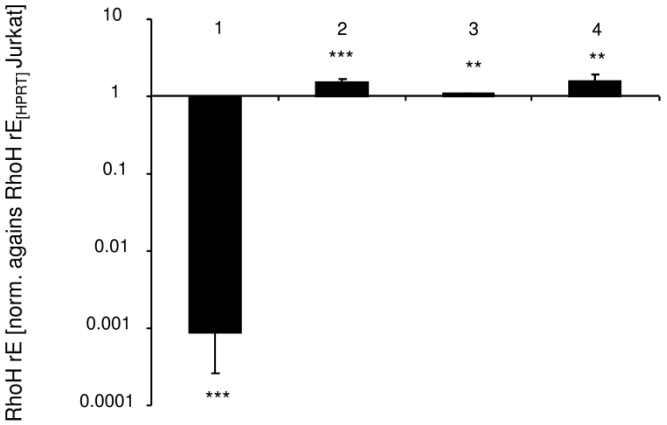

(C)	Cell line	Lineage/ cell type	Classification translocation
1	MCF-7	epithelial	Adenocarinoma
2	SUDHL6	B-cell	Mantle cell t(11:14)
3	NCEB	B-cell	B-NHL t(14:18)
4	Granta 519	B-cell	Mantle cell t(11:14)

(D)

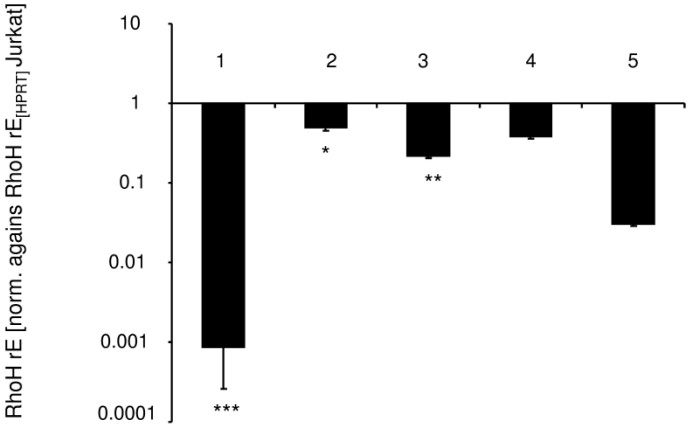

(D)	Cell line	Lineage/ cell type	Classification translocation
1	MCF-7	epithelial	Adenocarcinoma
2	OCILY1	B-cell	B-NHL, t(14:18)
3	SUDHL4	B-cell	B-NHL, t(14:18)
4	FL18	B-cell	B-NHL, t(14:18)
5	FL518	B-cell	B-NHL

Fig. 4.10 RhoH underexpression in lymphoma derived cell lines
RhoH mRNA was analysed from indicated cell lines, using quantitative SYBR green PCR and primers directed against human RhoH and the reference gene *HPRT*.The human breast cancer cell line MCF-7 served as negative control, while RhoH mRNA levels detected in Jurkat cells marked base line of *RhoH* expression. *RhoH* expression was normalised against *HPRT* and compared to expression levels detected in Jurkat cells. Statistical relevance was determined using Student`s t-test (n=3, mean± SD; *P≤0.05, **P≤0.01, ***P≤0.005)

Interestingly, almost all ALCL types showed a significant downregulation of RhoH expression, compared to that of Jurkat cells, indicated by the baseline. The most prominent downregulation could be detected in NPM-ALK$^-$ Mac2A cells, while the lowest regulation of RhoH was observed in the NPM-ALK$^+$ DEL cell line. However, a direct correlation between NPM-ALK fusion gene expression in ALCL cells and a certain RhoH expression pattern was not found. When comparing the results of RhoH expression in B-cell NHL, ALCL and B-cell mantle lymphomas there was a clear downregulation of RhoH detectable in ALCL and B-cell NHL cell lines. The two analysed B-cell mantle cell lymphomas, as well as the B-cell NHL cell line NCEB, showed an enhanced or almost equal level of RhoH expression in comparison to Jurkat cells.

4.1.9 Proteomics of RhoH in IL-3 dependent cell lines

To gain insight into how RhoH in detail interferes with IL-3 dependent signalling, GST-pulldown assays with recombinant GST-RhoH and lysates of BaF3 cells treated and untreated with IL-3 were performed. Resulting eluates were subject to mass spectrometric analysis with the aim to identify new interaction partners of RhoH, with special relevance for IL-3 dependent signalling events. To exclude unspecific binding two negative controls were used for pulldown assay. GST-only protein (25 kDa) was produced with *E. coli* transformed with GST-2T empty vector and additionally a T36A mutant variant of RhoH (resulting in an constitutive inactive variation of RhoH[85]) was cloned into GST-2T vector and the correlating recombinant protein was produced and used as an additional negative control **(Fig 4.11)**.

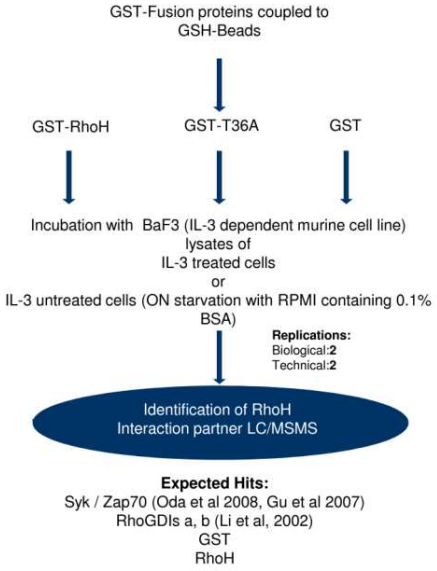

Fig. 4.11 Work-Flow Proteomics of RhoH
Produced GST fusion proteins were coupled to GSH Beads and incubated with lysates of BaF3 cells which were previously kept in IL-3 containing medium or were cultured 10-15 hours under IL-3 withdrawal in RMPI medium with 0.1 % BSA. Beads were washed and GST-fusion proteins were eluated from beads. After eluation samples were prepared for LC/MSMS and peptide fragments of interacting proteins were then identified using Mascot IPI software. Previously published or interaction partner of RhoH (Syk, Rho GDI 1 and 2), or expected hits (GST, RhoH) were identified and sorted out from hit-list.

The resulting recombinant GST-fusion proteins (45 kDa) were purified using columns packed with GSH-beads. SDS Page and Coomassie Blue staining of the purified proteins from the columns showed that there was indeed production of recombinant GST-fusion proteins of the expected size, as well as stable expression of GST-only protein detectable **(Fig. 4.12A).** However it should be mentioned that recombinant RhoH expression in *E.coli* is difficult to perform and requires six times the volume that is required, for instance for the production of GST-only protein (1 litre), since the induction of RhoH protein expression seems to be toxic

for bacteria. Additionally there was fragmentation of the final GST-RhoH-fusion protein **(Fig 4.12B).** The recombinant production of RhoH required stepwise substantial process improvement by careful selection of optimal production temperature, volume as well as the time frame of protein expression. Samples for mass spectrometric analysis were prepared from eluates collected from columns containing fusion-protein coupled beads which were incubated with lysates generated from either IL-3 treated or untreated cells.

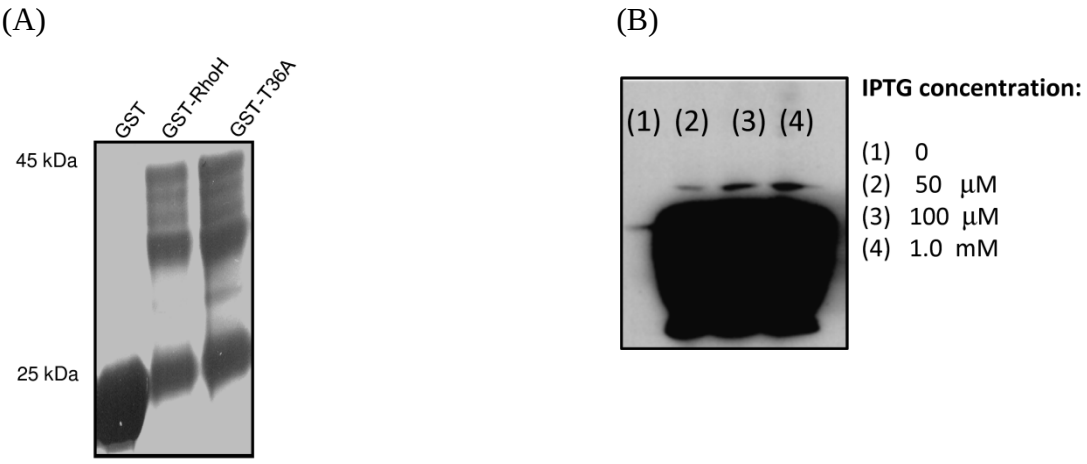

Fig. 4.12 Recombinantly produced GST-fusion proteins
(A) BL21 bacteria were transformed with GST-only, GST-RhoH and GST-RhoH-T36A, expression was induced and lysates prepared. After coupling to GSH beads, samples were run on gradient SDS-PAGE (4-20 %) (B) Western-blot analysis of GST-RhoH fusion protein production after induction of expression with different IPTG concentration, expression was allowed for 3 hours prior to lysis of BL21cells. Proteins were separated using 4-20% gradient SDS-PAGE.

4.1.9.1 Statistical evaluation of MS protein hits - Cytokine dependent binding events

Mass spectrometric data was analysed and related to proteins using the IPI-mouse databank. The results of two technical and two biological experiments, were combined and processed as follows: one peptide hits were considered as insolid hits and thereby removed, also proteins simultaneously occurring in GST-only, as well as in the RhoH and T36A samples, were removed. Known interaction partners (Zap70[89], Syk[114], GDI´s[61]) and GST, and RhoH itself were also considered as control proteins, and their identification was interpreted as indication for proper work-flow and experimental integrity. Next, redundant protein hits were combined and finally, to exclude further unspecific hits, results were checked for *E. coli* sequence homologues. Processed data was than manually sorted according to their "binding pattern" **(Appendix Tab. 6.1.1)**. For instance, some proteins were found to bind only to wt-RhoH and only when cells were treated with IL-3, others were binding exclusively to the T36A-RhoH protein and this again only when cells were treated with IL-3.

Tab. 4.1 Binding "pattern" of RhoH interaction partners

Binding „pattern"
RhoH (+ IL-3)
RhoH (– IL-3)
RhoH (+ IL-3) & (– IL-3)
T36 (+ IL-3)
T36 (– IL-3)
T36 (+ IL-3) & (– IL-3)
RhoH & T36 (+ IL-3)
RhoH & T36 (– IL-3)
RhoH & T36 (+ IL-3) & (– IL-3)
„No pattern"

Tab. 4.1 Binding patthern of RhoH interaction partners Listing of resulting groups of interaction partners when hits were sorted according to their binding behaviour to either wt-RhoH (RhoH) or T36A-RhoH indicated as T36 in regard of cytokine treatment (+/- IL-3)

From this interaction behaviour a chart with different binding conditions was postulated **(Tab.4.1).** Surprisingly, when protein interaction partners of wt RhoH and RhoH T36A were combined and statistically evaluated in a cytokine treatment dependent manner **(Fig 4.13)** it became clear that 115 proteins can bind to RhoH when cells were cultivated in IL-3 prior to their lysis, in addition, 133 proteins can bind to T36A under the same conditions. From these hits 31 were specific binding partners of wt-RhoH and 49 seem to be specific for T36A. Interestingly there was an overlap of 84 proteins being able to bind both the wt, and therefore active, GTP bound RhoH as well as the negative and conformational inactive variant T36A in a strictly IL-3 dependent manner **(Fig. 4.13A)**. Numbers of interacting proteins in IL-3 untreated samples were comparable between wt-RhoH (61), and T36A variant. Again there was an intersection of 38 proteins being able to bind to wt-RhoH and T36A variant **(Fig 4.13B)**. The examination of the numbers of the binding proteins in dependency of the cytokine treatment from these evaluations already suggested a strong relevance of IL-3 treatment. The numbers of the interacting proteins seem to decrease by 50% when recombinant proteins were incubated with lysates of cells cultured under IL-3 withdrawal **(Fig. 4.13 A, 4.13 B)**. This phenomenon becomes even more apparent when binding partners of the same recombinant sample are sorted according to their cytokine dependency **(Fig. 4.13C, 4.13D)**. From the total of 116 RhoH wt specific binding candidates, 83 are specifically occurring when cells are maintained in IL-3 prior to their lysis, only 28 proteins seem to bind only when cells were kept under starvation conditions and the binding of an intersection of 33 proteins remains to be unaffected by the cytokine treatment of the cells **(Fig. 4.13C)**. In the case of T36A a similar effect was observed **(Fig. 4.13D)**, from a total of 133 interaction partners for the T36A mutant of RhoH, 91 only bound when beads were incubated with IL-3 treated lysates, 24 were binding only when cells are not treated with IL-3 and an intersection of 42 proteins seemed to bind generally and independent of the IL-3 treatment **(Fig. 4.13D)**. These findings on the one hand indicated that there is a surprisingly high number of

interacting proteins which seem to be “blind” for the conformational changes of RhoH, induced by the T36A mutation. On the other hand, in line with the previous findings of this study, it was found that the binding of proteins interacting with RhoH seem to be strongly influenced by the IL-3 treatment of the cells, suggesting a specific IL-3 dependent role for RhoH in BaF3 cells. As aim of this work is to elucidate the role of RhoH in IL-3 dependent signalling the focus of further studies was directed towards hits occurring in wt-RhoH. For further studies in this work T36A specific hits were neglected.

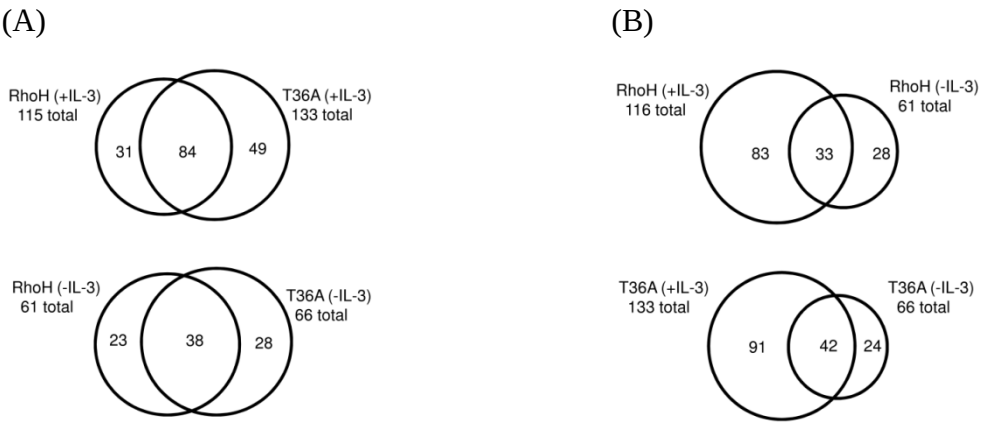

Fig. 4.13 Statistical evaluation of RhoH interaction partners: Venn diagrams
(A) Comparison of interaction partner, wt-RhoH (RhoH) versus T36A-RhoH (T36A) variant found in lysates of IL-3 treated BaF3 cells samples (upper panel), lower panel comparison of interaction RhoH versus RhoH T36A variant found in lysates of BaF3 cells after IL-3 withdrawal. (B) Comparison of detected interaction partner, form lysates of IL-3 treated BaF3 cells versus IL-3 untreated BaF3 cells, upper panel wt-RhoH lower panel T36A-RhoH variant.

To gain insight into the function of the RhoH wt binding proteins under different cytokine conditions a function dependent segmentation of the interacting protein hits was performed **(Fig 4.14)**. It was found that under IL-3 containing conditions, RhoH apppeared to bind preferentially to proteins, involved into metabolic processes in the cell **(Fig. 4.14A)**, these interactions occured to lesser extent when cells were kept under IL-3 withdrawal. This supported the previous findings in which RhoH inhibited cytokine induced proliferation.

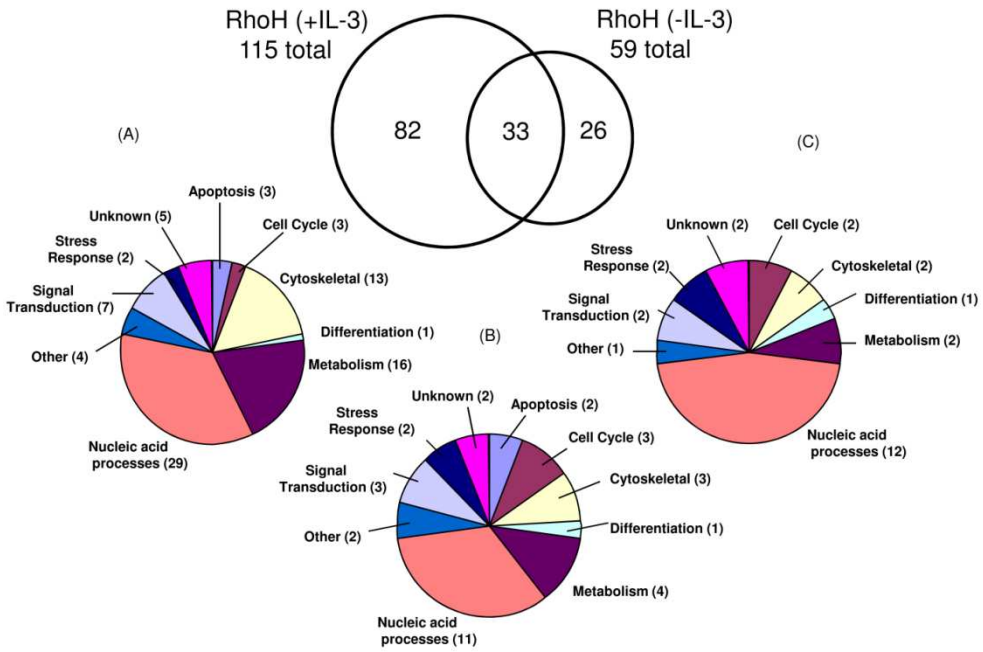

Fig. 4.14 Statistical evaluation of according to gene ontology of RhoH interacting proteins
(A) Gene ontology of RhoH interacting proteins binding exclusively when BaF3 cells were treated with IL-3 prior to lysis
(B) Gene ontology of RhoH interacting proteins binding independently of previous cytokine treatment of lysed cells.
(C) Gene ontology of RhoH interacting proteins found exclusively when cells were lysed after IL-3 deprivation -3.

4.1.9.2 Subcellular distribution of RhoH and T36A interacting proteins depends on IL-3

There are several publications in which RhoH is shown to be incorporated after posttranslational modifications on its CKIF motif into the lipid rafts of cells[68,87,89,115]. Cytokine stimulation is reported to induce protein trafficking and recruitment in the cell[116] which is important for various ongoing signal transducing mechanisms, such as cell proliferation. Cytokine induced posttranslational modifications of proteins can influence their ability to bind to certain adaptor proteins, which results in the accumulation of proteins into different cell compartments[117,118]. To clarify whether the capability of proteins to interact with RhoH changes with IL-3 treatment and to gain insight into possible consequences on functional and signal transduction of IL-3 withdrawal on RhoH mediated signalling, the interaction partners of RhoH, were sorted according to their localisation within the cell and in dependency of cytokine treatment.

By this, the importance of cytokine induced posttranslational modifications of cellular proteins leading to an enhanced binding capacity to RhoH would be clarified. Also the validation would address the question of whether there is a cytokine dependent influence of preferred RhoH binding to specific groups of proteins. Additionally, the data generated from the T36A mutant was also reviewed and checked for similarities in the subcellular distribution

between wt RhoH and T36A binding interaction partners since this mutant still inhabits a functional CAAX-box, which was reported to play an important role in protein-protein interaction[64].

First hits were sorted in different interaction patterns depending on the cytokine treatment **(Tab. 4.1)**. The majority of protein hits showed a clear affiliation to one of the resulting groups but there was also a cluster of proteins of randomly occurring hits. Assuming that these proteins are most likely unspecific interactions, the focus was set on the proteins of the remaining groups with clear affiliation patterns. Comparison of the statistical distribution of the hits detected in RhoH wt samples incubated with IL-3 treated cell lysates **(Fig. 4.15)** with the distribution pattern of interaction partners found in samples without IL-3 treatment or with samples of the T36A mutant, regardless of the cytokine treatment, it showed that 14% of interacting proteins were related to the cytoskeleton **(Fig. 4.15A)**. This was not present in all other samples **(Fig. 4.15B, C, D)**. Another remarkable observation was made when the section of "nuclear" located hits of the cytokine treated wt RhoH sample **(Fig. 4.15A)** was compared to the hits occurring in the other samples. The contingent of nuclear located proteins increased from 5% in RhoH wt samples with IL-3 treatment as high as 30% in the other samples **(Fig. 4.15B, C, D)**. The subcellular evaluation of the interaction partner indicated that RhoH seemed to be able to interact with differently localised proteins in the cell upon IL-3 treatment, most likely depending on their cytokine induced altered posttranslational conformation. Also this statistical read-out was interpreted as indication that RhoH might shuttle, depending on IL-3 treatment, between the nucleus and the cytoplasmic compartments of the cell. Furthermore it was clarified that although the T36A mutation of RhoH does not seem to directly influence the binding capacity of the GTPase, it did however decrease the ability of the protein to efficiently interact with proteins located in the cytoskeleton.

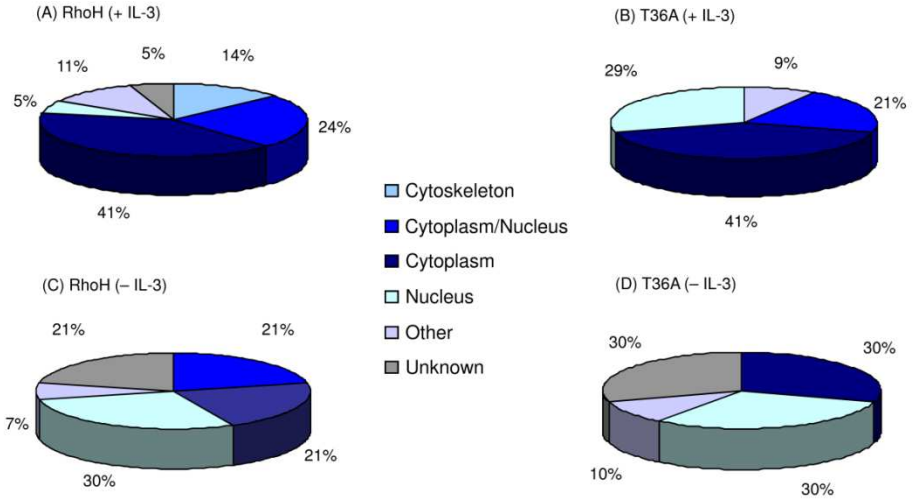

Fig. 4.15 Statistical evaluations of RhoH /RhoH T36A interacting proteins according to their subcellular localisation in dependency of IL-3 treatment
(A) Subcellular localisation of RhoH (wt) interacting proteins when recombinant GST-fusion proteins were incubated with lysates of IL-3 treated cells. (B) Subcellular localisation of RhoH (wt) interacting proteins when recombinant GST-fusion proteins were incubated with lysates of cells cultivated under IL-3 withdrawal. (C) Subcellular localisation of RhoH-T36A interacting proteins when recombinant GST-fusion proteins were incubated with lysates of IL-3 treated cells. (D) Subcellular localisation of RhoH-T36A interacting proteins when recombinant GST-fusion proteins were incubated with lysates of cells cultivated under IL-3 withdrawal.

4.1.9.2.1 IL-3 dependent localisation of RhoH

To address the question of whether there is an IL-3 depending "shuttling" of RhoH, as indicated by the mass spectrometry data, BaF3 cells were retrovirally infected with flag-tagged RhoH (**Fig. 4.16A)**. Transduced cells were either kept under IL-3 starvation conditions or were starved and restimulated with IL-3. They were then intracellularly stained with a FITC labelled flag-tag antibody. First microscopic analysis suggested that there might be an IL-3 dependent shuttling of RhoH, partly explaining the generated mass spectrometry analysis **(Fig. 4.16A)**. After IL-3 treatment however RhoH still is located in the nucleus but is also clearly to a higher percentage present in the cytoplasmic region of the cells. At the same time it seemed that starvation of IL-3 induces RhoH protein degradation **(Fig. 4.16A)**. Lysosomal processing of RhoH, and thereby regulation of RhoH, is already known to be an early event after proximal TCR activation[72]. Another initial experiment was performed to provide further insight to the intracellular distribution of RhoH on protein level **(Fig. 4.16B)**. IL-3 treated and untreated BaF3 cells were lysed to obtain nuclear and cytoplasmic fractions. Western-blot analysis of RhoH protein and β-Actin as an indicator for the cytoplasmic fraction, appeared to confirm the preliminary microscopy. In this experiment RhoH was detected in the cytoplasmic fraction of IL-3 treated cells, while in cells cultured without IL-3 no RhoH protein was detectable.

(A)

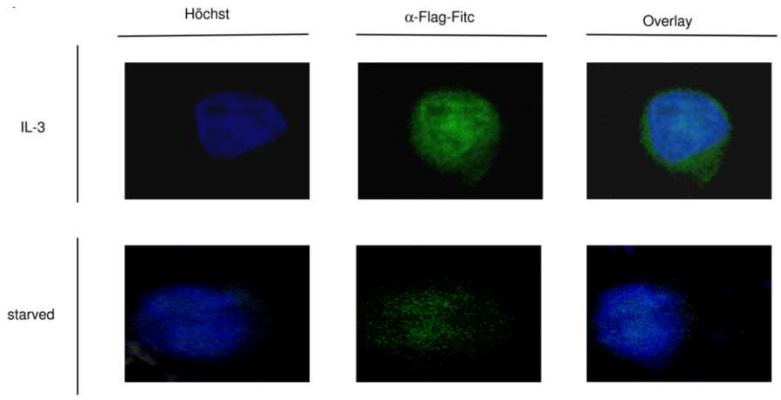

(B)

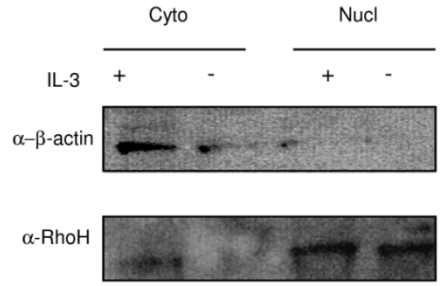

Fig.4.16 IL-3 dependent subcellular localisation of RhoH
(A) Confocal microscopy of IL-3 treated (upper panel) or starved (lower panel) BaF3 cells transduced with Flag-RhoH overexpressing vector. First row shows nuclear staining with Höchst, second row shows staining of Flag tagged RhoH with FITC labeled flag antibody, third row show overlay of Höchst and FITC staining (B) Following IL-3 cultivation or three hours of starvation BaF3 cells cell proteins were separated into nuclear and cytoplasmic fraction. Lysates were separated using 4-20 % gradient SDS-PAGE. Cytoplasmic contents were indicated by detection of β-actin.

In both conditions RhoH was detectable in the nuclear fraction. However, to make final conlusions the experiment needs to be repeated with more appropriate loading controls for the cytoplasmic (e.g Tubulin) instead of β-Actin, as well as for the nuclear fraction (e.g Lamin).

4.1.9.3 Verifying RhoH protein interactions – Cofilin-1 (Cof-1)

The mass spectrometry analysis revealed Cofilin-1 (Cof-1), a 19 kDa sized, ubiquitous protein as a RhoH interacting candidate in IL-3 treated samples. Cof-1 is a promoter of actin polymerisation and filament elongation[119]. As a downstream effector of the GTPases Rac1 and Cdc42 it is known as a key molecule of cytoskeleton rearrangement[74]. To verify the data obtained from the mass spectrometry experiments, the binding of RhoH to Cof-1 was tested in HEK cells. HEK cells were cotransfected with HA tagged RhoH and GFP-Cof-1. HEK cells lack IL-3 receptor surface expression, as such, HEK cells required treatment with sodium ortho vanadate (Na_3VO_4), which inactivates phosphatases and thereby mimics an IL-3 treated activation state. It was found that in HEK cells the interaction of Cof-1 and RhoH only occurred when cells were activated by Na_3VO_4 prior to lysis **(Fig. 4.17)**.

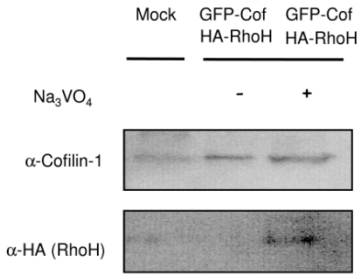

Fig. 4.17 Verification of RhoH interacting protein Cofilin-1 in HEK cells HEK cells were cotransfected with GFP-Cofilin-1 overexpression and HA-RhoH overexpression vectors or with empty vector only (control) for 48 hours. HEKcells were treated with 1mM Na_3VO_4 or left untreated, lysed and IP was performed using either antibody against Cofilin-1. Samples were separated using gradient (4-20%) SDS PAGE. Precipitated proteins were targeted using antibodies against RhoH (lower panel) and Cofilin-1 (upper panel) and were detected with enhanced chemiluminescence.

This binding of RhoH and Cof-1 confirms the results of the mass spectrometry analysis and also suggests that also in BaF3 cells the interaction of RhoH and Cof-1 would occur only after IL-3 treatment of the cells. This interaction partner of RhoH could contribute to future understanding of how RhoH takes part in cytoskeleton related processes such as migration of hematopoietic cells by a mechanism other than the previously reported inhibition of other GTPases[85,87].

4.1.9.4 Verifying RhoH protein interactions- Protein tyrosine phosphatase 1B (PTP1B)

The mass spectrometry analysis revealed the ubiquitously expressed phosphatase PTP1B, a 50 kDa sized protein, as a RhoH interacting candidate in IL-3 treated samples. Different publications show that PTP1B is able to target the JAK-STAT signalling pathway[20,120-122] and IL-3 dependent proliferation [123]. Therefore the potential interaction of RhoH with PTP1B may have contributed to the observed RhoH modulated IL-3 dependent effects. To verify the specificity of the binding of RhoH to PTB1B, HEK cells were cotransfected with flag-tagged RhoH and PTP1B. Again, because of the lack of IL-3 receptor on HEK cells, treatment with Na_3VO_4 was required. The results showed that in HEK cells the interaction of PTP1B and RhoH is only formed when cells were set in a state of activation, and is not detectable when cells remain in an inactivated state **(Fig. 4. 18)**.

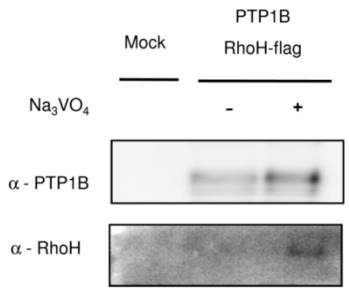

Fig. 4.18 Verification of RhoH interacting protein PTP1B in HEK cells
HEK cells were cotransfected with PTP1B overexpression and HA-RhoH overexpression vectors or with empty vector only (control), for 48 hours. HEK cells were treated with 1mM Na_3VO_4 or left untreated, lysed and IP was performed using antibody against PTP1B. Samples were separated using gradient (4-20%) SDS page. Precipitated proteins were targeted using antibodies against RhoH (lower panel) and PTP1B (upper panel) and were detected with enhanced chemiluminescence.

4.2 RhoH in IL-3 derived bone marrow MCs

The aim of this work included investigations of the physiological role of RhoH on IL-3 dependent processes in murine MC. In early studies supernatant derived from mitogen-activated T-cells was used to induce MC differentiation[124,125].IL-3 was identified to be the cytokine which directed the differentiation of $CD34^{+}$/c-Kit^{+} cells into functional MCs[126,127]. However, the details of the signalling cascade that triggers the differentiation to MCs remains fairly unknown. RhoH has been reported to be of importance for the development, survival and the differentiation of hematopoietic progenitor cells[85]. Together with the previous findings of this study regarding its relevance for IL-3 mediated signal transduction and its effect on CDKI expression it was decided to elaborate the impact of a lack of RhoH for IL-3 mediated differentiation and of murine hematopoietic progenitor cells to functional MCs in more detail.

4.2.1 RhoH mRNA expression in IL-3 derived murine MCs

The relevance of RhoH for IL-3 mediated MC development from HPC was investigated. It was assumed that unregulated or extremely low expression levels of RhoH would suggest a minor role for the atypical GTPase in the differentiation and function of murine MCs. Bone marrow cells (BMCs) isolated from C57BL/6 wt mice femurs were cultivated for 27-30 days in IL-3 containing medium. mRNA samples isolated from these progenitor cells at different time points and RhoH expression was measured using quantitative real-time PCR and GAPDH as reference gene **(Fig. 4.19)**. The results of the quantification of RhoH mRNA levels show a decrease of approx. 40% of RhoH mRNA on day 5 (compared to day 0), followed by an upregulation of RhoH mRNA and remains stably expressed at this level during the period of cultivation. From these results it was assumed that RhoH plays a defined role in the process of IL-3 dependent murine MC signalling.

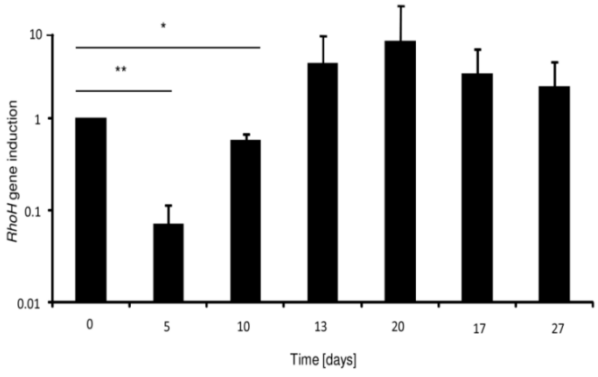

Fig. 4.19 RhoH mRNA expression in murine HPCs differentiating to mast cells over 27 days (4-weeks) wt mice BMCs were isolated (day 0) and cultivated in IL-3 containing medium for 4 weeks. At indicated time points, mRNA was prepared and RhoH expression was detected using *RhoH* specific primers, *GAPDH* served as reference. *RhoH* expression was normalised against *GAPDH* and are shown fold induction in comparison to day O. Presented results from one representative experiment performed in duplicates ± SD (n=3)

4.2.2 RhoH null HPCs show elevated IL-3 induced proliferation

It was tested whether the findings made in the BaF3 model system were transferable to the more physiologic system of MCs. Therefore the IL-3 dependent proliferation behaviour of yet undifferentiated hematopoietic progenitors from RhoH null mice in comparison to wt mice progenitor cells was observed. The proliferation assay was performed early after isolation of BMCs, which was posted between day three and day five after isolation of cells from the bone marrow. A Cell Titer Glo assay was performed to measure ATP levels after cells were cultivated for 24 hours at distinct IL-3 concentrations **(Fig. 4.20A)**. The read out of this assay showed that IL-3 concentrations higher than 0.01 ng/ml were able to induce proliferation of cells both, from RhoH null and wt mice origin. While wt progenitor cells reached a plateau of proliferation at 0.1 ng/ml, RhoH null progenitor cells showed a remarkable ongoing increase in proliferation **(Fig. 4.20A)**.

(A)

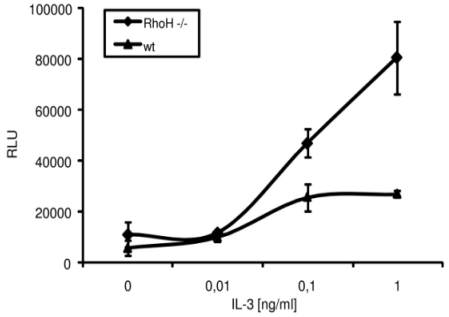

(B)

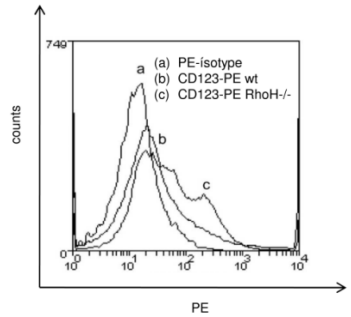

(C)

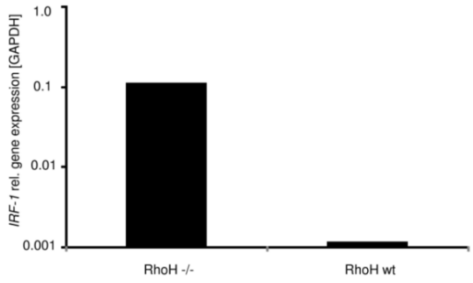

Fig. 4.20 IL-3 induced proliferation, IRF-1 expression and CD123 surface expression in progenitors from RhoH deficient are similar to that observed in siRhoH BaF3 cells
(A) IL-3 dose response curve of RhoH null and wt progenitor cells (day 3-5 after preparation) cultivated for 48 h in medium with indicated IL-3 concentrations. Viability of cells was analysed by ATP determination in a Cell Titer Glo assay. Presented results from one representative experiment performed in triplicates ± SD (n=2). (B) FACS analysis of CD123 surface expression on wt and RhoH null progenitor cells in IL-3 containing medium, was performed using a murine CD123-PE antibody. Antibody specifity was controlled by the usage of correlating PE-labeled antibody isotype reagent. Presented results from one representative experiment (n=3). (C) Normalised *IRF-1* mRNA levels detected in progenitor cells cultivated 3-5 days in IL-3 containing medium using quantitative SYBR green Real-Time PCR with *IRF-1* specific primers and *GAPDH* as a reference gene. Presented results from one representative experiment performed in duplicates (n=2).

The impressive observation of RhoH null proliferation response to cultivation in IL-3 containing medium confirmed that RhoH indeed functions as a negative regulator of IL-3 dependent proliferation not only in the BaF3 model system, but also in progenitor cells. From this experiment it was concluded that RhoH deficient progenitor cells show, similar to siRhoH cells, an increase in IL-3 induced proliferation. To clarify whether these increased proliferation rates were due to an increased sensitivity to IL-3 and thereby enhanced pro-proliferative signal delivery to the progenitor cells lacking RhoH expression, the surface expression of CD123 was determined using FACS analysis **(Fig. 4.20B).** Here again the previous results obtained from the model system BaF3 cells with knock-down of RhoH were able to be reproduced in RhoH null mice progenitor cells. Indeed RhoH deficient progenitor cells showed a substantially higher surface expression of CD123 than wt progenitors. This enhanced CD123 expression was detectable over the period of differentiation and mast-cell *in vitro* cultivation. Since the elevated CD123 levels in siRhoH cells were a result of enhanced expression of the STAT5 dependent trabscription factor IRF-1, IRF-1 mRNA levels of progenitor cells lacking RhoH in comparison to that found in wt mice were analysed using quantitative PCR to clarify whether the observed effects in MCs were related to that observed in siRhoH cells **(Fig. 4.20C)**. The results of the IRF-1 mRNA quantification suggested that there may be the same correlation between enhanced STAT5 dependent IRF-1 expressions which ended up in elevated CD123 surface expression in IL-3 cultivated progenitor cells.

4.2.3. RhoH null HPCs show lower $p21^{waf/cip1}$ and $p27^{kip1}$ mRNA expression only in early phase of IL-3 cultivation

It was hypothesised that the increased proliferation observed in RhoH null progenitors could be indicative of a defective ability to differentiate in response to IL-3 into MCs, due to a shorter duration phase of cells in the G1-phase. Studies made with pluripotent cells showed that upon decreased entry of cells into G1-phase, the differentiation and cell-fate-decision processes are introduced[128]. In turn, cells that show high rates of cell division seem to be more resistant to these processes[129]. The mRNA levels of the cell cycle inhibitors $p21^{waf/cip1}$ and $p27^{kip1}$ were measured in freshly isolated and in IL-3 cultivated bone marrow progenitor cells from RhoH null mice and wt mice **(Fig. 4.21A)**. The detected CDKI levels were normalised against GAPDH and were compared (fold induction). The results showed that $p21^{waf/cip1}$ and especially $p27^{kip1}$ show an increased expression than measured in hematopoietic progenitors from wt mice in the early stage of cultivation with IL-3. $P21^{waf/cip1}$ [34] showed a 4-fold higher mRNA expression in normal progenitor cells and $p27^{kip1}$ mRNA levels, were found to be 14-

fold higher in progenitor cells expressing RhoH in the early cultivation state. To check whether the decreased expression of $p21^{waf/cip1}$ and $p27^{kip1}$are stable during the differentiation of the RhoH null progenitor cells to MCs, $p21^{waf/cip1}$ and $p27^{kip1}$expression was tested in different stages of differentiation **(Fig. 4.21B)**. Interestingly, expression differences in $p21^{waf/cip1}$ and $p27^{kip1}$ were found to diminish after the early state of cultivation in IL-3 (day 3-5), and $p27^{kip1}$seem even to be slightly, increased in RhoH-/- cells. This dynamic recovery of $p21^{waf/cip1}$ and $p27^{kip1}$mRNA expression levels of RhoH ko mice indicated that RhoH deficient progenitors may proliferate with increased rates and show less duration in G1-phase in the very early state of *in vitro* culture in IL-3. Although there were clear differences in the early expression of $p21^{waf/cip1}$ and $p27^{kip1}$the proceeding efficient upregulation of CDKI expression levels indicated that proliferation rate of RhoH null progenitor cells will decrease during the course of MC differtentiation in IL-3 containing medium.

(A) (B)

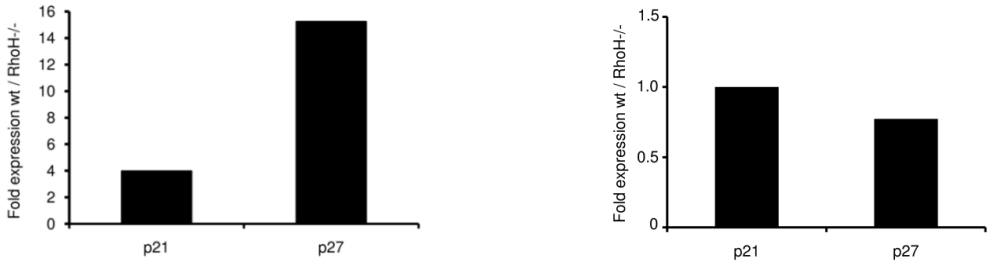

Fig. 4.21 RhoH null progenitor cells dynamically upregulate CDKIs during mast cell differentiation
(A) mRNA from BMC of wt and RhoH null mice, day 3-5 after preparation (cultivated in IL-3 containing medium)was prepared and analysed for CDKI *$p21^{waf/cip1}$* and *$p27^{kip1}$* expression with quantitative SYBR green real-time PCR. P*$21^{waf/cip1}$* and *$p27^{kip1}$* levels were normalised against the reference gene *GAPDH* and presented as fold induction compared to levels detected in wt mice. Presented results from one representative experiment performed in duplicates (n=2). (B) mRNA from progenitor cells of wt and RhoH null mice, after day 5 were cultivated in IL-3 containing medium was prepared and CDKI *$p21^{waf/cip1}$* and *$p27^{kip1}$* expression was quantified SYBR green real-time PCR and *$p21^{waf/cip1}$/$p27^{kip1}$* specific primer. *$P21^{waf/cip1}$* and *$p27^{kip1}$* levels were normalised against the reference gene *GAPDH* and presented as fold induction compared to levels detected in wt mice. Presented results from one representative experiment performed in duplicates (n=3) and presented as fold induction compared to wt mice.

4.2.4. RhoH null progenitors show no differences in the differentiation to MCs

The IL-3 induced differentiation capability of HPC of RhoH null mice to develop into MCs was tested by analysing the MC specific markers c-Kit and FcεRI during MC differentiation. For this purpose RhoH null and wt progenitors were cultivated 4 weeks in IL-3 containing medium. Each week the expression pattern of FcεRI and c-Kit receptor were analysed after IgE mediated activation of the cells. The FACS analysis of c-Kit and FcεRI expression of RhoH null MCs in comparison to RhoH wt MCs indicated no differences in MC development**(Fig. 4.22A)**, the same was true for all time points **(data not shown)**. To address

the question of morphologic differences between RhoH deficient and wt MCs, which could occur independently of the expression of MC specific surface markers MC specific histological Touluidine Blue staining of MCs was also performed. The metachromatic staining of MCs derived from RhoH null and wt mice indicated no obvious morphologic abnormalities between RhoH null and wt MCs **(Fig. 4.22B)**. Additional western-blot analysis of MC specific proteases confirmed that RhoH null progenitors can differentiate to MCs **(Fig. 4.22C)**.However, these *in vitro* experiments do not clarify the *in vivo* situation regarding MC development, number and distribution in RhoH KO mice.

(A)

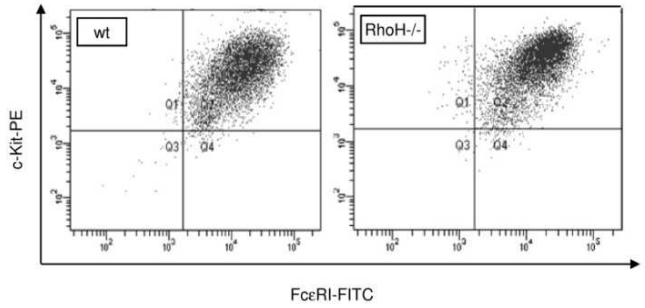

(B)

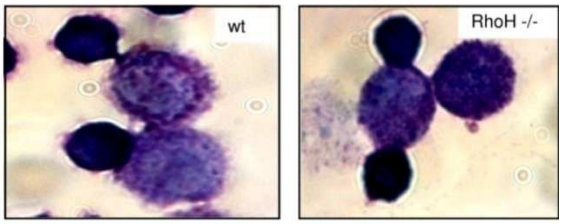

(C)

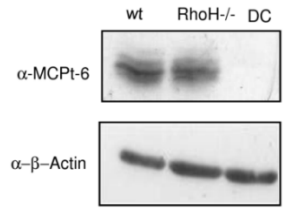

Fig. 4.22 RhoH-/- progenitor cells differentiate to morphological typical mast cells
(A)FACS analysis of mature MCs (right panel: wt, left panel: RhoH null) MCs were activated with 1% IgE overnight and co-stained with PE-c-KIT and FTIC-FcεRI antibody. Presented results from one representative experiment (n=3). (B) Cytopspins from bone marrow derived MCs (week 4) were prepared and stained with Touluidine Blue (n=2)(C) Lysates of MCs from RhoH ko and wt mice as well as dendritic cells (DCs) from control mice were prepared and separated using 12% SDS PAGE. Proteins were detected using enhanced chemicluminescence. Presented result from one representative experiment (n=2).

4.2.5. RhoH is important for FcεRI mediated degranulation of MCs

There were no obvious morphologic differences reported for neutrophils generated from RhoH ko mice. However, the GM-CSF induced neutrophil specific release of leucotriene, and thereby the function of neutrophils, was found to be impaired in RhoH ko mice[106]. To check whether the same would be true for MC specific functions of IL-3 derived RhoH ko MCs, showing previously no obvious morphologic or developmental defects, the antigen triggered

release of the major mediator of anaphylaxis, histamine, was measured. β-hexsosaminidase assays were performed using fully differentiated IL-3 derived MCs from RhoH ko and wt mice. Degranulation of MCs was triggered after the antigen, trinitrophenol (TNP)-haptenised ovalbumin (OVA), induced aggregation of the IgE bound FcεRI, therefore MCs were first incubated with 1% anti-TNP-OVA-IgE conditioned medium and then challenged with distinct concentrations of TNP-OVA (0-10 ng/ml). The released as well as the remaining intracellular MC mediators were measured. The measurement of this enzyme is a parameter allowing inferences on the release of MC specific mediators, including histamine. Interestingly, the results of the colourimetric reaction indicated defective MC antigen mediated degranulation of RhoH deficient MCs. At each TNP-OVA concentration RhoH deficient MCs were found to degranulate to a lesser extent than wt MCs. Most remarkably at the lowest TNP-OVA concentration of 0.0001 ng/ml RhoH ko MCs were found to degranulate to less than 25% of the degranulation potential detected in wt MCs **(Fig. 4.23)**. Even at the highest TNP-OVA concentration of 10 ng/ml the MCs lacking RhoH show degranulation decreased to 60% of the amount measured in wt MCs **(Fig. 4.23)**. These experiments suggest that even though RhoH does not play a role in the IL-3 dependent differentiation of MCs, the antigen mediated function of MCs, such as degranulation, seem to suffer from the lack of RhoH and that there may be defects in FcεRI mediated signal transduction.

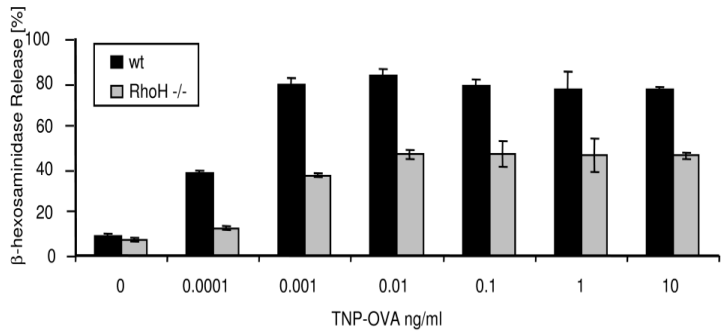

Fig. 4.23 Defective histamine release of RhoH null mast cells
Histamine release of MCs derived from RhoH null and wt mice BMCs, previously activated with 1% anti-TNP-OVA-IgE overnight and incubated with indicated concentrations of antigen TNP-OVA for 1h. Degranulation was determined by β-hexosaminidase release. Presented results from one representative experiment performed in triplicates (mean ± SD); n=2.

4.2.6. RhoH$^{-/-}$ MCs show impaired release of IL-6 and TNF-α

To address the question of functional defects caused by a lack of RhoH in MCs, cytokine release was determined. MCs are known to release pro-inflammatory cytokines in response to antigen challenge and thereby induce and promote immune responses in the organism[130]. Degranulation of MCs was again triggered by TNP-haptenised OVA induced aggregation of the IgE bound FcεRI. From previous hexsosaminidase experiment it was concluded that an antigen concentration of 0.1 ng/ml would be sufficient to trigger efficient MC cytokine release. The comparing the released cytokine concentrations showed that there were again

strong differences between MCs of wt and RhoH ko animals **(Fig. 4.24)**. The release of the pro-inflammatory cytokine IL-6, which is known to target immune cells such as T-cells and other cell types[131,132], was remarkably decreased in MCs of RhoH deficient mice **(Fig. 4.24A)**. In comparison to wt MCs, which released about 420 ng/ml of IL-6, RhoH deficient MCs were only capable of releasing less than the half this amount of IL-6, with a concentration of approx. 200 ng/ml. The decrease in TNF-α release, also playing a major role in host immune defence and inflammatory reactions[133] was even more impressive **(Fig. 4.24B)**. While antigen challenged wt MCs released about 380 ng/ml, of TNF-α the release from RhoH deficient MCs was negligible. Again this observed defect in antigen induced cytokine release indicated that downstream signalling of FcεRI mediated signals are impaired due to the lack of RhoH.

(A) (B)

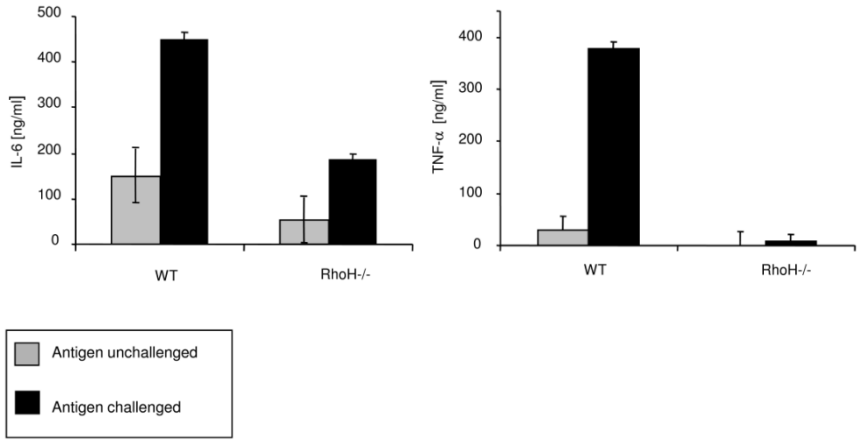

Fig. 4.24 Defective cytokine release of RhoH null mast cells
(A)IL-6 release of MCs derived from RhoH null and wt mice BMCs, previously activated with 1% anti-TNP-OVA-IgE overnight and either treated with 10 ng/ml TNP-OVA or left untreated for 5 h. Release was determined by IL-6 specific ELISA. Presented results from one representative experiment performed in triplicates (mean ± SD) n=2. (B) TNF-α release of MCs derived from RhoH null and wt mice BMCs, previously activated with 1% anti-TNP-OVA-IgE overnight and either treated with 10 ng/ml TNP-OVA or left untreated for 5 h. Release was determined by TNF-α specific ELISA. Presented results from one representative experiment performed in triplicates (mean ± SD) n=2.

5. Discussion

5.1 RhoH expression is regulated by IL-3 and modulates IL-3 induced proliferation

The results of this study have demonstrated that RhoH functions as an inhibitor of IL-3 dependent cell proliferation. Neither the starvation nor the long-term cultivation of IL-3 dependent BaF3 cells was shown to have an effect on the regulation of RhoH expression levels. Only treatment of starved cells with IL-3 caused a downregulation of RhoH mRNA levels within 5 hours **(Fig. 4.1)**. The results confirmed a transcriptional regulation of RhoH in IL-3 mediated signal transduction. Transcriptional regulation of RhoH was already shown by pervious studies to to be crucial for proper signalling in T-lymphocytes and neutrophils[61,106]. In contrast to this study the treatment of T-lymphocytes and neutrophils with PMA or GM-CSF led to an increase of RhoH expression and thereby the transcriptional upregulation of RhoH was interpreted as indication for a functional role of RhoH in the defined cell subsets by the investigators[61,106]. However, since RhoH is known to be a negative regulator of hematopoietic cell proliferation[85] it was assumed that IL-3 dependent induction of proliferation would most probably cause a decrease of endogenous RhoH levels to allow proproliferative signalling. The considerably high levels of RhoH, when cells are kept continuously in IL-3 containing medium and after IL-3 starvation **(Fig. 4.1)**, suggests that RhoH levels are dynamically upregulated and remain enhanced to control events involved in IL-3 mediated signalling. Analysis of IL-3 dependent cell proliferation with altered RhoH levels confirmed previous work of Liu in which high RhoH levels had a specific inhibitory effect on IL-3 dependent proliferation regardless of the IL-3 concentration[102] in comparison to parental BaF3 cells **(Fig. 4.3)**. In this study an additional control (Mock), as well as RhoH underexpressing cells were included into CTG proliferation analysis, proofing the reliability of the previous results[102]. While the proliferation assay with constant IL-3 concentrations shows rather small differences between the proliferation rates of the distinct cell lines **(Fig. 4.3A)**, the CTG assays clarify the inhibitory effect of RhoH on IL-3 mediated proliferation **(Fig. 4.3B)**. Assays were carried out with empty vector transduced cells as control. Since shRNA was used for knock-down of RhoH it should be considered to use BaF3 cell transduced with control shRNA containing vector as additional control for proliferation as well as signalling experiments to disclude shRNA mediated off-target effects.

However, since RhoH underexpressing cells seem to reach inhibitory levels of proliferation at latter time points, future experiments could include the investigation of proteins which are involved in contact inhibition of proliferation, which might be deregulated by a lack of RhoH [134,135]. RhoH is a known negative regulator of the adhesion protein LFA-1[136] and also of Rac1[61,87], several reports show that adhesion molecules, as well as the GTPase Rac1, are taking a substantial part in mediating growth inhibiton[134,135]. The results also highlighted that the inhibitory effects that RhoH had on proliferation were specific for IL-3 induced proliferation and are not detectable when the cytokine IL-3 is replaced by the growth factor Epo **(Fig 4.3C)**. Although, Epo does not belong to the IL-3 family of cytokines[15]. To check whether some of the observed effects may result from a RhoH dependent deregulated signalling of the common β chain of the IL-3 receptor further proliferation experiments with IL-5 and GM-CSF should be considered since JAK-STAT mediated signaltransduction, for example, is reported to depended partly on the on the common β chain of the IL-3 receptor[13]. Finally it would be interesting to investigate the consequences on IL-3 dependent proliferation of the T36A mutant variant of RhoH, since it is reported that SCF-1 mediated proliferation in HPCs remains unaffected when the T36A variant instead of wt RhoH is transduced into the cells.

5.2 RhoH: Fine-tuning of IL-3 dependent JAK-STAT signalling

The JAK-STAT pathway is one of the major signalling cascades in hematopoietic cells, controlling cell survival, proliferation and differentation[137,138]. STAT1 is known to initiate the transcription of genes leading to cell cycle arrest or apoptosis in cells[30]. RhoH expression was reported to induce apoptosis in HPCs, explaining the observed decreased cell counts[85]. Preliminary data from Lius` work suggest that increased RhoH levels modulate STAT1/STAT5 activity[102]. However, these experiments were performed with parental BaF3 cells as control cell line and did not include the investigation of RhoH underexpressing cells. In this study it was confirmed that increased RhoH expression amplified IL-3 induced STAT1 phosphorylation **(Fig. 4.4)** in comparison to empty vector transduced cell line. The FACS experiments imply slightly less IL-3 induced STAT1 phosphorylation in siRhoH cells compared to control cells. The significance of this difference however was not determined during this study and can be subject for future experiments. The STAT1 activation did not lead to enhanced apoptosis, instead it resulted in enhanced expression of the STAT1 dependent CDKIs $p21^{waf/cip1}$ and $p27^{kip1}$ [34, 30]**(Fig 4.5)**. However, as well as being regulated by

STAT1, $p27^{kip1}$ has also been described to be modulated following IL-3 treatment of cells[108]. The enhanced expression of CDKIs was a result of RhoH overexpression, suggesting an increasead G1 cell cycle arrest in RhoH cells. The induction of a cell cycle arrest however remains to be carried out in further experiments and would support the hypothesis that there is a different mechanism in the IL-3 dependent system by which RhoH can inhibit cell counts other than its known role in inducing apoptosis in HPCs[85].

While the induction of STAT1 by IL-3 is poorly described, IL-3 is well known as a potent inducer of STAT5 phosphorylation, which initiates the transcription of genes required for proliferation and survival [22]. Previously generated data from Liu suggested that RhoH overexpression results in decreased IL-3 induced STAT5 phosphorylation[102]. However, these studies used parental cells as control cell line instead of empty vector transfected cells. Analysis of empty vector transfected cells is of special importance since virus particle based transduction of cells may target immunestimulatory pathways[139] and thereby modulate STAT activity. Furthermore, the previous data did not provide solid information about the phosphorylation state of STAT5 in RhoH underexpressing cells[102]. In this study it was confirmed that enhanced RhoH expression is able to inhibit the phosporylation of STAT5 and thereby its activation following IL-3 treatment **(Fig. 4.6A)**, it was also found that the shRNA mediated regulation of RhoH expression resulted in enhanced levels of IL-3 induced STAT5 phosphorylation **(Fig. 4.6)**. The elevated STAT5 activation was difficult to reveal on the first sight using the STAT5 IP results, because of increased total STAT5 levels. However the signal quantification and additional FACS **(Fig. 4.6B)** experiments supported the increase in IL-3 induced STAT5 activation in siRhoH cells, which eventually leads to an increased transcription of genes, important for cell cycle progression and the recovery from IL-3 starvation. A potent downregulation of $p21^{waf/cip1}$ and $p27^{kip1}$ protein levels was not detectable in siRhoH BaF3 cells, compared to control cells. This could be a result of the already weak expression levels of RhoH in BaF3 cells[61]. Further, shRNA mediated downregulation of RhoH in BaF3 cells may not cause a decrease in the expression of the CDKIs as this could probably be detected when endogenous RhoH expression levels are on a higher level. To thest this hypothesis shRNA mediated knock-downs of RhoH, in IL-3 dependent cell lines with higher endogenous RhoH expression remain to be performed and tested on the expression changes of $p21^{waf/cip1}$ and $p27^{kip1}$.

Although low levels of RhoH did not protect cells from apoptosis caused by cytokine withdrawal in the first instance, cells underexpressing RhoH were found to be able to recover from long-term IL-3 withdrawal in comparision to control cells **(Fig. 4.7)**. This suggested that siRhoh cells are able to react with higher efficiency to the cytokine IL-3, while parental cells expressing higher levels of RhoH failed to respond with recovery and proliferation. This hyptothesis was confirmed by the finding that RhoH overexpressing cells showed decreased surface expression of the IL-3 receptor alpha chain CD123, while cells with low RhoH expression exhibited increased expression of CD123 **(Fig. 4.8A)**. This increased in CD123 surface expression in siRhoH cells was comparably low and showed high variation between experiments. It was assumed that the variations strongly depended on the shRNA mediated RhoH knock-down efficiency and that the slight increase in CD123 expression could be a result of already weak endogenous RhoH expression in BaF3 cells and further downregulation of RhoH as performed in this study would not lead to a stong induction of CD123 expression. Nevertheless, it was hypothised that low RhoH levels induce an enhanced activation of STAT5 in response to IL-3 and the elevated expression of the transcription factor IRF-1 **(Fig. 4.8B)**. The ability to recover from cytokine withdrawal as well as the increased proliferation rate of siRhoH cells can be dedicated to the enhanced delivery of proliferative and survival supporting signals by the increased IRF-1 mediated CD123 surface expression.

IRF-1 is classically known to be involved in interferon-1/STAT1 dependent signal transduction[140-142] but which was also reported to be a STAT5 dependent early response gene in G-CSF mediated signaltransduction in neutrophils[10]. The surface expression of CD123 is thought to be a result of STAT5 dependent IRF-1 expression in AML cells[110]. Interestingly, RhoH overexpressing cells also showed a slightly elevated level of IRF-1 expression **(Fig. 4.8B)** compared to control cells, which is not surprising considering the elevated STAT1 activation in response to IL-3 in RhoH BaF3 cells. As mentioned above, IRF-1 is classically described as a target of STAT1 mediated signalling[25] therefore the enhanced STAT1 phoshorylation in RhoH cells leads to elevated IRF-1 expression, with different signalling targets than the CD123 surface expression observed in siRhoH cells. Similar observations of insignificant STAT1 mediated IRF-1 regulation were made in studies investigating signalling pathways induced by G-CSF[10].

This result, in particular, highlights that RhoH expression may function as a tool to finetune IL-3 mediated proliferative and inhibitory STAT dependent signals by tandem activation of

either STAT1 or STAT5 and their target genes. In both cases, STAT5 and STAT1 activation, the outcome of experiments performed with an inactive RhoH mutant would be highly interesting. Although data from previously performed reporter gene assays of the Kubatzky lab exist, suggesting a RhoH modulated IL-3 dependent STAT1 and STAT5 transcriptional activity[102], futher investigations of the transcriptional activity of STAT5 specifically leading to IRF-1 expression in comparison to appropriate control cells need to be conducted. Additionally experiments to investigate the IRF-1 regulated CD123 expression in BaF3 cells, remain to be performed. Additionaly, CD123 expression should be tested on cells with higher endogenous RhoH levels after shRNA mediated RhoH knock-down to further investigate the increase in CD123 expression.

5.3 RhoH expression in THP-1 cells, correlates with increased IRF-1 and decreased CD123 expression

Enhanced CD123 expression, together with increased STAT5 phosphorylation and elevated IRF-1 expression are reported to be characteristic features of primitive AML cells[110]. The observed effects are described to result in higher cell proliferation rates and are considered as negative factors for patient prognosis[110,111]. Other investigations demonstrated that RhoH gene expression in AML cells is remarkably decreased and that lower RhoH levels are also considered as poor prognostic marker for patient survival[54]. In this study the observed effects in siRhoH cells were connected to the AML characteristic features using the AML derived monocytic cell line THP-1 as model system **(Fig. 4.9)**. It was demonstrated that reconstitution of RhoH expression in THP-1 cells lowered both IRF-1 expression and CD123 surface expression. RhoH reconstitution is suggested to inhibit the elevated STAT5 activation in these cells, thereby targeting the STAT5 induced IRF-1 expression, which finally leads to lower CD123 surface expression in THP-1 cells. However, complementary experiments showing the changes of STAT5 activation, following RhoH reconstitution in THP-1 cells remain to be carried out. Like in the BaF3 system, these studies need to include the investigation of eventually occurring RhoH dependent changes of the proliferation behaviour of THP-1 cells. Additionaly the transcriptional activity of IRF-1 remains to be determined to clarify the impact of RhoH modulated STAT5 activation. Studies investigating the treatment of AML have suggested targeting of CD123 on AML blasts with IL-3 ligand variants fused to catalytic portions of bacterial toxins[143]. However, the use of such a treatment in humans could cause unexpected and unfavourable adverse effects, since CD123 is also present on other cell types such as different progenitor subsets[144]. A promising approach to treat AML could therefore be

the targeted reconstitution of RhoH in AML cells or the attempt to find molecular candidates leading to an upregulation of endogenous RhoH expression in the malignant cells.

5.3.1 RhoH is underexpressed in lymphoma derived cell lines with abberant signalling patterns and immunophenotype

Elevated STAT5 activation, as well as the altered resistance to cytokine withdrawal and enhanced proliferation rates as observed in RhoH underexpressing cells during the course of this study, are broadly found among malignant hematopoetic disorders[145,146]. In a first attempt to identify additional hematopoietic malignancies where RhoH underexpression may be involved in cancer progression was performed by comparing the effects caused by a lack of RhoH with described leukemia features. Different cell lines derived from B-cell Non-Hodgkin lymphoma (B-NHL), as well as from ALCL lineages, were analysed upon their RhoH mRNA expression **(Fig. 4.10)**.

ALCL are described as a biologically and clinically heterogeneous subtype of peripheral T-cell lymphoma, with an aberrant immunophentotype[90]. ALCL can commonly be detected to inhabit chromosomal translocations, of which mostly the tyrosine kinase, ALK is found to be under the promoter control of the nucleolar phosphoprotein NPM[91-92]. Studies indicate that upon expression of NPM-ALK enhanced STAT3 and STAT5 phosphorylation results correlating with higher cell cycle progression rates and cytokine independent growth [95,96]. There is growing evidence that the constitutive activation of small GTPases such as Rac1 and Cdc42 are contributing to the oncogenic features of NPM-ALK rearrangements in systemic ALCL[97,98] and the enhanced expression of RhoH is reported to have an inhibitory effect on the activity of other GTPases, such as Rac1and Cdc42 [61,87]. Proteomic analysis of NPM-ALK positive and negative cells also revealed also the downregulation of the phosphatase PTP, which was demonstrated during this work to be an interaction partner of RhoH **(Fig 4.18)**, to the cancer progressive attributes of NPM-ALK positive cells[147]. Most interestingly ALCL cells are reported displaying peculiar T-cell immunophentoypes, which is the phenotype of cells of hematopoietic neoplasms defined according to their resemblance to normal T-cells. ALCL are commonly deficient for TCR and T-cell receptor associated molecules Zap70 and CD3 expression[148]and CD4/CD8 expression[148]. Studies of RhoH in T-cells revealed its importance for TCR mediated thymocyte selection and maturation and for TCR mediated CD3ζ phosphorylation and Zap70 recruitment to the immunological synapse, indicating that RhoH is a component of the TCR signalling complex[88,89]. Together with the previous findings

of this work, in which RhoH acted as an inhibitor of IL-3 induced proliferation via modulation of the JAK-STAT signalling pathway it was hypothised that in particular ALCL derived cell lines, and in more detail the NPM-ALK$^+$ ALCL types, because of their reported STAT signalling signature, would show a characteristic downregulation of RhoH. The analysis of the RhoH mRNA levels demonstrated that NPM-ALK positive, as well as NPM-ALK negative ALCL types, exhibited significantly lower expression of RhoH than control cells **(Fig. 4.10A, 4.10B)**. Further studies will be required to address the question of the role and consequences of a loss of RhoH expression in ALCL subtypes. Sequential phosphoproteomic analysis or cDNA microarrays performed with ALCL subtypes, or ALCL cells with different RhoH expression levels, could indicate in which direction the reconstitution of RhoH, which was shown to be required for proper TCR signalling, would drive the ALCL characteristic immonophenotype. In order to gain further insight into the role of RhoH in ALCL disease progression further investigations including the abnormal ALCL phentoype, will be cruical to our understanding of the molecular mechansims of this disease.

Interestingly most of the the analysed B-NHL subtypes also showed prominent and significant downregulation of RhoH on mRNA level **(Fig. 4.10D)**. This lymphoma type exhibits constitutive STAT5 activation, which allows the generation of B-cell precursors growing and surviving in a cytokine independent state[149]. Remarkably RhoH was reported to be targeted for aberrant somatic hypermutations[99,150], as well as aberrant chromosomal rearrangements[151] but not described to be underexpressed in this lymphoma subtype. The results of this study showed that these cells seem to underexpress RhoH as well, although the T-lymphocyte Jurkat served as a control cell line and not a B-cell line, which would be more comparable in terms of proper gene expression analysis. In the future studies of RhoH underexpression and its consequences should be subject of further investigation. However, cell lines of other B-cell lineages, the so called NHL mantle cell lymphoma subtypes, were also analysed to determine the RhoH expression levels. Surprisingly, in this subtype the RhoH expression was slightly higher than the expression levels detected in Jurkat cells **(Fig. 4.10C)**.

Mantle cell lymphoma, is an aggressive lymphoma type with t(11;14)(q13;q32) translocation that is reported to express uniquely high levels of cyclin D1, approximately four-fold higher than detected in other B-cell lymphoma types. The oncogenic protein cyclin D1 is a major activator of the cell cycle machinery and is described to be transcriptionally regulated by STAT5[152]. In healthy mature B-lymphocytes cyclin D1 is known to be downregulated [153].

Considering the connection of RhoH to the cell cycle machinery via counterregulating the IL-3 dependent STAT1 /STAT5 activation, in particular through the modulation of the STAT1 dependent CDKIs, the detected upregulation of RhoH in mantle cells could be the result of the cells effort to use inhibitory mechanisms to neutralise elevated cell cycle progression. However, mantle cell lymphoma shows an increased proteosomal degradation of CDKIs, leading to their depletion[154]. Therefore the attempt of the cell to inhibit cell cycle progression by enhanced RhoH expression is unlikely to succeed. Even so, studies made with B-cell chronic lymphocytic leukaemia (CLL) also showed an upregulation of RhoH mRNA levels, positively correlating with the expression of Zap70 which is a prognostic marker in aggressive CLL (approx. 65% of all diagnosed patient samples)[155]. Zap70, which enhances B cell receptor signalling and thereby contributes to the pathogenesis of CLL, is known to interact with RhoH in order to mediate proper T-cell receptor signalling[89]. It was demonstrated that the loss of RhoH contributes to a significant delay in disease progression[101]. However, only 8% of mantle cell lymphomas are found to overexpress Zap70 [155], which highlights that in the case of mantle cell lymphoma, RhoH may play a different functional role.

5.4 RhoH interaction partner binding is IL-3 dependent

Proteomics is a powerful tool for gaining insight into target protein interactions as well as signalling cascades involved in the function of the investigated protein. In order to obtain a detailed understanding of how RhoH interferes with IL-3 dependent signalling, and is thereby able to modify major hematopoietic signalling cascades such as the JAK-STAT pathway, GST-pulldown assays were performed with recombinant GST-fusion proteins. These assays were carried out with recombinant GST-fusion proteins of wt RhoH and the T36A effector domain mutant variant of RhoH, being incubated with lysates of IL-3 treated and untreated BaF3 cells. The resulting protein eluates were subject to mass spectrometry analysis **(Fig 4.18)**. The aim was to identify new interaction partners of RhoH, with particular relevance for IL-3 dependent signalling and more-over to understand other as yet unresolved questions about the function of RhoH in the IL-3 dependent cell system.

Mass spectrometry is a highly sensitive method, which increases the tendency for false positive hits. GST-fusion proteins were produced and purified from *E.coli*. In theory, only proteins with GST-tag should stick to GSH-beads. However, many bacterial proteins are

known to interact unspecifically with the target protein and the complete removal from the final GST-fusion protein is not possible. This is why the GST-only sample was included as a negative control into the experimental layout. Detected proteins from thsese samples were excluded for further evaluation. Additionally the results of all mass spectrometry runs were cross analysed in an *E.coli* peptide data base. This was required to exclude potential *E.coli* proteins from further investigations, although there is chance that some highly conserved proteins of eukaryotic origin might also be excluded. Another common source of error are protein clusters. Many proteins are forming signalling complexes by physical interactions. Even if only one candidate of the cluster is actually able to directly interact with the target protein there is a high possibility to detect several proteins of the cluster with mass spectrometry. Multiple washing steps within the purification procedure, as well as technical and biological replicates as applied in this study are thought to diminish but not to fully erase unspecific hits. To further optimize the statistical relevance of the detected hits irregular occurring peptides, such as non-reproducable hits (within the biological/technical replicates) and single peptide hits (from one protein, in one run) were also removed from the list of potential RhoH interaction candidates. Despite all these procedures, the resulting protein hits obtained from the mass spectrometry data were considered only as indications for a possible protein interaction between RhoH and the corresponding protein.

The statistical analysis of the results of these studies was remarkable and gave raise to a number of new questions. The study of protein binding to the target proteins resulting from the differently cytokine treated cells confirmed that protein binding and therefore downstream signalling of RhoH, depends to a great extend on the prior presence of the IL-3 stimulus **(Fig.4.13)**. A closer look at the gene ontology function of the identified IL-3 dependent interaction partners, confirmed not only that the number of binding partners differs, but also their mediated cellular functions **(Fig. 4.15)**. 35% of the candidates interacting with RhoH under IL-3 treated conditions were found to be involved in nucleic acid processes. The precentage of interacting partners with the same gene ontology increases to 46% when cells were starved before. Another example for the functional shift depending on the IL-3 treatment are proteins with functional responsibilities in the cytoskeleton. The proportion of proteins found in lysates of cytokine treated cells is about 16% and drops, in regard to the total number of interactions, to 9% in the group of cytokine independent bindings and is even lower with 7% after cytokine withdrawal **(Tab. 6.1.2.1 Appendix)**.

The explanation for this phenomenon of the cytokine treatment dependent changes of the function of interacting proteins, are most likely posttranslational modifications. The previous cytokine treatment leads to the activation or inactivation of proteins allowing or preventing specific interactions with RhoH. However, not only posttranslational modifications can depend on cytokine treatment, but also the protein expression of the found interaction partners may be affected by the cytokine treatment. The transcription and protein expression of particular genes is initiated when the IL-3 signal is received. Posttranslational modifications initiated by cytokines are broadly reported and are known to influence the protein interaction ability of proteins. The same is true for the expression and synthesis of new proteins, which is only efficiently promoted when cells are receiving sufficient signals to enter the interphase state. Also, IL-3 deprivation of BaF3 cells is able to introduce apoptosis leading to the subsequent degradation of proteins which otherwise would be able to interact with RhoH. Taken together these data support the IL-3 dependent involvement of RhoH in signalling pathways through altered protein binding patterns depending on IL-3 treatment.

5.4.1 Similar proteins can bind to RhoH and to its effector domain mutant variant

An unexpected functional conlusion was made about RhoH regarding its ability to interact with proteins when studying the interactions occurring between wt RhoH and with its supposed loss-of-function mutant T36A. The effector domain T36 in GTP binding proteins is reported to be fundamental for GTP binding, as well as for the interaction with downstream effectors[60]. The analysis of the binding patterns of proteins **(Tab. 4.1)** to the different RhoH versions suggested that there are indeed several proteins which are able to bind to RhoH despite the T36A mutation. As these interactions never occurred in GST-only samples the detected candidates were considered to be solid and specific interactions. There is only one report using the T36A variation of RhoH as an inactive control, for HPC growth assays. The proliferation assays performed with the mutant variant demonstrated that the inhibitory function of RhoH on SCF-1 mediated proliferation is lost when cells were transduced with the T36A mutant variant instead of wt RhoH[85]. The authors suggest that this is simply due to the inability of the protein to interact with its downstream effectors[85,156]. However, the results of the RhoH proteomic analysis performed in this study suggest a broader answer to the observed phenomenon.

The observations of this study indicate that in the case of the atypical GTPase RhoH a simple mutation of its key threonin, located at the switch region, is not sufficient to abolish possible interactions in IL-3 mediated signalling. Even if the T36A mutation is still crucial for the RhoH mediated suppression of growth factor induced effects in HPCs[85], there could be different interactions and functions of RhoH, still mediated by its other Rho protein typical structural compartments **(Fig. 5.1)**. Different publications have described the importance of the C-terminal CAAX-box of small GTPases, which is required for the proper localisation of GTPases for protein interactions, as well as for the GTPase function and for the interaction of GTPases with other proteins[68,157]. Similar observations were made for RhoH´s C-terminal CKIF motif, where the cross-talk between RhoH and Rac1 in the regulation of the actin cytoskeleton of hematopoietic progenitor cells was proven to depend on RhoH CAAX box[83]. RhoH also inhabits a unique ITAM motif, which most likely serves as a docking site for Zap70[89] and Syk[101,114]. In this study the interaction of RhoH with Syk was only detectable among the interactions which were able to bind to wt RhoH (when cells were previously treated with IL-3). Other reported interaction partners of RhoH are GDIs[61]. In contrast to the interaction of RhoH with Syk, the α isoform of RhoGDI detected during the mass spectrometry analysis, appeared as an interaction partner of RhoH that seems to bind independent of the presence of threonine on position 36 in RhoH, **(Tab.6.1.1.2 Appendix)** but only in IL-3 treated cells. To further clarify and understand the importance of structural key elements of RhoH and their importance for RhoH modulated IL-3 dependent signal transduction it is required to continue the mass spectrometry based, as well as biochemical and immunological protein interaction, investigations of RhoH interacting proteins with different structural modified versions of RhoH, such as the deletion of the putative NLS in the polybasic region, the CKIF motif as well as with mutation variants of the RhoH ITAM-motif and again the T36A variant of RhoH.

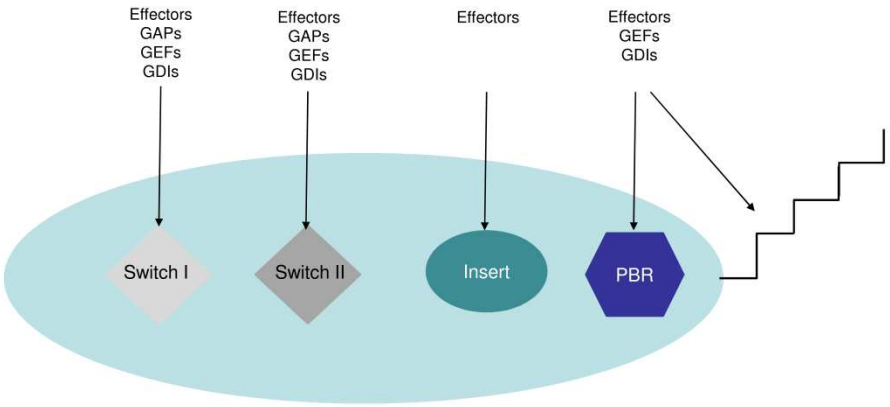

Fig. 5.1 Structural domains of GTPases serving as protein interaction sites
The different regions of RhoGTPases are serving as interaction sites for regulatory and effector proteins (switch I, switch II, Rho insert, Polybasic region (PBR), CAAX motif) (modified from DerMardirossian and Bokoch, 2005)

5.4.2 IL-3 treatment determines the subcellular localisation of RhoH interacting proteins

Cytokine stimulation causes protein trafficking and recruitment in the cell. This process of protein recruitment is important for various ongoing signal transduction mechanisms inducing cell proliferation, polarisiation, migration and motility. Cytokine induced posttranslational modifications of proteins can influence their ability to bind to certain adaptor proteins, which introduce the accumulation of proteins into different cell compartments[117,157] The subdivision of all detected interaction partner of each sample (wt, T36A-RhoH) under each condition (with IL-3 treatment, without IL-3 treatment) according to their "classical" cellular localisation gave further insight on the subcellular mechanisms RhoH may be involved in **(Fig. 4.15)**. The majority of protein hits showed a clear affiliation to one of the resulting groups but there was also a cluster of proteins of randomly occurring hits **(Tab. 4.1)** "No pattern"). Assuming that these proteins are most likely unspecific interactions, this study focused on the proteins of the remaining groups with clear affiliation patterns. IL-3 treatment caused interactions of RhoH with proteins that were localised to the cytoskeleton, while this compartment disappeared when comparing to the sorted T36A group. This compartment also was not present in the samples of the cytokine withdrawed samples **(Fig. 4.15)**. On the other hand, among the hits specifically for IL-3 starved samples and for the mutant RhoH variant, there were increased fractions of nuclear proteins detectable **(Fig. 4.15)**. This strongly indicated that the stimulation level not only defined the interacting protein but in more detail also seemed to affects the localisation and the functional role of the interacting protein. The mutation of T36A(+IL-3), which is thought to result in a loss-of-function mutant of RhoH, showed remarkable differences in the subcellular distribution of the binding partners when compared to those found in wt RhoH. This circumstance, however, highlights that this region of fundemental functional importance for typical GTPases, may also play a profound role in RhoH, when defining the origin of proteins that can bind to RhoH.

5.4.3.1 IL-3 dependent subcellular localisation of RhoH

The statistical evaluation of the mass spectrometry data implied a cytokine dependent cycling of RhoH into different cell compartments since the absence or presence of the cytokine was a major factor in defining the nature and the subcellular distribution of the interacting candidates. The Rho GTPase Rac1 facilitates different functions in the cell which are specified by its subcellular localisation, it is shown to cycle between cytoplasm and the

nucleus where it is thought to play a role in cell proliferation[158]. In response to growth factors and chemokines, Rho GTPases such as Rac1 and RhoA are known to accumulate in the cell membrane where they direct cytokineses and focal adhesion[159]. Initial experiments with the IL-3 dependent cell line BaF3 suggested that at least in the IL-3 dependent system, there may be an IL-3 induced recruitment of RhoH from the cytoplasmic fraction to the nuclear compartment **(Fig. 4.16B)**. Cytokine withdrawal seem to drive the GTPase RhoH to nuclear compartments, while shortly after retreatment with cytokine there is an ubiquitous distribution of the GTPase. Several Rho GTPases, such as Rac1, do contain a canonical NLS within their polybasic region (PBR)[160]. PBRs are of importance for the proper function of the GTPases as well as for their membrane localisation[160]. In the case of Rac1 it was shown that the NLS, is of importance for the regulation of its nuclear transport, when it is coupled to larger protein complexes that are unable to pass through nuclear pores[161,162]. It remains to be clarified whether the polybasic region of RhoH which lacks the canonical NLS, as described by Williams[160], is still able to mediate a regulated transport of RhoH to the nucleus. If this IL-3 induced transport turns out to be the case then the consequences would be a more thorough understanding of how RhoH is able to interfere with the IL-3 dependent JAK-STAT signalling pathway. If the PBR of RhoH does not induce the nuclear localisation of RhoH, another interesting aspect would be the identification of the nuclear transport mechanism of RhoH. A possible mechanism could be the binding to the protein Importin containing complexes, which were observed to facilitate the nuclear import of Rac1-STAT5 complexes as well[163]. Moreover if there is a cytokine dependent recruitment of RhoH to the nucleus by starvation; this should be validated by investigations of recruitment-kinetics. The microscopical analysis of the cells implies additionally reduced RhoH protein levels after starvation **(Fig. 4.16A)**. The western-blot, as well as the microscopic analysis of RhoH localisation are only initial experiments and of low quality, for instance future western-blot anaylsis, need to include proper controls for the cytoplasmic and nuclear compartmens. RhoH is known to be subject to proteosomal degradation after TCR stimulation[72]. Follow-up investigations need to include the observation of RhoH degradation at the protein level in order to gain further insight into the functional role of RhoH and the mechanisms by which it can be regulated in the IL-3 dependent system.

5.4.3 RhoH interacts with Cofilin-1 in HEK cells

Western-blot validations of the mass spectrometry detected interaction partners in HEK cells involved Cofilin-1, were carried out **(Fig. 4.17)**. Commonly known as a downstream effector of the GTPases Rac1 and Cdc42, Cofilin-1 is a key molecule of cytoskeleton rearrangement [74]. Rac1 and Cdc42 regulate Cofilin-1 induced actin turn-over by the activation of the p21-activated kinase (PAK1) which is able to induce the Cofilin-1 inhibiting LIM-kinase [58]. RhoH itself is reported to take part in the regulation of chemotaxis and homing of hematopoietic progenitor cells, mainly by inhibiting proper Rac1 activation and recruitment[85,87]. However, the direct protein interaction of RhoH and Cofilin-1 implies that there could be different mechanisms, by which RhoH can modulate cytoskeleton mediated processes. Besides of the known "classical" cytoskeleton dependent processes, signal transduction is also known to be affected by the cytoskeleton[164]. JAK-STAT signalling is described to be modulated by actin polymerisation events. The downregulation of Growth Hormone (GH) mediated STAT5 activation is reported to strongly depend on a functional cytoskeleton, since the treatment with actin polymerisation inhibitors causes prolonged STAT5 activity[165]. In this study a lack of RhoH was reported to enhance IL-3 induced STAT5 phosphorylation, additionally there were preliminary data suggesting a prolonged STAT5 activation as well. However, a possible IL-3 induced interaction of RhoH with Cofilin-1 could be indicative for the stabilisation of the required actin remodelling in the cytoskeleton. In this role, a lack of RhoH would cause a disruption in Cofilin-1 mediated actin polymerisation, which eventually leads to the observed prolonged STAT5 activity. Also, the observed enhanced STAT5 phosphorylation **(Fig. 4.6)** could be a direct result of the cytoskeletal disturbance as in cells with functional cytoskeleton the downregulation of the signal would work more efficient than in cells with defective actin polymerisation[165]. To clarify whether the binding of RhoH modulates the activation of Cofilin-1, experiments in which the IL-3 dependent phosphorylation state of Cofilin-1, with and without cotransfection of RhoH should be carried out. The experiments in this study were carried out in HEK cells, providing high transfection efficiency and uncomplicated handling. However, to address the role of the IL-3 stimulus in the formation of the RhoH-Cofilin-1 binding, the interaction has to be examined in BaF3 cells. Also the initial experiments performed in HEK cells require further controls such as a GFP only containing vector transduced sample to exclude unspecific protein binding.

5.4.4 RhoH interacts with PTP1B in HEK cells

Another interaction of RhoH in the IL-3 dependent system occurs with the protein tyrosine phosphatase PTP1B **(Fig. 4.18)**. This interaction was again due to uncomplicated handling and high transfection efficiency validated in HEK cells. PTP1B is widely expressed in tissues and, due to a C-terminal hydrophobic stretch, (exclusively) localised at the cytoplasmatic face endoplasmatic reticulum (ER)[122]. Different reports confirm PTP1Bs regulatory effect on the JAK-STAT pathway [19,120,166]. JAK2, TYK 2 as well as both isoforms of STAT5 were found to serve as PTP1B substrates. Additionally this phosphatase was found to negatively regulate IL-3 induced proliferation[123]. RhoH contains five possible tyrosine phosphorylation sites. In the case of the reported interactions between RhoH and Zap70/Syk the phosphorylation of the tyrosines in the ITAM motif seem to play a pivotal role[89,114], although recent studies are controversely discussing the phosphorylation of the putative ITAM in RhoH[167]. The RhoH-PTP1B interaction in HEK cells indicates that tyrosine phosphorylated RhoH may serve as a substrate for PTP1B. Dephosphorylation of RTKs, by PTP1B, requires the internalisation of the phosphorylated receptor[168]. After dephosphorylation the RTKs are targeted for lysosomal degradation[169,170]. The re-localisation or accumulation of the Rho GTPases at the ER however, is indicative for their lysosmal degradation [66]. RhoH is thought to be targeted for lysosomal degradation with and without activation of the TCR-complex[72]. To be functional in TCR signalling, RhoH is thought to be phosphorylated at its specific ITAM tyrosines[89]. If IL-3 induced signal transduction requires RhoH phosphorylation either on its ITAM or on its remaining tyrosines this could raise the need for the involvement of a tyrosine phosphatase in RhoH modulated IL-3 mediated signal transduction, which introduces the lysosomal processing of RhoH by its dephosphorylation. The binding of PTP1B to RhoH was not detectable in the Na_4VO_3 untreated sample, at the same time the results imply lower expression level of PTP1B in the same **(Fig. 4.18)** which could explain why the interaction was not detectable in this sample. To learn more about RhoH and its regulatory mechanisms it needs to be clarified whether in BaF3 cells, the interaction of RhoH and PTP1B is indeed IL-3 dependend, and furthermore, if, and on which tyrosines, RhoH gets phosphorylated by the IL-3 stimulus. PTP1B recognise substrates containing the aa sequence (E/D)-pY-pY-(R/K). The screening of the RhoH aa sequence shows no clear evidence for this recognition motif **(Appendix 6.2)**, indicating that RhoH might serve as a PTP1B substrate, via a yet unknown recognition motif.

5.5 Summary and outlook (I): RhoH modulates IL-3 induced proliferation by fine-tuning IL-3 dependent JAK-STAT signalling

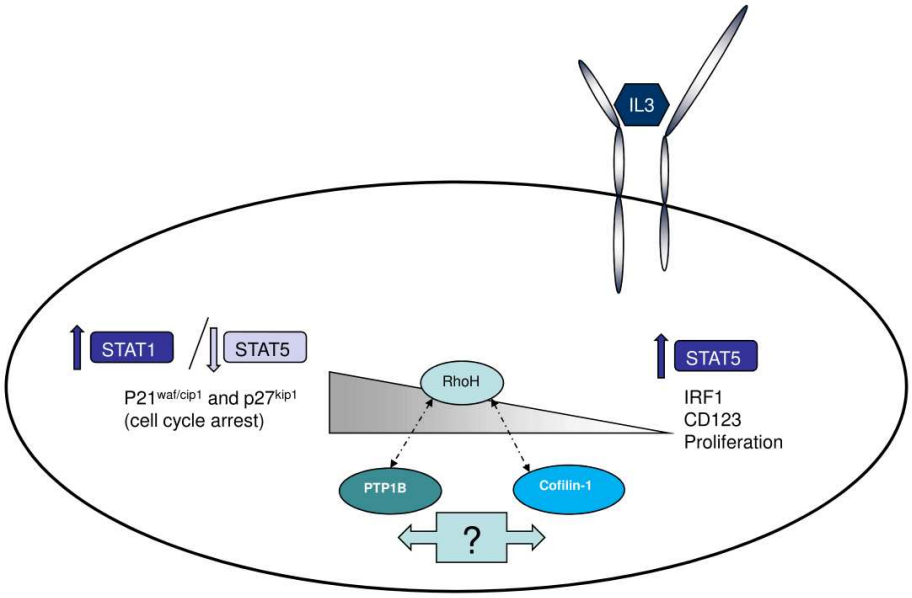

Fig. 5.3 Proposed model for RhoH modulated IL-3 induced signaling
In the case of low RhoH expression IL-3 induces enhanced STAT5 activation followed by an induction of the transcriptionfactor IRF-1 which results in enhanced CD123 surface expression eventually leading to increased cell proliferation. High RhoH expression leads to enhanced STAT1 phosphorylation and less STAT5 activation. RhoH modulated STAT1 activation causes an upregulation of CDKIs $p21^{cip1}$ and $p27^{kip1}$ and decreased cell counts by the induction of cell cycle arrest.The physical interaction of RhoH with PTP1B and Cofilin-1 are most likely taking part in tandem regulation of IL-3 mediated STAT5/STAT1 activation. However, the mechanistic details and functional consequences of these interactions remain to be clarified

Of particular interest would be in the future to investigate the effects of T36A variant of RhoH on IL-3 mediated proliferation, the phosphorylation of STAT5/STAT1 and on the induced gene expression of IRF-1 and CD123. These investigations can be essential to address the structural key elements of RhoH for signal transduction and as a negative control for experimental procedures. It is of particular interest to address the function of RhoH in IL-3 mediated signal transduction to the interaction of one or two of the identified interaction candidates in this work, to be able to complete the IL-3-RhoH mediated signaltransduction pathway. The interaction of RhoH with PTP1B and Cofilin-1 are required to be verified in the IL-3 dependent BaF3 system to determine the role of cytokine treatment for the interaction of RhoH with its interaction partners. To gain better insight into the function of RhoH structural key elemets such as the CKIF motif within the PBR, or the conserved T36, the use of different mutant variants for protein interaction and signalling experiments need to be carried out. For the future a strong focus could be set on eventually occurring posttranslational modifications, also in regard on distinct structural features of RhoH, following IL-3 treatment. This work

suggests the involvement of a protein tyrosine phosphatase in RhoH modulated IL-3 signalling, it needs to be clarified whether IL-3 stimulation is able to induce targeted posttranslational modifications of RhoH, such as tyrosine phosphorylation or targeted lipid modifications. The overerxpression of different tyrosine mutant variants could further resolve the question of the functional importance of the tyrosine phosphorylated residues. The use of prenylation inhibitors could provide additional insight into the relevance of C-terminal modifications for RhoH modulated IL-3 induced signalling. Also of importance is to draw final conlusions about the IL-3 dependent shuttling of RhoH between nuclear and cytoplasmic compartments and the relevance of this process for IL-3 mediated signalling. Future work needs to further clarify RhoHs involvement in hematopoetic malignancies. In this study the focus was set on malignancies which potentially bear siRhoH related “phenotype”. The accumulating knowledge about RhoH involvement into TCR signalling was also used to profile potential malignancies with RhoH involvement. Ongoing investigations need to include RhoH reconsitution experiments in lymphoma derived cell lines, to be able to investigate the impact on cancer progression and signalling. Of particular interest could be the reconstutiton of RhoH in ALCL gernerated cells and the effects RhoH reconstitution would have on the described T-cell phenotype in ALCL gernerated cells and whether RhoH expression modulates disease progression or previously described prognostic markers.

5.6 The function of RhoH in IL-3 mediated MC differentiation and function

Mast cells are most commonly known as mediators of anaphylactic reactions; however, these cells also play important roles in innate and adaptive immunity[44,171]. IL-3 plays a central role in the differentiation and maturation of erythroid, megakaryocytic and myeloid lineages[172], such as MCs[171]. Processes regulating stem-cell self-renewal and cell differentiation are thereby controlled and influenced by cellular signalling pathways which can be activated by IL-3[13] such as STAT5 activation[173,174]. STAT5 was also demonstrated to play a pivotal role in MC development since MCs were reported to be completly absent in tissues of STAT5 a/b null mice. *In vitro* generation of STAT5 deficient MCs was only successful when cells were incubated with both cytokines IL-3 and SCF-1. The lack of STAT5 also had a large impact on cell cycle progression and cell survival and on late phase response of MCs [37,175]. STAT1 activation, however, is known to play an important role in MC survival and MC mediated inflammation[176]. The studies discussed in this work demonstrated that expression levels of RhoH strongly modulated IL-3 dependent STAT5/ STAT1 induced processes in the model cell line BaF3. To gain further insight into the physiologic relevance of RhoH and its involvement in IL-3 dependent differentiation and signalling, as well as its role for allergic reactions, the studies of RhoH in the IL-3 dependent system were continued and emerged using murine MCs *in vitro* differentiated in a strictly IL-3 dependent manner from murine femur progenitor cells.

5.6.1 RhoH mRNA expression is regulated during MC differentiation

The expression of the GTPase RhoH was previously reported to be restricted on hematopoietic lineages[82]. As RhoH is an atypical member of the Rho GTPases lacking an intrinsic GTPase activity it is assumed that transcriptional control is an important regulatory mechanism for RhoH[86]. To get a basic idea of the involvement and regulation of RhoH during IL-3 dependent MC development, BMCs from wt mice were generated into MCs and RhoH mRNA level at distinct time points were measured **(Fig 4.19)**. The outcome of this experiment showed a relatively high RhoH expression in freshly isolated bone marrow cells, which drops after 5 days of cultivation in IL-3 containing medium. However, this decrease in RhoH levels may be explained by a strong IL-3 induced expansion of precursor cells in the early phases of differentiation which would most probably require the downregulation of

RhoH, a described inhibitor of HPC proliferation[85]. The IL-3 containing medium suppositionally induces a boost in proliferation in the early phases of MC differentiation, which would be accompanied by a lower differentiation potential of the progenitor cells. Wt BMMCs are described to show a high level of S-phase progression in response to IL-3 or SCF-1, peaking by 36 h[37]. However, cell fate decisions are known to be assessed mainly during G1 phase, when cells are in a state of cell cycle arrest[177]. During the course of MC differentiation however, RhoH levels are increasing until the attainment of a plateau value which is approx. 2-fold the relative mRNA expression from day 5. This observation strongly implicated that RhoH in general seem to play an important role in MC development and signalling. Studies investigating the stimulus dependent RhoH mRNA alterations performed in T cell derived cell lines or in primary neutrophils were interpreted as indications for a cell type specific functional role of RhoH[61,106]. For final conclusions about the role of RhoH during the early phase of IL-3 dependent MC development and in particular for its significance for IL-3 induced differentiation, endogenous RhoH levels need to be measured in progenitor cells during different states of MC differentiation, in response to SCF-1 another reported MC differentiation factor[178]. A similar RhoH induction caused by SCF-1 during MC development would be indicative for an IL-3 independent regulatory mechanism of RhoH in MCs. Due to highly varying mRNA levels, the presented results were from one representative experiment from a series of 3 independently performed experiments, showing the clearest RhoH mRNA differences between day 5 and the following days. However scientifly solid data should summarise the outcome of different experiments to provide insight into biologic and statistical relevance.

5.6.2 RhoH null MC progenitors show enhanced proliferation in early phases of cultivation in IL-3 containing medium

To test whether the progenitor cells of RhoH null mice cultivated in IL-3 would show similar proliferation behaviour as siRhoH cells, a Cell Titer Glo assay was performed using freshly isolated cells (Day 3-5 after bone marrow preparation) **(Fig. 4.20 A)**. Several studies showed that *in vitro* exposure of HPCs to cytokines causes a dramatic shift of gene expression patterns in which cell division genes are turned on or off in different phases than genes responsible for cell engraftment [179-181]. The early time frame was chosen upon the hypothesis that with proceeding maturation level of the cells the proliferation potential of hematopetiec cells decreases considerably[182], which would have complicated the detection of proliferation differences. However, the results of ATP measurement showed an impressive proliferative

difference in response to IL-3 between RhoH null and wt mice progenitors. This leads to the conclusion that the lack of RhoH in progenitor cells results, as expected, in elevated proliferation. A similar observation was made in siRhoH cells, where RhoH underexpression was demonstrated to result in enhanced IL-3 dependent STAT5 phosphorylation leading to accelerated proliferation and increased IRF-1 dependent CD123 surface expression. However, the observed altered proliferation rate of RhoH deficient progenitors is supposally a result of enhanced IL-3 induced STAT5 activation, which is reported to be essential for progenitor cell and MC proliferation[36,37,109]. For final conclusions about the effects caused by lack of RhoH, impacting specifically IL-3 induced proliferation of HPCs, the investigation of HPC expansion in response to SCF-1 is required. To address the relevance of RhoH for IL-3 dependent MC development the effects of SCF-1 on progenitor cells deficient for RhoH need to be compared. Furthermore, the hypothesis of increased STAT5 activity in RhoH deficient progenitor cells in response to IL-3 remain to be confirmed and ideally compared to STAT5 activation in response to SCF-1, since both cytokines are described to have fairly similar effects on STAT activation in MC deveopment[178]. Again this experiment was performed twice and due to high variance between the results only the proliferation assay with optimal outcome was presented. For final conlusions however, the assay needs to be optimized for solid understanding of the role of RhoH for progenitor proliferation in IL-3 containing medium.

To understand the extent of the similarities between the model system BaF3 and the primary progenitor cells lacking RhoH, further analysis of the CD123 receptor surface expression was performed **(Fig. 4.20B)**. CD123 presence on RhoH null progenitor cells was elevated as detected in siRhoH cells. Finally, the mRNA analysis of IRF-1 was also found to be upregulated in RhoH null progenitor cells **(Fig. 4.20C)**. Gene expression pattern in stem and progenitor cells are changing during developmental processes in response to a cytokine, especially the expression of cell cycling genes[179-181]. Future experiments need to clarify whether the altered CD123 and IRF-1 expression, observed in freshly isolated progenitors, would be detectable at latter time points, when cells have fully differentiated into MCs. Another interesting aspect would be to observe whether SCF-1 as differentiation factor would cause similar effects in regard to IRF-1 and CD123 expression in RhoH null progenitors. Given the case that SCF-1 and IL-3 mediated MC differentiation of RhoH deficient progenitor have different effects regarding proliferation and STAT5 mediated IRF-1 and CD123 activation, cDNA microarrays and comparison of the gene expression shifts during

differentiation could be used to identify particular genes that are significantly regulated by a lack of RhoH leading to the final cytokine dependnent phenotype, and eventually to the compensation of altered gene expression caused by a lack of RhoH.

The observed enhanced proliferation in response of IL-3 of MC progenitors is in particular interesting, since abnormal MC expansion is a major feature of mastocytosis[183]. Mastocytosis is a myeloproliferative disease with unknown prevalence and variants and is known to have complex pathologic consequences[183,184]. Furthermore, the progenitor cells of a subset of patients suffering from mastocytosis were found to express higher levels of CD123 surface receptor[183,184], similar findings were made with progenitors of AML patients[185]. Nevertheless altered CD123 is not described as a diagnostic marker for mastocytosis. It needs to be clarified whether RhoH deficiency contributes to the abnormal proliferation pattern of mastocytic cells. Also neoplastic MCs in mastocytosis are reported to show altered STAT5 activation, which is another parallel to the effects detected in siRhoH cells[186]. To define a role of RhoH in mastocytosis, RhoH expression pattern in a subset of systemic and coutaneous mastocytosis samples should be determined and the correlation with the STAT5 activation found in the samples needs to be investigated. Since mastocytosis and its different subtypes are considered to be difficult to distinguish from each other and from other diseases such as the hypereosinophilic syndrome[187-188], RhoH expression patterns could serve as a additional prognostic or diagnostic marker. In the human MC system the functions of the cytokine IL-3 is replaced by IL-4[189]. Follow-up studies could include work with human MCs to further clarify the context between RhoH and the MC relevant cytokine. The question of whether RhoH serves as an IL-3 specific inhibitor of proliferation in this system remains to be speculative, since SCF-1 dependent proliferation studies made with RhoH overexpressing murine progenitor cells indicated similar inhibitory effects of RhoH on cell proliferation[85]. Due to highly varying IRF-1 mRNA levels, the presented results were from one representative experiment from only two successfully performed experiments, showing the clearest IRF-1 mRNA differences. This is a relatively reduced set of data and the parallels between the primary cells and the BaF3 model system remain questionable as long results are not standardised.

5.6.3 No morphologic differences between RhoH null and wt MC

Mature MCs can be distinguished from other cell types such as eosinophils or basophils by the expression of the surface markers FcεRI and c-Kit [44]. The IL-3 dependent generation of

progenitors to MCs in this study was observed by weekly (4 weeks) measurements of the FcεRI and c-Kit surface expression, after IgE mediated activation of the cells **(Fig.4.22)**. In contrast to Lius` experimental outcomes [102], the results of these experiments suggested no obvious developmental abnormalities of RhoH deficient MCs when analysing MC surface marker c-Kit and FcεRI. Additionally, the proper expression of the MC specific protease MMP-6 was demonstrated and MC specific Toluidine Blue staining of RhoH KO MCs was performed showing no developmental differences between wt and ko MCs. However, alcian blue stainings[190] as well as the analysis of CD13 and T1/ST2[191] expression could help to draw final conclusions about the proper MC morphology and development. During the course of this study, the group of Shirai published their work, investigating FcεRI signalling in RhoH KO MCs, in which they confirmed normal MC development of RhoH deficient MCs *in vivo* and *in vitro*[114].

Normal MC development of RhoH KO progenitors was unexpected considering the earlier finding of the elevated proliferation rates detected in RhoH KO progenitors, which were thought to be indicative for impaired cell development. Since stem cells and the derivative progenitor cells are very complex systems and in particular the differentiation of MCs is reported to be influenced by numerous factors of their microenviroment[49,50] it can be assumed that MCs inhabit regulatory feedback mechanisms which can eventually compensate possible developmental consequences. It is reported that CDKIs such as $p21^{waf/cip1}$ and $p27^{kip1}$, are important key molecules contributing to cell fate decisions in HPCs[192-196]. HSCs from mice lacking CDKIs were found to proliferate at elevated rates, and showed altered differentiation potential[192,193]. In the BaF3 model system RhoH-BaF3 cells showed decreased IL-3 induced proliferation, resulting from enhanced CDKI levels. It was hypothised that in contrast to the observations in siRhoH cells, due to a complete lack of RhoH in the KO animal, the $p21^{waf/cip1}$ and $p27^{kip1}$ may be decreased in early time points after isolation, leading to the enhanced proliferation rates in RhoH KO progenitor cells. The results of $p21^{waf/cip1}$ and $p27^{kip1}$ mRNA measurements in freshly isolated (day 3-5 after preparation) progenitor cells from RhoH null and wt mice, cultivated in the presence of IL-3, confirmed this hypothesis **(Fig 4.21A)**. It was further hypothised that intracellular feedback mechanisms may be induced, during the course of cultivation, which were rapidly regulating the expression of $p21^{waf/cip1}$ and $p27^{kip1}$ to a normal level, to compensate developmental defects. Repeated measurements of $p21^{waf/cip1}$ and $p27^{kip1}$ mRNA levels at latter time points (after day 7) consistently showed comparable expression levels in RhoH null and wt mice **(Fig 4.21B)**. This observed dynamic adjustment

of CDKI levels in RhoH ko progenitors explains at least partly the lack of any developmental failures in RhoH ko MCs. The enhancement of the CDKI expression could be a result of a stronger regulation of other signalling pathways such as NOTCH2 signalling[197] or transcripton factors such as members of the EBF family of transcription factors[198], which were reported to be involved into cell fate decision determination and cell cycle regulation. Also an upregulation of STAT1 phosphorylation and activation in RhoH null progenitiors in response to IL-3, induced by a RhoH independent, alternative pathway remain to be carried out.

5.6.4 The lack of RhoH causes functionial defects in IL-3 derived MCs

Earlier studies made with RhoH ko mice only reported a strong T-cell related phenotype[88,89] . Nevertheless, later studies performed with *in vitro* generated neutrophils derived from RhoH KO mice showed that these cells exhibited functional defects, despite the lack of developmental deficiencies or morphologic abnormalities[106]. Therefore, and because of the significant similarities between Zap70 mediated TCR and Syk mediated FcεRI signalling in MCs[199-201], it was necessary to gain insight into the functional attributes of RhoH ko MCs. The reported T-cell defects in RhoH ko mice were found to be related to the defective recruitment and phosphorylation of Zap70 to the immunological synapse[89]. Syk, which is a Zap70 homologue, plays a similar role in FcεRI mediated MC signalling and initiating of down-stream effects such as histamine release and cytokine production, following MC activation[202]. Preliminary experiments of Liu already indicated possible functional defects of RhoH ko MCs regarding FcεRI mediated β-hexosaminidase release[102]. These initial functional experiments were repeated because in contrast to Lius` data no developmental deficiencies in MC development were detectable in this study. Antigen mediated histamine release between RhoH null and wt MCs was compared, when antigen was applied in different concentrations.

In RhoH deficient MCs reduced amounts of β-hexosaminidase (indicative for histamine) were detectable **(Fig 4.23)**; the measurement of the reduced histamine levels was thought to be either caused by defective synthesis of the MC mediators, or by inappropriate production of the mediators as a consequence of defective FcεRI signalling following antigen challenge. A scenario in which both defective mediator production, as well as defective mediator release

leads synergistically to the detected results was also considered as possible. Shirais` group published their work during the course of this study and they also demonstrated reduced histamine release from RhoH null MCs[114]. In their studies, they included an ionomycin control. Ionomycin leads to the perforation of the cell membrane and helps to gain insight into the over-all content of intracellular mediators. Their results showed that RhoH null MCs are able to produce equal amounts of histamine indicating that RhoH is dispensable for granule biogenesis, which lead them to the conclusion that these RhoH deficient MCs show, instead, impaired FcεRI mediated degranulation. They also checked for passive systemic anaphylaxis and found that indeed RhoH KO mice also show *in vivo* defects of proper MC response[114]. During the studies of this thesis, it was aimed to further characterise functional defects in RhoH null mice by the quantification of the main MC cytokines: IL-6 and TNF-α **(Fig. 4.24)**[44]. The released TNF-α is upregulating endothelilal and epithelial adhesion molecules, enhances bronichial responsiveness and inhibits tumor progression[44]. The release of IL-6 by MCs is known to contribute to MC mediated immune stimulatory functions, such as host defense during bacterial infections[203,204]. The outcome of this study showed that at least the release of these important cytokines was dramatically impaired in RhoH null mice **(Fig. 4.24)**. Again, studies of the Sharai group confirmed the observed effects and they additionaly showed that this defect was not based on impaired exocytosis of the cytokines, but instead demonstrated that upon antigen treatment already mRNA levels, indicative for a lower expression of these cytokines was significantly reduced[114]. The functional deficiencies in MCs are indicative for impaired FcεRI mediated signalling. The group of Shirai observed impaired ion-flux as a result of inefficient phosphorylation of FcεRI downstream positioned adaptor proteins PLCγ1, PLCγ2, SLP76 and LAT upon activation of FcεRI. They assumed that the activation upstream of the adaptor proteins might be the cause for the lack of phosphorylation detected in RhoH deficient MCs. Since the given similarities between TCR and MC signalling[205] and the impaired recruitment and phosphorylation of Zap70 (Syk in MCs) in TCR mediated signal transduction in RhoH KO mice[88,89], they investigated the phosphorylation of the Syk kinase in response to antigen challenge. It was found that the phosphorylation and activation of the kinase Syk in MCs strongly depends on the presence of RhoH and that Syk is able to bind to RhoH in a MC unstimulated and even stronger after activation of the FcεRI, which most likely indicates that RhoH similar to its identified role in TCR signalling is necessary to mediate activation and recruitment of Syk to the proper signalling subunits in MCs to guarantee proper MC activation.

5.7 Summary and outlook (II): The consequences of RhoH deficiency for IL-3 derived MCs

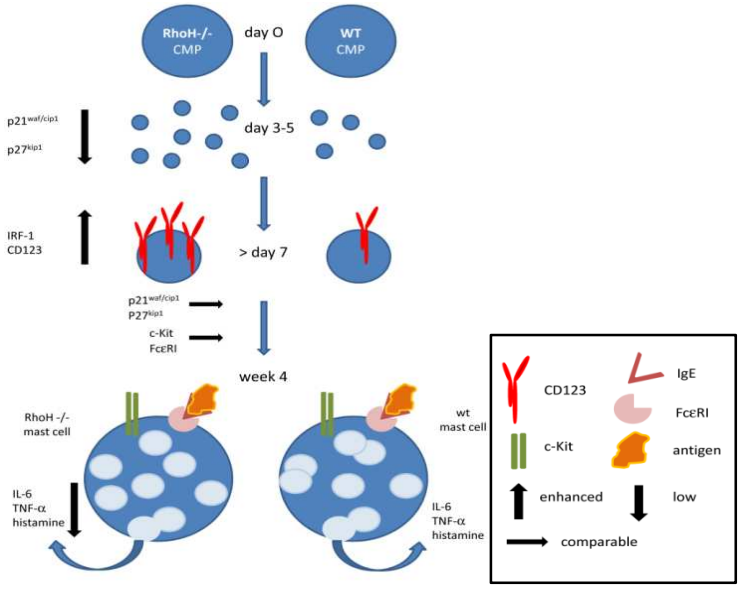

Fig. 5.4 Effects of RhoH deficiency for IL-3 derived mast cells
RhoH -/- progenitors show increased proliferation and decreased $p21^{waf/cip1}$ and $p27^{kip1}$ levels in early phase of cultivation. (after d 7) RhoH null progenitors show enhanced CD123 surface expression correlating with increased IRF-1 mRNA levels, while $p21^{waf/cip1}$, $p27^{kip1}$ levels as well as MC specific marker expression are comparable to that of wt cells. Fully differentiated MCs show decreased histamine release and secreation of the cytokines IL-6 and TNF-α following FcεRI activation.

The results from IL-3 derived RhoH null MCs suggest that although RhoH is not essential for the development of MCs the lack of RhoH causes functional defects in FcεRI mediated signal transduction, most likely through a defective activation of the Syk kinase. However to cut down the relevance of IL-3 and IL-3 mediated signalling in MCs, the observed effects such as enhanced proliferation of RhoH deficient progenitor cells need to be further investigated and compared to results obtained from experiments using the MC differentiation factor SCF-1. RhoH deficiency resulted in enhanced MC progenitor proliferation in IL-3 containing medium. The proliferation rate of mature RhoH ko MCs remains to be determined and also whether the altered proliferation correlates with increased STAT5 activity. In this context, it should be clarified whether the dynamic upregulation of CDKIs during MC maturation is able to decrease the observed proliferation rate at latter time points. Future studies should include the investigation of endogenous pathways responsible for the compensation of the effects caused by the lack of RhoH. The answer to this question could potentially provide major insight into RhoH modulated pathways. Due to high variations between biologic replicates, the data obtained from analysis of primary MCs are widely speculative. In the future experimental layouts have to be standardised to receive trustworthy results which will help to understand the biology of this highly interesting GTPase

6. Appendix

6.1 Supplementary tables

6.1.1 Thesis relevant protein hits

6.1.1.1 RhoH wt +IL3

Accession #	Gene	Aliases
IPI00139795	Rplp2	Renal carcinoma antigen NY-REN-44, P2,RPP2, 60S acidic ribosomal protein P2
IPI00225634	Rps12	ribosomal protein S12
IPI00113377	Rplp1	acidic ribosomal protein P1, RLA1,PI, RPP1
IPI00115477	Ccdc46	Isoform 1 of Coiled-coil domain-containing protein 46
IPI00132352	Cxorf26 homo	CXO26,
IPI00848599	Dnahc7l	Hsp40 homolog subfamily B , member14
IPI00121297	Naca	HSD48, NAC-alpha 3, Nascent polypeptide-associated complex subunit alpha
IPI00111265	Capza2	F-actin-capping protein subunit alpha-2
IPI00269481	Capzb	f F-actin-capping protein subunit beta
IPI00896602	Ppfia1	Liprin alpa 1, LIP1, PTPRF interacting protein alpha 1
IPI00132966	Ppid	PPIase, Cyclophilin-40, CYP40
IPI00623545	Ppp1r14b	Protein phosphatase 1 regulatory subunit 14B, PHI1 PLCB3N
IPI00265471	Adsl	ASL, adenylosuccinate lyase
IPI00118757	Phpt1	PHP14,HSPC141, Protein janus-A homolog
IPI00228633	Gpi1	PIG-Q, phosphatidylinositol glycan, class Q 1, Glucose-6-phosphate isomerase
IPI00122565	Gdi2 Iso	Rab GDI beta, Rab GDP dissociation inhibitor beta iso1
IPI00266281	Txnl1	TPR32, TXL1, Thioredoxin-like protein 1
IPI00856350	Clip1	restin, RSN, CYLN1
IPI00110753	Tuba1a	Tubulin alpha-1A chain
IPI00307837	Eef1a1	CTCL tumor antigen, Leukocyte receptor cluster member 7
IPI00169707	Tpm3	Tropomyosin3, gamma
IPI00227918	Tpm2	tropomyosin2, DA2B,TMSB
IPI00136929	Actg1	Actin gamma actin like
IPI00123039	**Ptpn1**	**PTP-1B, Tyrosine-protein phosphatase non-receptor type 1**
IPI00621468	EG665964	similar to ubiquitin A-52
IPI00377342	EG383341	similar to ubiquitin A-52
IPI00114894	Myh11	Myosin1 isoform1
IPI00129105	Sae1 Iso1	Sua, AOS, SUMO1 activating enzyme subunit 1
IPI00648513	Zc3h18 Iso1	NHN1, zinc finger CCCH-type containing 18
IPI00845851	Syne2	nesprin2, NUA, NUANCE, synaptic nuclear envelope 2
IPI00119959	Banf1	BAF, BCRG1, Barrier-to-autointegration factor
IPI00331146	Cmpk1	KCY, CM, KCytidylate kinase , UMP-CMP kinase
IPI00606189	Jarid1a	Jumonji, AT rich interactive domain 1A (RBBP2-like), 14 kDa phosphohistidine phosphatase
IPI00131186	Btf3 Iso2	basic transcription factor 3
IPI00129417	Hnrpdl	JKT41-binding protein, JKTBP1, Heterogeneous nuclear ribonucleoprotein D-like
IPI00463344	Dnajc8	DnaJ (Hsp40) homolog, subfamily C, member 8

6.1.1.2 RhoH wt and T36A +IL-3

Accession #	Gene	Aliases
IPI00118892	Lcp1	L-Plastin, Lymphocyte cytosolic protein 1,Plastin2
IPI00453599	Cfdp1	Craniofacial development protein 1, CP27, bucentaur
IPI00331556	Hspa4	Heat shock 70 kDa protein 4, APG4
IPI00127989	ptges3	Prostaglandin E synthase 3
IPI00125923	Ostf1	Osteoclast-stimulating factor 1
IPI00323600	Coro1a	Coronin-1A, p57

IPI00111560	SET Iso 1	SET translocation, leukemia associated protein SET, Iso 1
IPI00322312	**Arhgdia**	**Rho GDP-dissociation inhibitor 1**
IPI00555059	Prdx6	Peroxiredoxin-6, PRX6
IPI00405227	Vcl	Vinculin
IPI00131459	Nme1;	Nucleoside diphosphate kinase A, expressed in non-metastatic cells 1
IPI00227392	Ywhah 14-3-3 ε	tyrosine 3-monooxygenase
IPI00230707	Ywhag 14-3-3γ	14-3-3 gamma
IPI00465786	Tln1	Talin-1
IPI00377351	Apoa4	Apolipoprotein A-IV, apo A-IV
IPI00230427	Mif r	Macrophage migration inhibitory facto
IPI00221402	Aldoa	Fructose-bisphosphate aldolase A
IPI00109061	Tubb2b	Tubulin beta 2b, Tubulin beta-2B chain
IPI00119458	Aldoc	Aldolase C,zebrin2, fructose-biphosphate
IPI00273646	GAPDH	Glyceraldehyde-3-phosphate dehydrogenase
IPI00123181	Myh9	Myosin-9
IPI00113870	Pcna	Proliferating cell nuclear antigen
IPI00128904	Pcbp1	Poly(rC)-binding protein 1
IPI00123199	Nap1l11	Nucleosome assembly protein 1-like
IPI00230139	Fkbp4	p59, FK506 binding protein 4
IPI00462934	Khsrp	KH type splicing regulatory protein, FUSE-binding protein 2,
IPI00474446	Eif2s1	Eukaryotic translation initiation factor 2 subunit 1
IPI00890117	**Cfl1**	**Cofilin-1**
IPI00622235	Vcp	valosin containing protein, p97
IPI00320645	Zfp830	Ccdc16, Zinc finger protein 830
IPI00117011	Hcls1	haematopoietic cell specific Lyn substrate 1
IPI00131138	Flna Isoform 1	Filamin alpha
IPI00138892	Uba52;	ubiquitin and ribosomal protein L40, ubiquitin-CEP52
IPI00223253	Hnrnpk Isoform 1	KBBP, NOVA, Heterogeneous nuclear ribonucleoprotein K isof 1
IPI00225307	Sars	Seryl-aminoacyl-tRNA synthetase, isoform CRA_b, seryl-tRNA synthetase
IPI00277930	Capg	gesolin like capping protein
IPI00321147	Samsn1	,SH3 domain and nuclear localization signals, 1, isoform CRA_SAM domainb
IPI00407130	Pkm2	PK3, pyruvate kinase, muscle Isoform M2, CTHBP, THBP1
IPI00467266	Dut	Deoxyuridine triphosphatase, isoform CRA_a
IPI00469103	Kars	lysyl-tRNA synthetase isoform 1, KRS, LysRS
IPI00756894	Nsfl1c	p47 , SHP1 homolog, UBX domain protein 2,cNSFL1 (P97) cofactor
IPI00850795	A-52	residue ribosomal protein fusion product 1 isoform 1, similar to ubiquitin
IPI00330767	Cnbp	Isoform 1 of Cellular nucleic acid-binding protein
IPI00108206	Mela	melanoma antigene, Gag-Pol polyprotein
IPI00118676	Eif4a1 I	Eukaryotic translation initiation factor 4A-
IPI00121427	S100a6	Calcyclin
IPI00130883	Rbm3	RNA-binding motif protein 3
IPI00132080	Pgls 6	6- phosphogluconolactonase
IPI00137409	Tkt	Transketolase, p68
IPI00317309	Anxa5	Annexin A5

6.1.2 Gene ontology

6.1.2.1 Gene ontology in precent

RhoH wt	Hits	%	Hits	%	Hits	%
Treatment	**(+)IL-3**	**(+)IL-3**	**(+/-)IL-3**	**(+/-)IL-3**	**(-) IL-3**	**(-) IL-3**
Total	82	100%	33	100%	26	100%
Apoptosis	3	4%	2	6%	0	0
Signal transduction	7	9%	3	9%	2	8%
Cell cycle	3	4%	3	9%	2	8%

Cytoskeletal	13	16%	3	9%	2	8%
Differentiation	1	1%	1	3%	1	4%
Metabolism	16	20%	4	12%	2	8%
Nucleic Acid	29	35%	11	33%	12	46%
Stress response	2	2%	2	6%	2	8%
Unkown	5	6%	2	6%	2	8%
Others	4	5%	2	6%	1	4%

6.2 RhoH protein sequence (mouse)

(Sequence as obtained from: http://www.ncbi.nlm.nih.gov/protein/AAH94937.1)

```
1       MLSSIKCVLV GDSAVGKTSL LVRFTSETFP EAYKPTVYEN TGVDVFMDGI QISLGLWDTA
61      GNDAFRSIRP LSYGGADVVL MCYSVANHNS FLNLKNKWIS EIRSNLPCTP VLVVATQTDQ
121     REVGPHRASC INAIEGKRLA QDVRAKGYLE CSALSNRGVQ QVFECAVRTA VNQARRRNRR
181     KLFSINECKIF
```

7. Bibliography

1. Migliaccio, A.R., Migliaccio, G. & Adamson, J.W. Effect of recombinant hematopoietic growth factors on proliferation of human marrow progenitor cells in serum-deprived liquid culture. *Blood* **72**, 1387-1392 (1988).
2. Zhu, J. & Emerson, S.G. Hematopoietic cytokines, transcription factors and lineage commitment. *Oncogene* **21**, 3295-3313 (2002).
3. Garland, J.M., Dexter, T.M. & Testa, N.G. Colony-stimulating factors: future prospects. *Immunol Ser* **49**, 465-467 (1990).
4. van Leeuwen, B.H., Martinson, M.E., Webb, G.C. & Young, I.G. Molecular organization of the cytokine gene cluster, involving the human IL-3, IL-4, IL-5, and GM-CSF genes, on human chromosome 5. *Blood* **73**, 1142-1148 (1989).
5. Ozaki, K. & Leonard, W.J. Cytokine and cytokine receptor pleiotropy and redundancy. *J Biol Chem* **277**, 29355-29358 (2002).
6. Miyajima, A., Mui, A.L., Ogorochi, T. & Sakamaki, K. Receptors for granulocyte-macrophage colony-stimulating factor, interleukin-3, and interleukin-5. *Blood* **82**, 1960-1974 (1993).
7. Lopez, A.F., *et al.* Interleukin-5, interleukin-3, and granulocyte-macrophage colony-stimulating factor cross-compete for binding to cell surface receptors on human eosinophils. *J Biol Chem* **266**, 24741-24747 (1991).
8. Rapoport, A.P., Luhowskyj, S., Doshi, P. & DiPersio, J.F. Mutational analysis of the alpha subunit of the human interleukin-3 receptor. *Blood* **87**, 112-122 (1996).
9. Rapoport, A.P. & DiPersio, J.F. Sequence analysis and functional studies of interleukin-3 receptor alpha subunit-encoding cDNAs amplified from KG-1 leukemic cells and normal human marrow. *Gene* **137**, 333-337 (1993).
10. Tian, S.S., *et al.* Multiple signaling pathways induced by granulocyte colony-stimulating factor involving activation of JAKs, STAT5, and/or STAT3 are required for regulation of three distinct classes of immediate early genes. *Blood* **88**, 4435-4444 (1996).
11. Guthridge, M.A., *et al.* Mechanism of activation of the GM-CSF, IL-3, and IL-5 family of receptors. *Stem Cells* **16**, 301-313 (1998).
12. Brumatti, G., Salmanidis, M. & Ekert, P.G. Crossing paths: interactions between the cell death machinery and growth factor survival signals. *Cell Mol Life Sci* **67**, 1619-1630 (2010).
13. Reddy, E.P., Korapati, A., Chaturvedi, P. & Rane, S. IL-3 signaling and the role of Src kinases, JAKs and STATs: a covert liaison unveiled. *Oncogene* **19**, 2532-2547 (2000).
14. Inhorn, R.C., Carlesso, N., Durstin, M., Frank, D.A. & Griffin, J.D. Identification of a viability domain in the granulocyte/macrophage colony-stimulating factor receptor beta-chain involving tyrosine-750. *Proc Natl Acad Sci U S A* **92**, 8665-8669 (1995).
15. Wang, X., Lupardus, P., Laporte, S.L. & Garcia, K.C. Structural biology of shared cytokine receptors. *Annu Rev Immunol* **27**, 29-60 (2009).
16. Kisseleva, T., Bhattacharya, S., Braunstein, J. & Schindler, C.W. Signaling through the JAK/STAT pathway, recent advances and future challenges. *Gene* **285**, 1-24 (2002).
17. Leonard, W.J. & O'Shea, J.J. Jaks and STATs: biological implications. *Annu Rev Immunol* **16**, 293-322 (1998).
18. Schindler, C., Levy, D.E. & Decker, T. JAK-STAT signaling: from interferons to cytokines. *J Biol Chem* **282**, 20059-20063 (2007).
19. Xu, D. & Qu, C.K. Protein tyrosine phosphatases in the JAK/STAT pathway. *Front Biosci* **13**, 4925-4932 (2008).
20. Aoki, N. & Matsuda, T. A nuclear protein tyrosine phosphatase TC-PTP is a potential negative regulator of the PRL-mediated signaling pathway: dephosphorylation and deactivation of signal transducer and activator of transcription 5a and 5b by TC-PTP in nucleus. *Mol Endocrinol* **16**, 58-69 (2002).
21. Mui, A.L., Wakao, H., Kinoshita, T., Kitamura, T. & Miyajima, A. Suppression of interleukin-3-induced gene expression by a C-terminal truncated Stat5: role of Stat5 in proliferation. *EMBO J* **15**, 2425-2433 (1996).
22. Mui, A.L., Wakao, H., O'Farrell, A.M., Harada, N. & Miyajima, A. Interleukin-3, granulocyte-macrophage colony stimulating factor and interleukin-5 transduce signals through two STAT5 homologs. *EMBO J* **14**, 1166-1175 (1995).
23. Nagata, Y. & Todokoro, K. Interleukin 3 activates not only JAK2 and STAT5, but also Tyk2, STAT1, and STAT3. *Biochem Biophys Res Commun* **221**, 785-789 (1996).

24. Regis, G., Pensa, S., Boselli, D., Novelli, F. & Poli, V. Ups and downs: the STAT1:STAT3 seesaw of Interferon and gp130 receptor signalling. *Semin Cell Dev Biol* **19**, 351-359 (2008).
25. Fulda, S. & Debatin, K.M. IFNgamma sensitizes for apoptosis by upregulating caspase-8 expression through the Stat1 pathway. *Oncogene* **21**, 2295-2308 (2002).
26. Bernabei, P., *et al.* Interferon-gamma receptor 2 expression as the deciding factor in human T, B, and myeloid cell proliferation or death. *J Leukoc Biol* **70**, 950-960 (2001).
27. Conti, L., *et al.* In the absence of IGF-1 signaling, IFN-gamma suppresses human malignant T-cell growth. *Blood* **109**, 2496-2504 (2007).
28. Choi, E.A., *et al.* Stat1-dependent induction of tumor necrosis factor-related apoptosis-inducing ligand and the cell-surface death signaling pathway by interferon beta in human cancer cells. *Cancer Res* **63**, 5299-5307 (2003).
29. Kim, H.S. & Lee, M.S. STAT1 as a key modulator of cell death. *Cell Signal* **19**, 454-465 (2007).
30. Stephanou, A., Brar, B.K., Knight, R.A. & Latchman, D.S. Opposing actions of STAT-1 and STAT-3 on the Bcl-2 and Bcl-x promoters. *Cell Death Differ* **7**, 329-330 (2000).
31. Dimberg, A., Karlberg, I., Nilsson, K. & Oberg, F. Ser727/Tyr701-phosphorylated Stat1 is required for the regulation of c-Myc, cyclins, and p27Kip1 associated with ATRA-induced G0/G1 arrest of U-937 cells. *Blood* **102**, 254-261 (2003).
32. Ramana, C.V., *et al.* Regulation of c-myc expression by IFN-gamma through Stat1-dependent and -independent pathways. *EMBO J* **19**, 263-272 (2000).
33. Xiao, S., *et al.* RIG-G as a key mediator of the antiproliferative activity of interferon-related pathways through enhancing p21 and p27 proteins. *Proc Natl Acad Sci U S A* **103**, 16448-16453 (2006).
34. Chin, Y.E., *et al.* Cell growth arrest and induction of cyclin-dependent kinase inhibitor p21 WAF1/CIP1 mediated by STAT1. *Science* **272**, 719-722 (1996).
35. Lord, J.D., McIntosh, B.C., Greenberg, P.D. & Nelson, B.H. The IL-2 receptor promotes lymphocyte proliferation and induction of the c-myc, bcl-2, and bcl-x genes through the trans-activation domain of Stat5. *J Immunol* **164**, 2533-2541 (2000).
36. Debierre-Grockiego, F. Anti-apoptotic role of STAT5 in haematopoietic cells and in the pathogenesis of malignancies. *Apoptosis* **9**, 717-728 (2004).
37. Shelburne, C.P., *et al.* Stat5: an essential regulator of mast cell biology. *Mol Immunol* **38**, 1187-1191 (2002).
38. de Groot, R.P., Raaijmakers, J.A., Lammers, J.W. & Koenderman, L. STAT5-Dependent CyclinD1 and Bcl-xL expression in Bcr-Abl-transformed cells. *Mol Cell Biol Res Commun* **3**, 299-305 (2000).
39. Liang, Q.C., *et al.* Inhibition of transcription factor STAT5b suppresses proliferation, induces G1 cell cycle arrest and reduces tumor cell invasion in human glioblastoma multiforme cells. *Cancer Lett* **273**, 164-171 (2009).
40. Xiong, H., *et al.* Inhibition of STAT5 induces G1 cell cycle arrest and reduces tumor cell invasion in human colorectal cancer cells. *Lab Invest* **89**, 717-725 (2009).
41. Ahonen, T.J., *et al.* Inhibition of transcription factor Stat5 induces cell death of human prostate cancer cells. *J Biol Chem* **278**, 27287-27292 (2003).
42. Yamashita, H., Iwase, H., Toyama, T. & Fujii, Y. Naturally occurring dominant-negative Stat5 suppresses transcriptional activity of estrogen receptors and induces apoptosis in T47D breast cancer cells. *Oncogene* **22**, 1638-1652 (2003).
43. Galli, S.J., Grimbaldeston, M. & Tsai, M. Immunomodulatory mast cells: negative, as well as positive, regulators of immunity. *Nat Rev Immunol* **8**, 478-486 (2008).
44. Stone, K.D., Prussin, C. & Metcalfe, D.D. IgE, mast cells, basophils, and eosinophils. *J Allergy Clin Immunol* **125**, S73-80 (2010).
45. Arinobu, Y., Iwasaki, H. & Akashi, K. Origin of basophils and mast cells. *Allergol Int* **58**, 21-28 (2009).
46. Holowka, D., Sil, D., Torigoe, C. & Baird, B. Insights into immunoglobulin E receptor signaling from structurally defined ligands. *Immunol Rev* **217**, 269-279 (2007).
47. Abram, C.L. & Lowell, C.A. The expanding role for ITAM-based signaling pathways in immune cells. *Sci STKE* **2007**, re2 (2007).
48. Metcalfe, D.D., Baram, D. & Mekori, Y.A. Mast cells. *Physiol Rev* **77**, 1033-1079 (1997).
49. Kitamura, Y. & Fujita, J. Regulation of mast cell differentiation. *Bioessays* **10**, 193-196 (1989).
50. Ryan, J.J., *et al.* Mast cell homeostasis: a fundamental aspect of allergic disease. *Crit Rev Immunol* **27**, 15-32 (2007).
51. Messner, H.A. & Griffin, J.D. Biology of acute myeloid leukaemia. *Clin Haematol* **15**, 641-667 (1986).
52. McCulloch, E.A., Minden, M.D., Miyauchi, J., Kelleher, C.A. & Wang, C. Stem cell renewal and differentiation in acute myeloblastic leukaemia. *J Cell Sci Suppl* **10**, 267-281 (1988).
53. Jordan, C.T., *et al.* The interleukin-3 receptor alpha chain is a unique marker for human acute myelogenous leukemia stem cells. *Leukemia* **14**, 1777-1784 (2000).

54. Iwasaki, T., *et al.* Prognostic implication and biological roles of RhoH in acute myeloid leukaemia. *Eur J Haematol* **81**, 454-460 (2008).
55. Colicelli, J. Human RAS superfamily proteins and related GTPases. *Sci STKE* **2004**, RE13 (2004).
56. Vetter, I.R. & Wittinghofer, A. The guanine nucleotide-binding switch in three dimensions. *Science* **294**, 1299-1304 (2001).
57. Wennerberg, K., Rossman, K.L. & Der, C.J. The Ras superfamily at a glance. *J Cell Sci* **118**, 843-846 (2005).
58. Heasman, S.J. & Ridley, A.J. Mammalian Rho GTPases: new insights into their functions from in vivo studies. *Nat Rev Mol Cell Biol* **9**, 690-701 (2008).
59. Wennerberg, K. & Der, C.J. Rho-family GTPases: it's not only Rac and Rho (and I like it). *J Cell Sci* **117**, 1301-1312 (2004).
60. Spoerner, M., Herrmann, C., Vetter, I.R., Kalbitzer, H.R. & Wittinghofer, A. Dynamic properties of the Ras switch I region and its importance for binding to effectors. *Proc Natl Acad Sci U S A* **98**, 4944-4949 (2001).
61. Li, X., *et al.* The hematopoiesis-specific GTP-binding protein RhoH is GTPase deficient and modulates activities of other Rho GTPases by an inhibitory function. *Mol Cell Biol* **22**, 1158-1171 (2002).
62. Etienne-Manneville, S. & Hall, A. Rho GTPases in cell biology. *Nature* **420**, 629-635 (2002).
63. Tcherkezian, J. & Lamarche-Vane, N. Current knowledge of the large RhoGAP family of proteins. *Biol Cell* **99**, 67-86 (2007).
64. Faure, J. & Dagher, M.C. Interactions between Rho GTPases and Rho GDP dissociation inhibitor (Rho-GDI). *Biochimie* **83**, 409-414 (2001).
65. DerMardirossian, C. & Bokoch, G.M. GDIs: central regulatory molecules in Rho GTPase activation. *Trends Cell Biol* **15**, 356-363 (2005).
66. Boulter, E., *et al.* Regulation of Rho GTPase crosstalk, degradation and activity by RhoGDI1. *Nat Cell Biol* **12**, 477-483 (2010).
67. Burridge, K. & Wennerberg, K. Rho and Rac take center stage. *Cell* **116**, 167-179 (2004).
68. Roberts, P.J., *et al.* Rho Family GTPase modification and dependence on CAAX motif-signaled posttranslational modification. *J Biol Chem* **283**, 25150-25163 (2008).
69. Lang, P., *et al.* Protein kinase A phosphorylation of RhoA mediates the morphological and functional effects of cyclic AMP in cytotoxic lymphocytes. *EMBO J* **15**, 510-519 (1996).
70. Wang, H.R., *et al.* Regulation of cell polarity and protrusion formation by targeting RhoA for degradation. *Science* **302**, 1775-1779 (2003).
71. Forget, M.A., Desrosiers, R.R., Gingras, D. & Beliveau, R. Phosphorylation states of Cdc42 and RhoA regulate their interactions with Rho GDP dissociation inhibitor and their extraction from biological membranes. *Biochem J* **361**, 243-254 (2002).
72. Schmidt-Mende, J., Geering, B., Yousefi, S. & Simon, H.U. Lysosomal degradation of RhoH protein upon antigen receptor activation in T but not B cells. *Eur J Immunol* **40**, 525-529 (2010).
73. Bishop, A.L. & Hall, A. Rho GTPases and their effector proteins. *Biochem J* **348 Pt 2**, 241-255 (2000).
74. Jaffe, A.B. & Hall, A. Rho GTPases: biochemistry and biology. *Annu Rev Cell Dev Biol* **21**, 247-269 (2005).
75. Karlsson, R., Pedersen, E.D., Wang, Z. & Brakebusch, C. Rho GTPase function in tumorigenesis. *Biochim Biophys Acta* **1796**, 91-98 (2009).
76. Montaner, S., Perona, R., Saniger, L. & Lacal, J.C. Multiple signalling pathways lead to the activation of the nuclear factor kappaB by the Rho family of GTPases. *J Biol Chem* **273**, 12779-12785 (1998).
77. Perona, R., *et al.* Activation of the nuclear factor-kappaB by Rho, CDC42, and Rac-1 proteins. *Genes Dev* **11**, 463-475 (1997).
78. Kawashima, T., *et al.* A Rac GTPase-activating protein, MgcRacGAP, is a nuclear localizing signal-containing nuclear chaperone in the activation of STAT transcription factors. *Mol Cell Biol* **29**, 1796-1813 (2009).
79. Arulanandam, R., Geletu, M., Feracci, H. & Raptis, L. Activated Rac1 requires gp130 for Stat3 activation, cell proliferation and migration. *Exp Cell Res* **316**, 875-886.
80. Park, E.J., *et al.* Rac1 contributes to maximal activation of STAT1 and STAT3 in IFN-gamma-stimulated rat astrocytes. *J Immunol* **173**, 5697-5703 (2004).
81. Williams, D.A., Zheng, Y. & Cancelas, J.A. Rho GTPases and regulation of hematopoietic stem cell localization. *Methods Enzymol* **439**, 365-393 (2008).
82. Dallery, E., *et al.* TTF, a gene encoding a novel small G protein, fuses to the lymphoma-associated LAZ3 gene by t(3;4) chromosomal translocation. *Oncogene* **10**, 2171-2178 (1995).
83. Fueller, F. & Kubatzky, K.F. The small GTPase RhoH is an atypical regulator of haematopoietic cells. *Cell Commun Signal* **6**, 6 (2008).
84. Tybulewicz, V.L. & Henderson, R.B. Rho family GTPases and their regulators in lymphocytes. *Nat Rev Immunol* **9**, 630-644 (2009).

85. Gu, Y., Jasti, A.C., Jansen, M. & Siefring, J.E. RhoH, a hematopoietic-specific Rho GTPase, regulates proliferation, survival, migration, and engraftment of hematopoietic progenitor cells. *Blood* **105**, 1467-1475 (2005).
86. Dallery-Prudhomme, E., *et al.* Genomic structure and assignment of the RhoH/TTF small GTPase gene (ARHH) to 4p13 by in situ hybridization. *Genomics* **43**, 89-94 (1997).
87. Chae, H.D., Lee, K.E., Williams, D.A. & Gu, Y. Cross-talk between RhoH and Rac1 in regulation of actin cytoskeleton and chemotaxis of hematopoietic progenitor cells. *Blood* **111**, 2597-2605 (2008).
88. Dorn, T., *et al.* RhoH is important for positive thymocyte selection and T-cell receptor signaling. *Blood* **109**, 2346-2355 (2007).
89. Gu, Y., *et al.* RhoH GTPase recruits and activates Zap70 required for T cell receptor signaling and thymocyte development. *Nat Immunol* **7**, 1182-1190 (2006).
90. Stein, H., *et al.* The expression of the Hodgkin's disease associated antigen Ki-1 in reactive and neoplastic lymphoid tissue: evidence that Reed-Sternberg cells and histiocytic malignancies are derived from activated lymphoid cells. *Blood* **66**, 848-858 (1985).
91. Harris, N.L., *et al.* The World Health Organization classification of neoplasms of the hematopoietic and lymphoid tissues: report of the Clinical Advisory Committee meeting--Airlie House, Virginia, November, 1997. *Hematol J* **1**, 53-66 (2000).
92. Savage, K.J., *et al.* Favorable outcome of primary mediastinal large B-cell lymphoma in a single institution: the British Columbia experience. *Ann Oncol* **17**, 123-130 (2006).
93. Nieborowska-Skorska, M., *et al.* Role of signal transducer and activator of transcription 5 in nucleophosmin/ anaplastic lymphoma kinase-mediated malignant transformation of lymphoid cells. *Cancer Res* **61**, 6517-6523 (2001).
94. Fornari, A., Piva, R., Chiarle, R., Novero, D. & Inghirami, G. Anaplastic large cell lymphoma: one or more entities among T-cell lymphoma? *Hematol Oncol* **27**, 161-170 (2009).
95. Zamo, A., *et al.* Anaplastic lymphoma kinase (ALK) activates Stat3 and protects hematopoietic cells from cell death. *Oncogene* **21**, 1038-1047 (2002).
96. Mosse, Y.P., Wood, A. & Maris, J.M. Inhibition of ALK signaling for cancer therapy. *Clin Cancer Res* **15**, 5609-5614 (2009).
97. Ambrogio, C., *et al.* The anaplastic lymphoma kinase controls cell shape and growth of anaplastic large cell lymphoma through Cdc42 activation. *Cancer Res* **68**, 8899-8907 (2008).
98. Colomba, A., *et al.* Activation of Rac1 and the exchange factor Vav3 are involved in NPM-ALK signaling in anaplastic large cell lymphomas. *Oncogene* **27**, 2728-2736 (2008).
99. Pasqualucci, L., *et al.* Hypermutation of multiple proto-oncogenes in B-cell diffuse large-cell lymphomas. *Nature* **412**, 341-346 (2001).
100. Galiegue-Zouitina, S., Delestre, L., Dupont, C., Troussard, X. & Shelley, C.S. Underexpression of RhoH in Hairy Cell Leukemia. *Cancer Res* **68**, 4531-4540 (2008).
101. Sanchez-Aguilera, A., *et al.* Involvement of RhoH GTPase in the development of B-cell chronic lymphocytic leukemia. *Leukemia* **24**, 97-104 (2010).
102. Liu, H. Die Rolle der hämatopoetischen GTPase, RhoH in der IL-3 vermittelten Signaltransduktion in BaF3 Zellen und in der Funktion und der Differenzierung in murine Knochmark abstammenden Mastzellen. *Diploma Thesis Fakultät für Biologie der Albert-Ludwigs-Universität Freiburg i. Br.* (2007).
103. Karasuyama, H. & Melchers, F. Establishment of mouse cell lines which constitutively secrete large quantities of interleukin 2, 3, 4 or 5, using modified cDNA expression vectors. *Eur J Immunol* **18**, 97-104 (1988).
104. Kinsella, T.M. & Nolan, G.P. Episomal vectors rapidly and stably produce high-titer recombinant retrovirus. *Hum Gene Ther* **7**, 1405-1413 (1996).
105. Ozawa, K., Yamada, K., Kazanietz, M.G., Blumberg, P.M. & Beaven, M.A. Different isozymes of protein kinase C mediate feedback inhibition of phospholipase C and stimulatory signals for exocytosis in rat RBL-2H3 cells. *J Biol Chem* **268**, 2280-2283 (1993).
106. Daryadel, A., *et al.* RhoH/TTF negatively regulates leukotriene production in neutrophils. *J Immunol* **182**, 6527-6532 (2009).
107. Liu, X., *et al.* Generation of mammalian cells stably expressing multiple genes at predetermined levels. *Anal Biochem* **280**, 20-28 (2000).
108. Parada, Y., *et al.* BCR-ABL and interleukin 3 promote haematopoietic cell proliferation and survival through modulation of cyclin D2 and p27Kip1 expression. *J Biol Chem* **276**, 23572-23580 (2001).
109. Nosaka, T., *et al.* STAT5 as a molecular regulator of proliferation, differentiation and apoptosis in hematopoietic cells. *EMBO J* **18**, 4754-4765 (1999).
110. Guzman, M.L., *et al.* Expression of tumor-suppressor genes interferon regulatory factor 1 and death-associated protein kinase in primitive acute myelogenous leukemia cells. *Blood* **97**, 2177-2179 (2001).

111. Testa, U., *et al.* Elevated expression of IL-3Ralpha in acute myelogenous leukemia is associated with enhanced blast proliferation, increased cellularity, and poor prognosis. *Blood* **100**, 2980-2988 (2002).
112. Testa, U., *et al.* Interleukin-3 receptor in acute leukemia. *Leukemia* **18**, 219-226 (2004).
113. Amin, H.M. & Lai, R. Pathobiology of ALK+ anaplastic large-cell lymphoma. *Blood* **110**, 2259-2267 (2007).
114. Oda, H., *et al.* RhoH plays critical roles in Fc epsilon RI-dependent signal transduction in mast cells. *J Immunol* **182**, 957-962 (2009).
115. Aspenstrom, P., Ruusala, A. & Pacholsky, D. Taking Rho GTPases to the next level: the cellular functions of atypical Rho GTPases. *Exp Cell Res* **313**, 3673-3679 (2007).
116. Johnson, H.M., *et al.* Hypothesis: ligand/receptor-assisted nuclear translocation of STATs. *Proc Soc Exp Biol Med* **218**, 149-155 (1998).
117. Eulenfeld, R. & Schaper, F. A new mechanism for the regulation of Gab1 recruitment to the plasma membrane. *J Cell Sci* **122**, 55-64 (2009).
118. Stokoe, D., Caudwell, B., Cohen, P.T. & Cohen, P. The substrate specificity and structure of mitogen-activated protein (MAP) kinase-activated protein kinase-2. *Biochem J* **296 (Pt 3)**, 843-849 (1993).
119. Ghosh, M., *et al.* Cofilin promotes actin polymerization and defines the direction of cell motility. *Science* **304**, 743-746 (2004).
120. Myers, M.P., *et al.* TYK2 and JAK2 are substrates of protein-tyrosine phosphatase 1B. *J Biol Chem* **276**, 47771-47774 (2001).
121. Simoncic, P.D., Lee-Loy, A., Barber, D.L., Tremblay, M.L. & McGlade, C.J. The T cell protein tyrosine phosphatase is a negative regulator of janus family kinases 1 and 3. *Curr Biol* **12**, 446-453 (2002).
122. Lu, X., *et al.* PTP1B is a negative regulator of interleukin 4-induced STAT6 signaling. *Blood* **112**, 4098-4108 (2008).
123. Gelderloos, J.A. & Anderson, S.M. Over-expression of protein tyrosine phosphatase 1 (PTP1) alters IL-3-dependent growth and tyrosine phosphorylation. *Oncogene* **13**, 2367-2378 (1996).
124. Nabel, G., Galli, S.J., Dvorak, A.M., Dvorak, H.F. & Cantor, H. Inducer T lymphocytes synthesize a factor that stimulates proliferation of cloned mast cells. *Nature* **291**, 332-334 (1981).
125. Nagao, K., Yokoro, K. & Aaronson, S.A. Continuous lines of basophil/mast cells derived from normal mouse bone marrow. *Science* **212**, 333-335 (1981).
126. Ihle, J.N., *et al.* Biologic properties of homogeneous interleukin 3. I. Demonstration of WEHI-3 growth factor activity, mast cell growth factor activity, p cell-stimulating factor activity, colony-stimulating factor activity, and histamine-producing cell-stimulating factor activity. *J Immunol* **131**, 282-287 (1983).
127. Razin, E., *et al.* Interleukin 3: A differentiation and growth factor for the mouse mast cell that contains chondroitin sulfate E proteoglycan. *J Immunol* **132**, 1479-1486 (1984).
128. Mummery, C.L., van den Brink, C.E. & de Laat, S.W. Commitment to differentiation induced by retinoic acid in P19 embryonal carcinoma cells is cell cycle dependent. *Dev Biol* **121**, 10-19 (1987).
129. Singh, A.M. & Dalton, S. The cell cycle and Myc intersect with mechanisms that regulate pluripotency and reprogramming. *Cell Stem Cell* **5**, 141-149 (2009).
130. Theoharides, T.C., Kempuraj, D., Tagen, M., Conti, P. & Kalogeromitros, D. Differential release of mast cell mediators and the pathogenesis of inflammation. *Immunol Rev* **217**, 65-78 (2007).
131. Gabay, C. Interleukin-6 and chronic inflammation. *Arthritis Res Ther* **8 Suppl 2**, S3 (2006).
132. Scheller, J., Ohnesorge, N. & Rose-John, S. Interleukin-6 trans-signalling in chronic inflammation and cancer. *Scand J Immunol* **63**, 321-329 (2006).
133. Okayama, Y. Mast cell-derived cytokine expression induced via Fc receptors and Toll-like receptors. *Chem Immunol Allergy* **87**, 101-110 (2005).
134. Gordon, M.Y., *et al.* Contact-mediated inhibition of human haematopoietic progenitor cell proliferation may be conferred by stem cell antigen, CD34. *Hematol J* **1**, 77-86 (2000).
135. Punzel, M., Gupta, P. & Verfaillie, C.M. The microenvironment of AFT024 cells maintains primitive human hematopoiesis by counteracting contact mediated inhibition of proliferation. *Cell Commun Adhes* **9**, 149-159 (2002).
136. Cherry, L.K., Li, X., Schwab, P., Lim, B. & Klickstein, L.B. RhoH is required to maintain the integrin LFA-1 in a nonadhesive state on lymphocytes. *Nat Immunol* **5**, 961-967 (2004).
137. Rane, S.G. & Reddy, E.P. JAKs, STATs and Src kinases in hematopoiesis. *Oncogene* **21**, 3334-3358 (2002).
138. Baker, S.J., Rane, S.G. & Reddy, E.P. Hematopoietic cytokine receptor signaling. *Oncogene* **26**, 6724-6737 (2007).
139. Baum, C., *et al.* Side effects of retroviral gene transfer into hematopoietic stem cells. *Blood* **101**, 2099-2114 (2003).
140. Darnell, J.E., Jr. STATs and gene regulation. *Science* **277**, 1630-1635 (1997).

141. Kimura, T., *et al.* Involvement of the IRF-1 transcription factor in antiviral responses to interferons. *Science* **264**, 1921-1924 (1994).
142. Taniguchi, T., Ogasawara, K., Takaoka, A. & Tanaka, N. IRF family of transcription factors as regulators of host defense. *Annu Rev Immunol* **19**, 623-655 (2001).
143. Testa, U., *et al.* Diphtheria toxin fused to variant human interleukin-3 induces cytotoxicity of blasts from patients with acute myeloid leukemia according to the level of interleukin-3 receptor expression. *Blood* **106**, 2527-2529 (2005).
144. Ford, A.M., *et al.* Multilineage phenotypes of interleukin-3-dependent progenitor cells. *Blood* **79**, 1962-1971 (1992).
145. Lewis, R.S. & Ward, A.C. Stat5 as a diagnostic marker for leukemia. *Expert Rev Mol Diagn* **8**, 73-82 (2008).
146. Zhao, W.L. Targeted therapy in T-cell malignancies: dysregulation of the cellular signaling pathways. *Leukemia* **24**, 13-21 (2010).
147. Lim, M.S., *et al.* The proteomic signature of NPM/ALK reveals deregulation of multiple cellular pathways. *Blood* **114**, 1585-1595 (2009).
148. Bonzheim, I., *et al.* Anaplastic large cell lymphomas lack the expression of T-cell receptor molecules or molecules of proximal T-cell receptor signaling. *Blood* **104**, 3358-3360 (2004).
149. Malin, S., McManus, S. & Busslinger, M. STAT5 in B cell development and leukemia. *Curr Opin Immunol* **22**, 168-176 (2010).
150. Gaidano, G., *et al.* Aberrant somatic hypermutation in multiple subtypes of AIDS-associated non-Hodgkin lymphoma. *Blood* **102**, 1833-1841 (2003).
151. Preudhomme, C., *et al.* Nonrandom 4p13 rearrangements of the RhoH/TTF gene, encoding a GTP-binding protein, in non-Hodgkin's lymphoma and multiple myeloma. *Oncogene* **19**, 2023-2032 (2000).
152. Matsumura, I., *et al.* Transcriptional regulation of the cyclin D1 promoter by STAT5: its involvement in cytokine-dependent growth of hematopoietic cells. *EMBO J* **18**, 1367-1377 (1999).
153. Gladkikh, A., Potashnikova, D., Korneva, E., Khudoleeva, O. & Vorobjev, I. Cyclin D1 expression in B-cell lymphomas. *Exp Hematol* (2010).
154. O'Connor, O.A. Mantle cell lymphoma: identifying novel molecular targets in growth and survival pathways. *Hematology Am Soc Hematol Educ Program*, 270-276 (2007).
155. Carreras, J., *et al.* Immunohistochemical analysis of ZAP-70 expression in B-cell lymphoid neoplasms. *J Pathol* **205**, 507-513 (2005).
156. John, J., *et al.* Kinetic and structural analysis of the Mg(2+)-binding site of the guanine nucleotide-binding protein p21H-ras. *J Biol Chem* **268**, 923-929 (1993).
157. Stokoe, D., Macdonald, S.G., Cadwallader, K., Symons, M. & Hancock, J.F. Activation of Raf as a result of recruitment to the plasma membrane. *Science* **264**, 1463-1467 (1994).
158. Michaelson, D., *et al.* Rac1 accumulates in the nucleus during the G2 phase of the cell cycle and promotes cell division. *J Cell Biol* **181**, 485-496 (2008).
159. Ridley, A.J. & Hall, A. The small GTP-binding protein rho regulates the assembly of focal adhesions and actin stress fibers in response to growth factors. *Cell* **70**, 389-399 (1992).
160. Williams, C.L. The polybasic region of Ras and Rho family small GTPases: a regulator of protein interactions and membrane association and a site of nuclear localization signal sequences. *Cell Signal* **15**, 1071-1080 (2003).
161. Lanning, C.C., Daddona, J.L., Ruiz-Velasco, R., Shafer, S.H. & Williams, C.L. The Rac1 C-terminal polybasic region regulates the nuclear localization and protein degradation of Rac1. *J Biol Chem* **279**, 44197-44210 (2004).
162. Lanning, C.C., Ruiz-Velasco, R. & Williams, C.L. Novel mechanism of the co-regulation of nuclear transport of SmgGDS and Rac1. *J Biol Chem* **278**, 12495-12506 (2003).
163. Kawashima, T. & Kitamura, T. Rac and nuclear translocation of signal transducers and activators of transcription factors. *Methods Enzymol* **439**, 171-180 (2008).
164. Romanova, L.Y., *et al.* Regulation of actin cytoskeleton in lymphocytes: PKC-delta disrupts IL-3-induced membrane ruffles downstream of Rac1. *J Cell Physiol* **179**, 157-169 (1999).
165. Rico-Bautista, E., Negrin-Martinez, C., Novoa-Mogollon, J., Fernandez-Perez, L. & Flores-Morales, A. Downregulation of the growth hormone-induced Janus kinase 2/signal transducer and activator of transcription 5 signaling pathway requires an intact actin cytoskeleton. *Exp Cell Res* **294**, 269-280 (2004).
166. Gu, F., *et al.* Protein tyrosine phosphatase 1B attenuates growth hormone-mediated JAK2-STAT signaling. *Mol Cell Biol* **23**, 3753-3762 (2003).
167. Wang, H., Zeng, X., Fan, Z. & Lim, B. RhoH modulates pre-TCR and TCR signalling by regulating LCK. *Cell Signal* (2010).

168. Haj, F.G., Verveer, P.J., Squire, A., Neel, B.G. & Bastiaens, P.I. Imaging sites of receptor dephosphorylation by PTP1B on the surface of the endoplasmic reticulum. *Science* **295**, 1708-1711 (2002).
169. Levkowitz, G., *et al.* Ubiquitin ligase activity and tyrosine phosphorylation underlie suppression of growth factor signaling by c-Cbl/Sli-1. *Mol Cell* **4**, 1029-1040 (1999).
170. Joazeiro, C.A., *et al.* The tyrosine kinase negative regulator c-Cbl as a RING-type, E2-dependent ubiquitin-protein ligase. *Science* **286**, 309-312 (1999).
171. Gurish, M.F. & Boyce, J.A. Mast cells: ontogeny, homing, and recruitment of a unique innate effector cell. *J Allergy Clin Immunol* **117**, 1285-1291 (2006).
172. Mangi, M.H. & Newland, A.C. Interleukin-3 in hematology and oncology: current state of knowledge and future directions. *Cytokines Cell Mol Ther* **5**, 87-95 (1999).
173. Wierenga, A.T., Vellenga, E. & Schuringa, J.J. Maximal STAT5-induced proliferation and self-renewal at intermediate STAT5 activity levels. *Mol Cell Biol* **28**, 6668-6680 (2008).
174. Moore, M.A., Dorn, D.C., Schuringa, J.J., Chung, K.Y. & Morrone, G. Constitutive activation of Flt3 and STAT5A enhances self-renewal and alters differentiation of hematopoietic stem cells. *Exp Hematol* **35**, 105-116 (2007).
175. Morales, J.K., Falanga, Y.T., Depcrynski, A., Fernando, J. & Ryan, J.J. Mast cell homeostasis and the JAK-STAT pathway. *Genes Immun* (2010).
176. Mann-Chandler, M.N., *et al.* IFN-gamma induces apoptosis in developing mast cells. *J Immunol* **175**, 3000-3005 (2005).
177. Pardee, A.B. G1 events and regulation of cell proliferation. *Science* **246**, 603-608 (1989).
178. Shelburne, C.P., *et al.* Stat5 expression is critical for mast cell development and survival. *Blood* **102**, 1290-1297 (2003).
179. Lambert, J.F., *et al.* Marrow stem cells shift gene expression and engraftment phenotype with cell cycle transit. *J Exp Med* **197**, 1563-1572 (2003).
180. Quesenberry, P.J., *et al.* Expression of cell cycle-related genes with cytokine-induced cell cycle progression of primitive hematopoietic stem cells. *Stem Cells Dev* **19**, 453-460 (2010).
181. Dooner, G.J., Colvin, G.A., Dooner, M.S., Johnson, K.W. & Quesenberry, P.J. Gene expression fluctuations in murine hematopoietic stem cells with cell cycle progression. *J Cell Physiol* **214**, 786-795 (2008).
182. Cronkite, E.P. Hemopoietic stem cells: An analytic review of hemopoiesis. *Pathobiol Annu* **5**, 35-69 (1975).
183. Metcalfe, D.D. Mast cells and mastocytosis. *Blood* **112**, 946-956 (2008).
184. Metcalfe, D.D. Classification and diagnosis of mastocytosis: current status. *J Invest Dermatol* **96**, 2S-4S; discussion 4S, 60S-65S (1991).
185. Florian, S., *et al.* Detection of molecular targets on the surface of CD34+/CD38-- stem cells in various myeloid malignancies. *Leuk Lymphoma* **47**, 207-222 (2006).
186. Baumgartner, C., *et al.* Expression of activated STAT5 in neoplastic mast cells in systemic mastocytosis: subcellular distribution and role of the transforming oncoprotein KIT D816V. *Am J Pathol* **175**, 2416-2429 (2009).
187. Maric, I., *et al.* KIT D816V-associated systemic mastocytosis with eosinophilia and FIP1L1/PDGFRA-associated chronic eosinophilic leukemia are distinct entities. *J Allergy Clin Immunol* **120**, 680-687 (2007).
188. Bain, B.J. Systemic mastocytosis and other mast cell neoplasms. *Br J Haematol* **106**, 9-17 (1999).
189. Bischoff, S.C. Role of mast cells in allergic and non-allergic immune responses: comparison of human and murine data. *Nat Rev Immunol* **7**, 93-104 (2007).
190. Stevens, R.L., Rothenberg, M.E., Levi-Schaffer, F. & Austen, K.F. Ontogeny of in vitro-differentiated mouse mast cells. *Fed Proc* **46**, 1915-1919 (1987).
191. Chen, C.C., Grimbaldeston, M.A., Tsai, M., Weissman, I.L. & Galli, S.J. Identification of mast cell progenitors in adult mice. *Proc Natl Acad Sci U S A* **102**, 11408-11413 (2005).
192. Walkley, C.R., Fero, M.L., Chien, W.M., Purton, L.E. & McArthur, G.A. Negative cell-cycle regulators cooperatively control self-renewal and differentiation of haematopoietic stem cells. *Nat Cell Biol* **7**, 172-178 (2005).
193. Walkley, C.R., McArthur, G.A. & Purton, L.E. Cell division and hematopoietic stem cells: not always exhausting. *Cell Cycle* **4**, 893-896 (2005).
194. Stepanova, L. & Sorrentino, B.P. A limited role for p16Ink4a and p19Arf in the loss of hematopoietic stem cells during proliferative stress. *Blood* **106**, 827-832 (2005).
195. Cheng, T., Rodrigues, N., Dombkowski, D., Stier, S. & Scadden, D.T. Stem cell repopulation efficiency but not pool size is governed by p27(kip1). *Nat Med* **6**, 1235-1240 (2000).
196. Cheng, T., *et al.* Hematopoietic stem cell quiescence maintained by p21cip1/waf1. *Science* **287**, 1804-1808 (2000).

197. Sakata-Yanagimoto, M., *et al.* Coordinated regulation of transcription factors through Notch2 is an important mediator of mast cell fate. *Proc Natl Acad Sci U S A* **105**, 7839-7844 (2008).
198. Liao, D. Emerging roles of the EBF family of transcription factors in tumor suppression. *Mol Cancer Res* **7**, 1893-1901 (2009).
199. Bradshaw, J.M. The Src, Syk, and Tec family kinases: distinct types of molecular switches. *Cell Signal* **22**, 1175-1184 (2010).
200. Turner, M., Schweighoffer, E., Colucci, F., Di Santo, J.P. & Tybulewicz, V.L. Tyrosine kinase SYK: essential functions for immunoreceptor signalling. *Immunol Today* **21**, 148-154 (2000).
201. van Oers, N.S. & Weiss, A. The Syk/ZAP-70 protein tyrosine kinase connection to antigen receptor signalling processes. *Semin Immunol* **7**, 227-236 (1995).
202. Gilfillan, A.M. & Rivera, J. The tyrosine kinase network regulating mast cell activation. *Immunol Rev* **228**, 149-169 (2009).
203. Galli, S.J. & Tsai, M. Mast cells in allergy and infection: versatile effector and regulatory cells in innate and adaptive immunity. *Eur J Immunol* **40**, 1843-1851 (2010).
204. Sutherland, R.E., Olsen, J.S., McKinstry, A., Villalta, S.A. & Wolters, P.J. Mast cell IL-6 improves survival from Klebsiella pneumonia and sepsis by enhancing neutrophil killing. *J Immunol* **181**, 5598-5605 (2008).
205. Kraft, S. & Kinet, J.P. New developments in FcepsilonRI regulation, function and inhibition. *Nat Rev Immunol* **7**, 365-378 (2007).

8. Publications and Presentations

Publication

M.S. Gündogdu, H. Liu, D. Metzdorf, D. Hildebrand, M. Aigner, K. Aktories, K. Heeg and K.F. Kubatzky "The haemtopoietic GTPase RhoH modulates IL3 signalling through regulation of STAT activity and IL3 receptor expression"
Molecular Cancer, August 2010, (9:225)

Posters

11/2007 **"**RhoH modulates IL3 dependent signalling" **M.S. Gündogdu**, H. Liu, K. Aktories and K.F. Kubatzky
Signal Transduction Society Meeting, Signal Transduction: Receptors, Mediators and Genes; Weimar, Germany, November 2007

08/2009 "RhoH modulates IL3 dependent signalling through regulation of STAT activity and IL3 Receptor expression" **M.S. Gündogdu**, H. Liu, K. Aktories, K. Heeg, and K.F. Kubatzky,
FEBS Lecture Course, Molecular Mechanisms in Signal transduction and Cancer;
Speetses, Greece, August 2009

11/2009 "Proteomics profiling of RhoH interaction networks in IL-3 mediated signalling" **M.S. Gündogdu**, E.S. Simon, K. Heeg. P.C. Andrews and K.F. Kubatzky,
Signal Transduction Society Meeting, Signal Transduction: Receptors, Mediators and Genes; Weimar, Germany, November 2009

Talks

03/2008 **M.S. Gündogdu** "RhoH modulates IL-3 dependent signalling through modulation of STAT activity"
Mini-Symposium of Infection and Immunology Rothenfels;
Rothenfels, Germany, March 2008.

08/2009 **M.S. Gündogdu** "RhoH modulates IL-3 dependent signalling through regulation of STAT activity and IL-3 Receptor expression"
FEBS Lecture Course, Molecular Mechanisms in Signal transduction and Cancer;
Speetses, Greece, August 2009

Acknowledgment

Allen voran möchte ich mich bei Frau **Dr. Kubatzky** bedanken, die ich bereits während der Diplomarbeit kennengelernt habe und die mir als ehemalige FH Studentin eine Chance gab. Sie stellte großzügig die interessante Themenstellung zur Verfügung und stand mir mit Ratschlägen zur Seite. Dem gesamten **Labor Kubatzky** danke ich für die anregende Arbeitsatmosphere.

Mein besonderer Dank gilt Herrn **Prof. Dr. Alexander Dalpke**, einem außerordentlichen Mensch und Wissenschaftler. Seine Unterstützung und sein Beistand kamen genau zur rechten Zeit.

Herrn **Prof. Dr. Klaus Heeg** danke ich für die herzliche Aufnahme in seine Abteilung, die Unterstützung die ich genießen durfte und für alle Möglichkeiten die er uns Doktoranden offenstellt.

He Liu möchte ich für die in Ihrer Diplomarbeit geleistete Vorarbeit danken, da diese das Fundament dieser Arbeit darstellen.

Peter Sahlstom und **Marie Lork** haben mir bei wesentlichen Teilen dieser Arbeit geholfen.
Vielen, vielen Dank! ich hoffe, ich konnte euch wenigstens ein bisschen von dem zurückgeben was Ihr mir gegeben habt. Der gesamten **Medizinischen Mikrobiologie** und im besonderen **Saskia Ziegler** danke ich für die schöne Zeit, den regen wissenschaftlichen und privaten Austausch und nicht zuletzt für die Bekanntschaften und Freundschaften die kamen und wieder gingen und doch immer etwas Besonderes hinterlassen haben.

Dr. Megan Lim für die gute Zusammenarbeit und zur Verfügungstellung der Lymphoma Zellinien und **Adam Kronk** aus dem BSRB für den technischen Support und den Spaß während der Versuche.
Prof. Phil Andrews, für die schöne Kooperation sowie für das Bereitstellen seines Labors, Equipments und seiner Experten während unserer Kooperation. Allen **Mitarbeitern des NRPP** und im Besonderen meinen Kollegen **Donna Veine**, **Dr. Takis Papoulias** sowie **Dr. Eric Simon**, sie haben mich aufgenommen und prägen meine schönsten Erinnerungen an die USA. Ausserdem haben sie dafür gesorgt das alles lief und weiter läuft und haben mich aufgerichtet wenns mal nicht so lief wie es sollte ;-)

Euch, meinen lieben Rosinenbombern, kann ich gar nicht genug Danken: **Judith Bauer**, **Laura Dittmar** und **Nicole Kilian**

My special thanks to **Dr. Jospeh Regan** (London) and **Jay** (Zürich).

Für musikalische Unterstützung und kompensation von Motivationstiefs danke ich **Phil May** und **John Lee Hooker** (RIP).

Dafür, dass sie immer ein offenes Ohr haben und so sind wie sie halt sind, danke ich **Dr. Flo Bott** und **Mehtap Sirin**.

Und niemals werde ich den Support der **„bayrischen Heimatfront“** vergessen! zu dieser expliziten Auswahl von überaus außergewöhnlichen Menschen gehören unter anderem: **Alexander Dämon+Familie**, **Werner Dämon**, **Toni Weweck**, **Chrissi Engelhard**, **Lothar Dybbert**, **Edina Jelecevic, Daniel Romahn** (alias Mind-Bender), **Victor Litterati-Lootz, Josip Curic** und natürlich der einizigartige **David “Dave“ Zanatta**.